HARVARD T.H. CHAN
SCHOOL OF PUBLIC HEALTH
CENTER FOR NANOTECHNOLOGY AND NANOTOXICOLOGY
http://hsph.harvard.edu/nano

Karolinska Institutet

End-of-life of nano-enabled products by thermal decomposition: Possible environmental health and safety implications

Georgios A. Sotiriou[1,2], Dilpreet Singh[2], Fang Zhang[2], Lutz Hoering[3], Wendel Wohlleben[2,3], Philip Demokritou[2]

[1]Department of Microbiology, Tumor and Cell Biology (MTC), Karolinska Institutet, Stockholm, Sweden.

[2]Center for Nanotechnology and Nanotoxicology, Department of Environmental Health, T.H. Chan School of Public Health, Harvard University, USA. www.hsph.harvard/nano

[3]BASF SE, Material Physics, Germany.

email: georgios.sotiriou@ki.se

Visit our lab website: www.sotirioulab.net

sotirioulab

Nanotoxicity: Realistic exposure scenarios?

- **So far**: Nanotoxicity evaluation of "raw" nanomaterials, which is great for:
  - → Mechanistic understanding
  - → Occupational exposures
- Realistic exposures?
- Transformations of nanomaterials during their life-cycle[1]

[1]

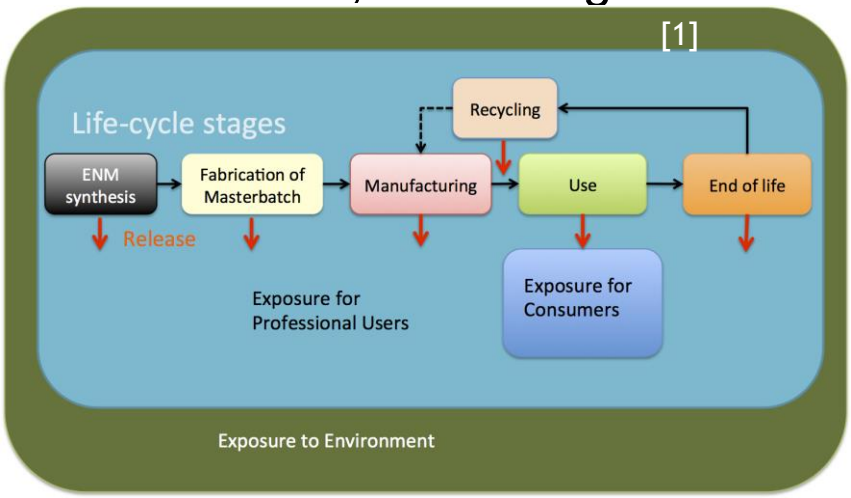

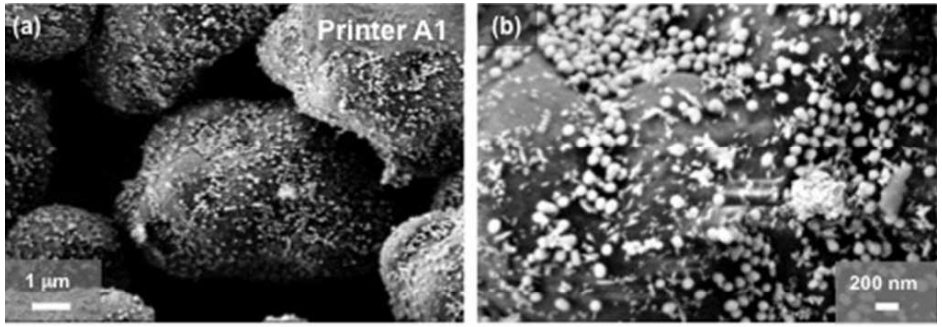

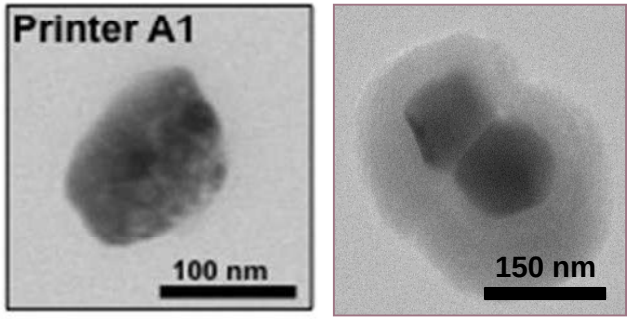

[2]

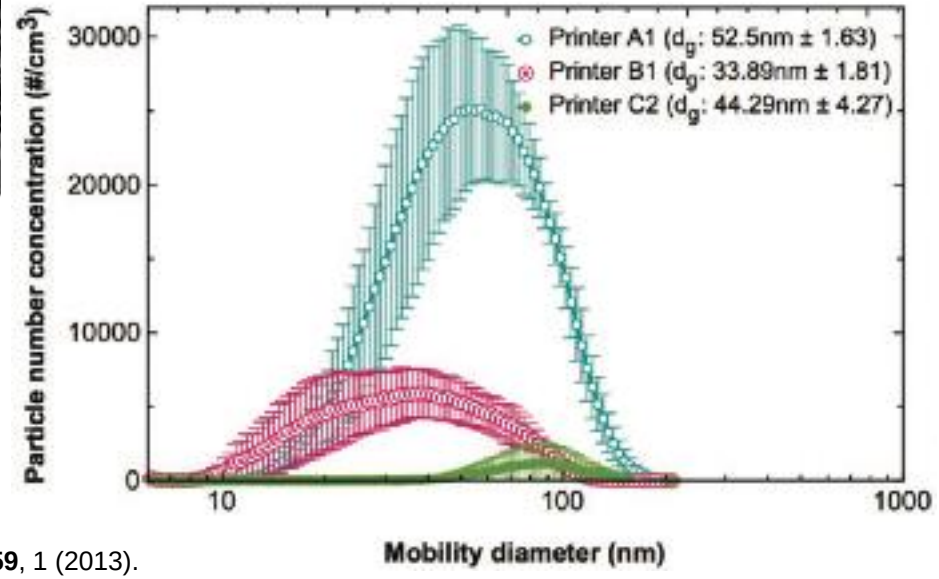

[1] Nowack, David, Fissan, Morris, Shatkin, Stintz, Zepp, Brouwer. *Environ. Int.* **59**, 1 (2013).
[2] Pirela, Sotiriou, Bello, Shafer, Bunker, Castranova, Thomas, Demokritou. *Nanotoxicology* **9**, 760 (2015).

Knowledge gaps of nano-release at End-of-Life

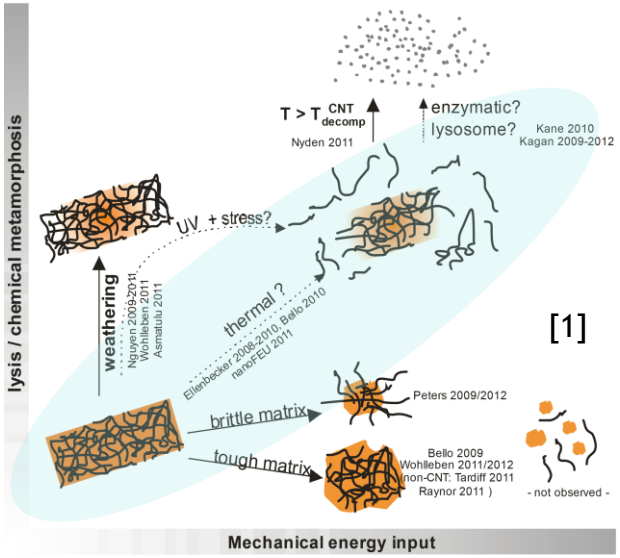

Our TARGET

- Obtain fundamental understanding on what factors influence the physicochemical and morphological properties of released materials
- ***Burning*** question: Is there a nanofiller-specific effect?

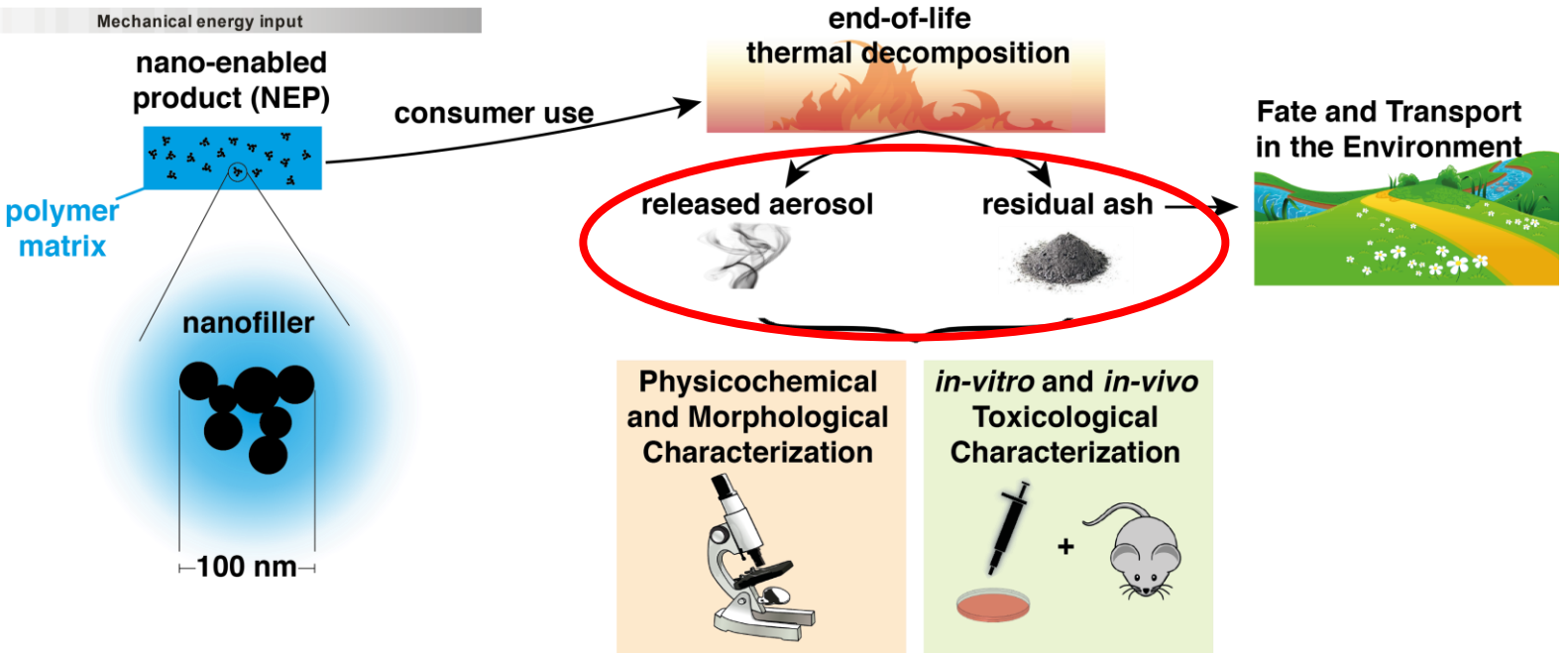

[1] Wohlleben, Meier, Vogel, Landsiedel, Cox, Hirth, Tomovic. *Nanoscale* **5**, 369 (2013).

Integrated Exposure Generation System (*INEXS*)

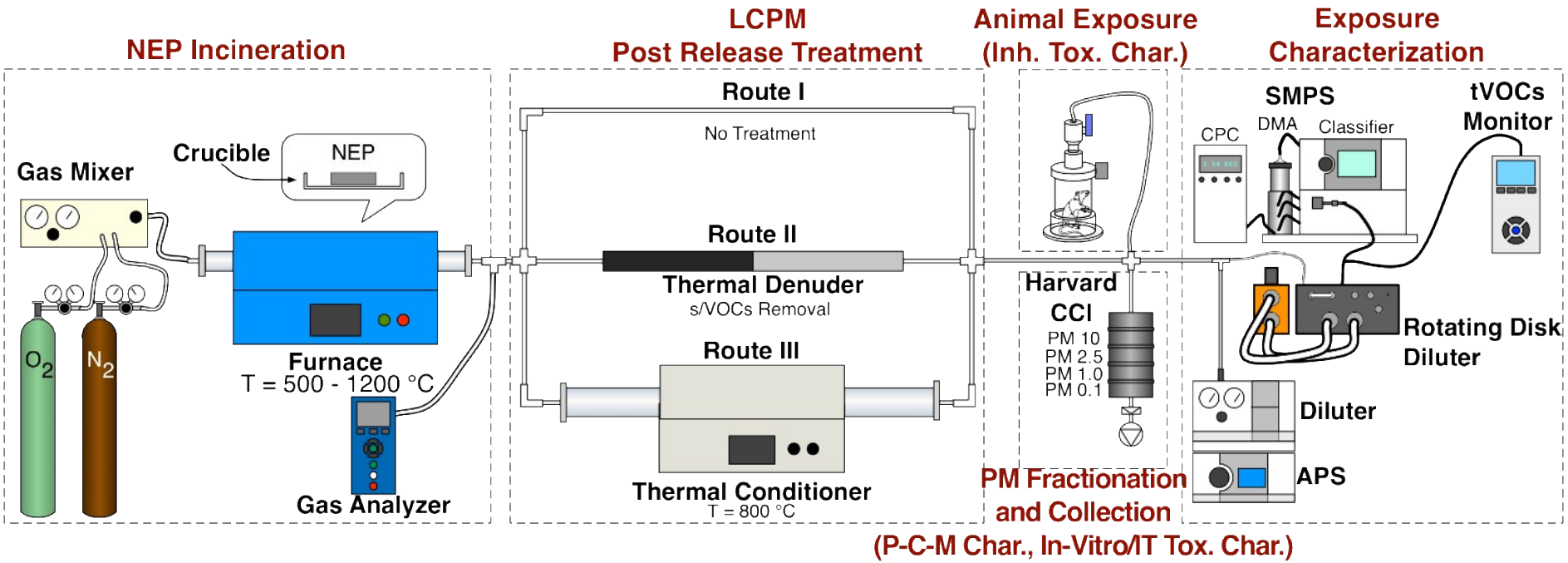

Advantages

- Versatile: Easy to change thermal decomposition scenario
- Real time equipment: Monitor particle concentration, size and composition
- Collection of **mg** of aerosol: Allows sufficient characterization and tox studies
- In situ inhalation studies: Direct aerosol in animal chambers
- Facile collection of residual ash

NEPs panel

	Matrix	nanofiller	nanofiller loading	application
MARINA	Polyurethane (PU)	-	-	automotive, buildings, textiles
		carbon black (CB)	0.1%	
		carbon nanotubes (CNT)	0.1%	
BASF	Polyethylene (PE)	-	-	packaging, buildings, constructions
		Fe_2O_3	1-5%	
		organic filler	2%	
		organic filler + UV agent	2%	
Umass Lowell	Polycarbonate (PC)	-	-	automotive, electronics
		CNT	3%	
	Polypropylene (PP)	-	-	packaging, electronics
		CNT	3%	
	Ethylene vinyl acetate (EVA)	-	-	packaging, biomedics
		TiO_2	1-15%	
	Medicinal waste	Ag		biomedics

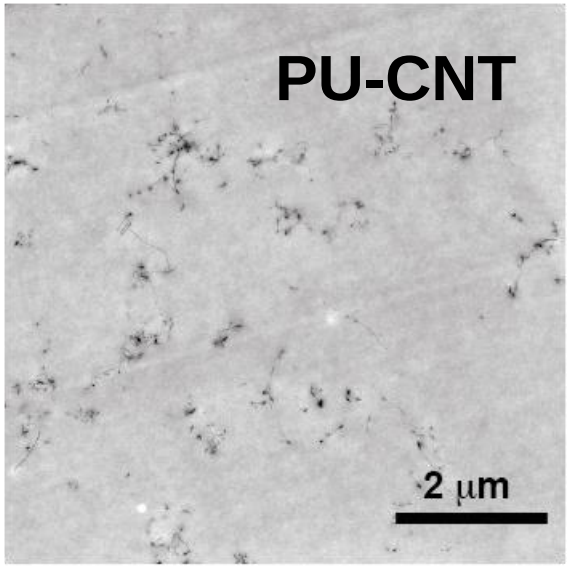

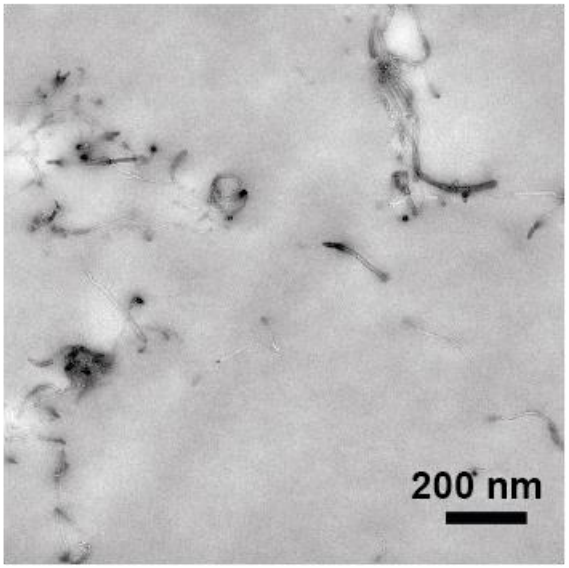

Nanofiller effect on aerosol size & concentration?

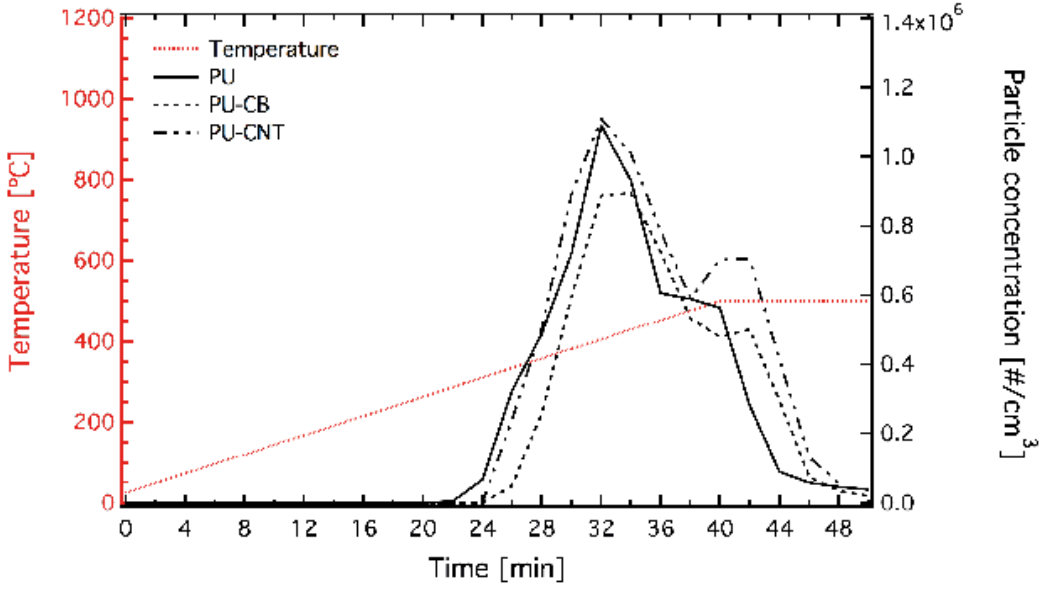

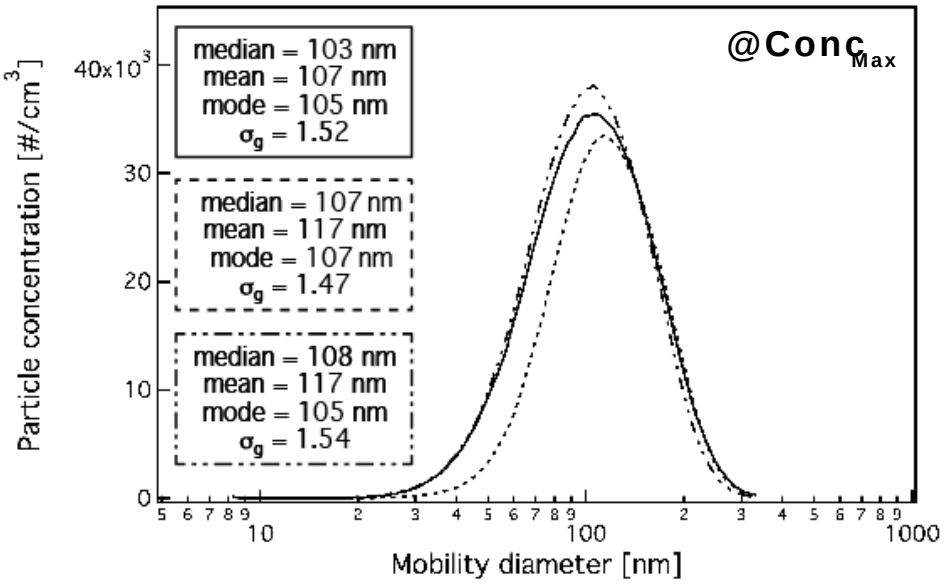

- PU-based NEPs
  - → Pure and with two different nanofillers (carbon black-CB, and carbon nanotubes-CNTs)
- No effect on released aerosol concentration and size due to the nanofiller presence
- Host polymer dictates the released PM
- >99% organic carbon, independent of nanofiller presence

Is there any nanofiller in the released aerosol?

SEM
after dispersion in alcohol and drying on SEM substrate

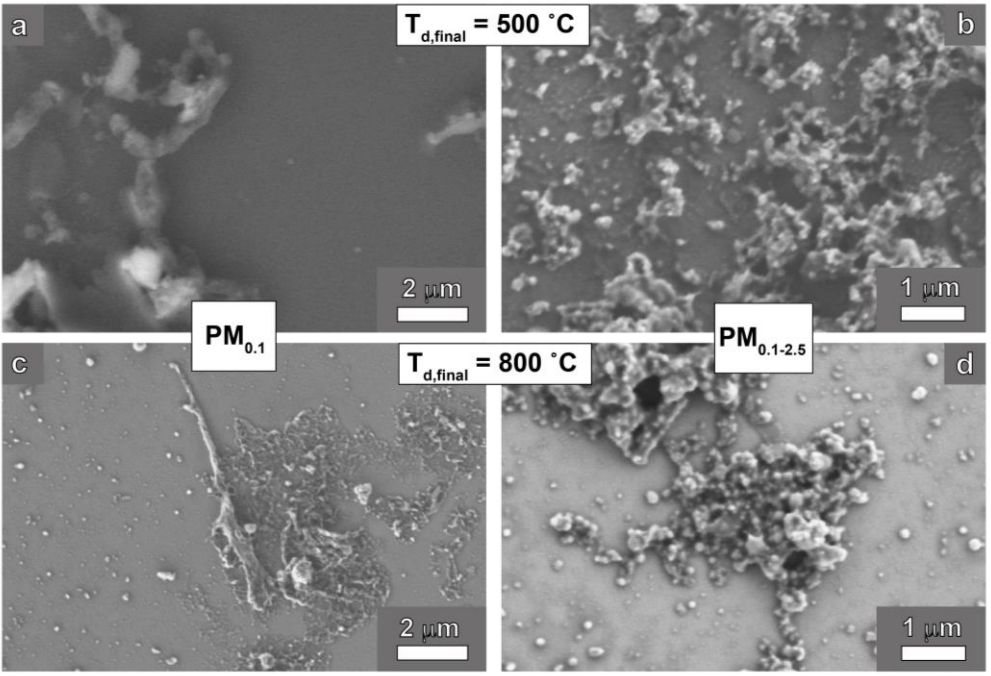

PU-CNT

TEM
in-situ deposition on TEM grids in CCI

PU-CNT (800 ˚C)

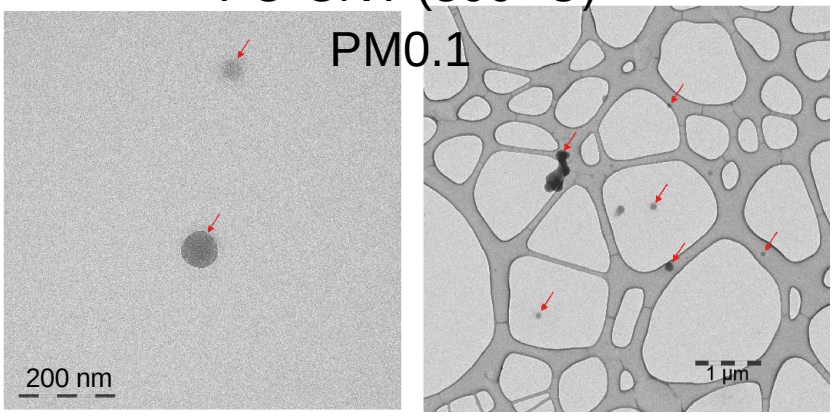

PE-Fe_2O_3 (800 ˚C)

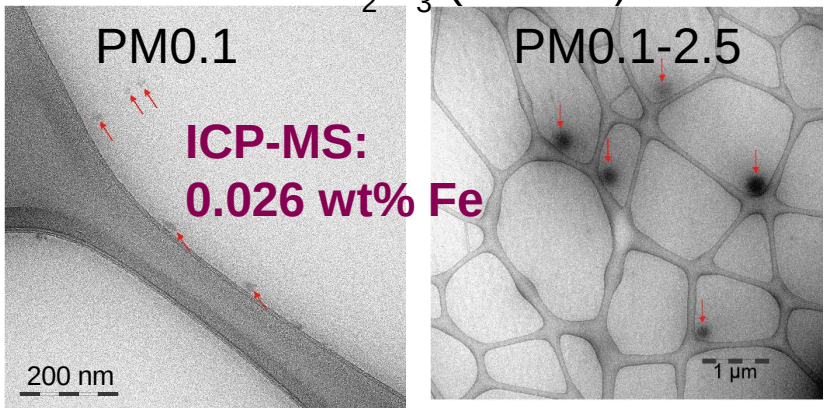

Nanofiller effect on chemistry of aerosol?

- TGA-FTIR (in situ detection of off-gases), ex-situ NMR

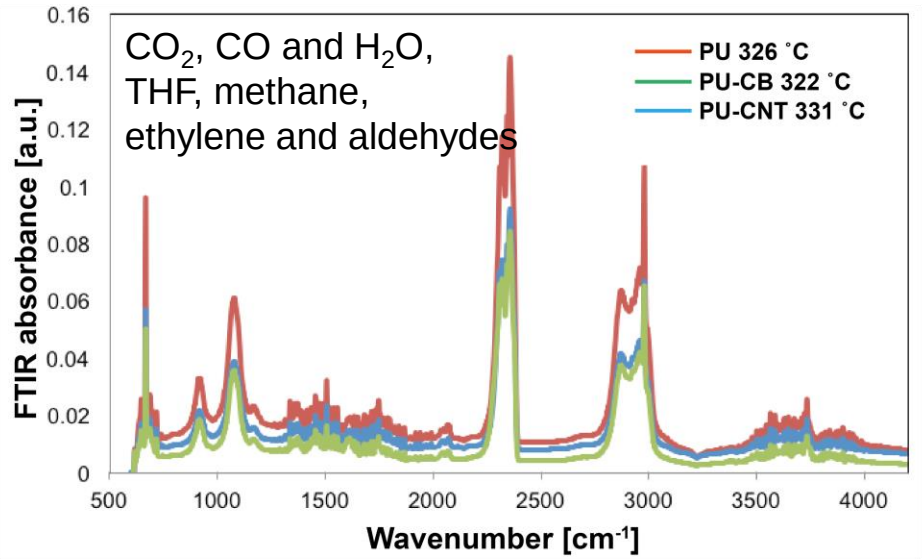

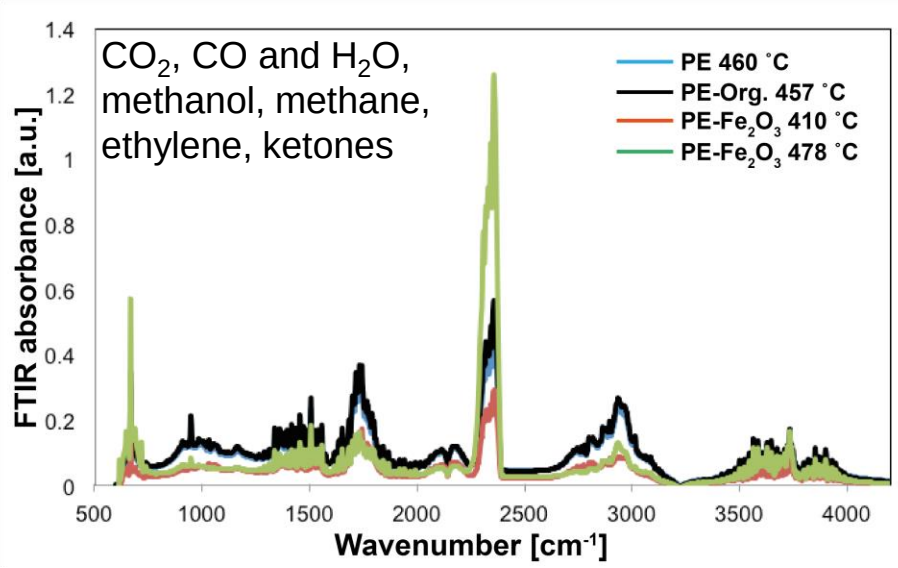

Total organic H

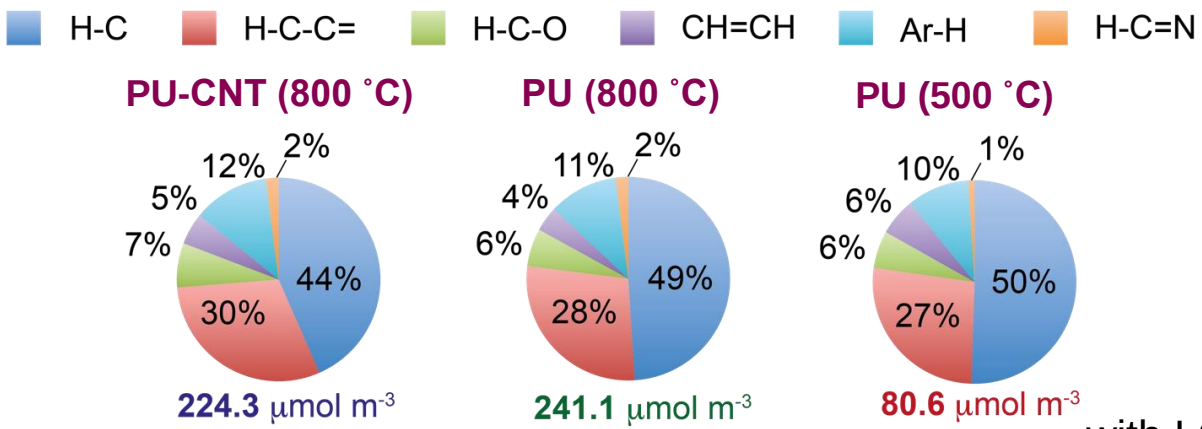

with I.G. Kavouras, Univ Arkansas

Polycyclic aromatic hydrocarbon (PAH) species

- 16 Environmental Protection Agency (EPA)-priority polycyclic aromatic hydrocarbon (PAH) species

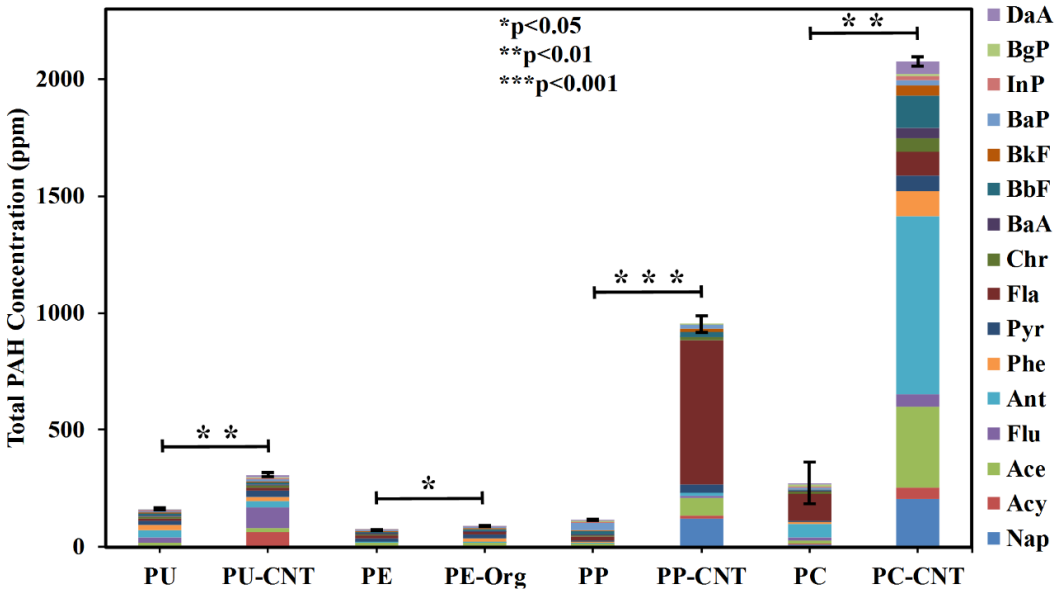

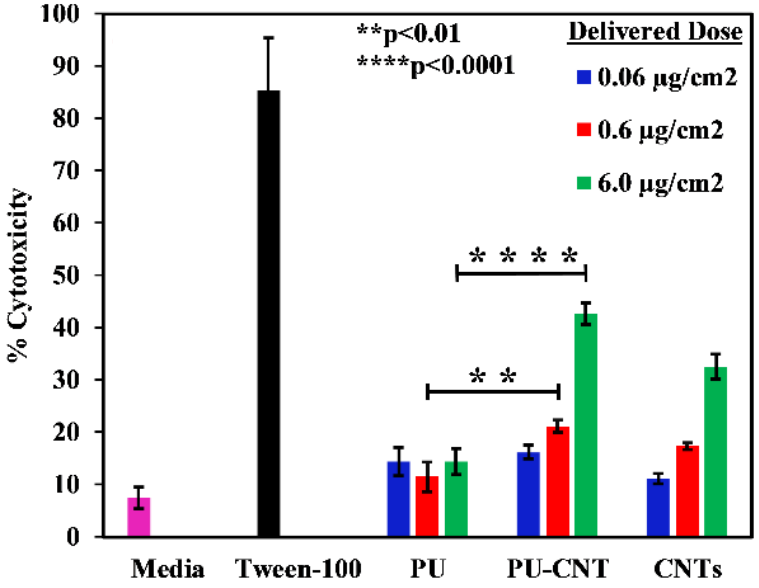

Singh et al., in preparation (2016).

with V. Craver, Univ Rhode Island

Is there nanofiller in the residual ash?

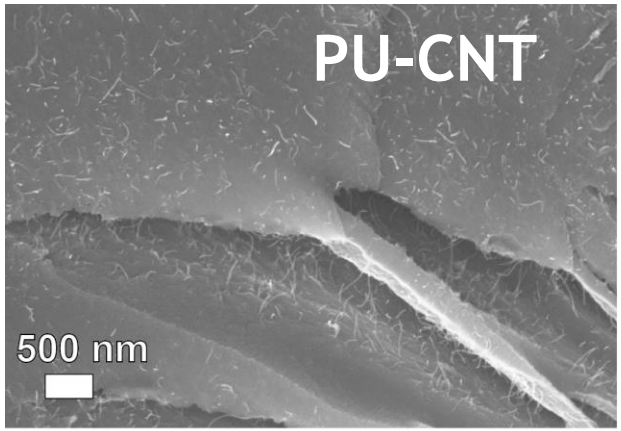

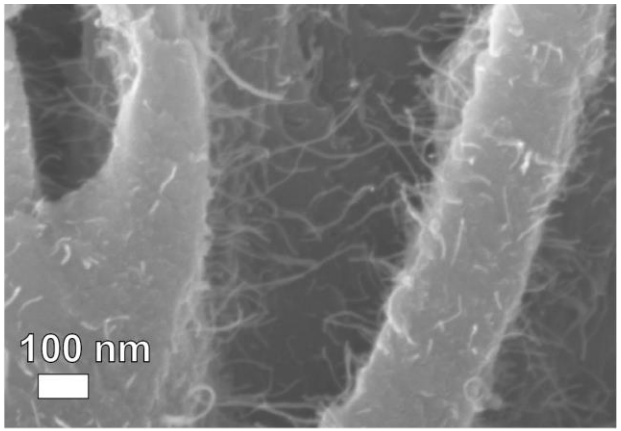

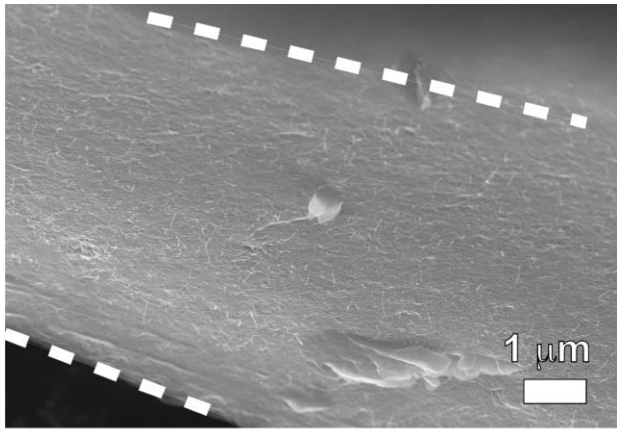

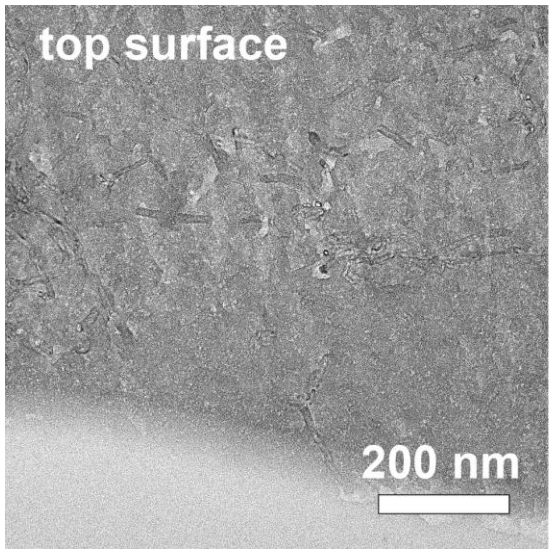

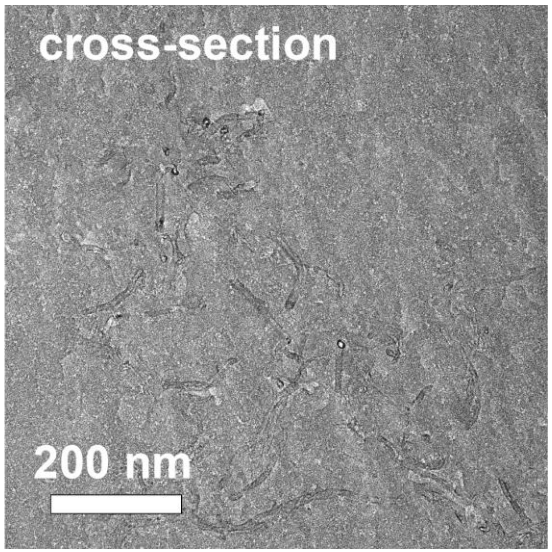

- CNTs in residual ash
- Homogeneously dispersed throughout the ash
- 18 times higher concentration than raw NEP

	500 °C	
	EC (%)	OC (%)
PU	85	15
PU-CB	77	23
PU-CNT	82	18

Effect of nanofiller on residual ash composition

- $T_{d,final}$ = 500˚C (PE-Fe_2O_3)

- Presence of Fe_2O_3 facilitates full polymer decomposiiton

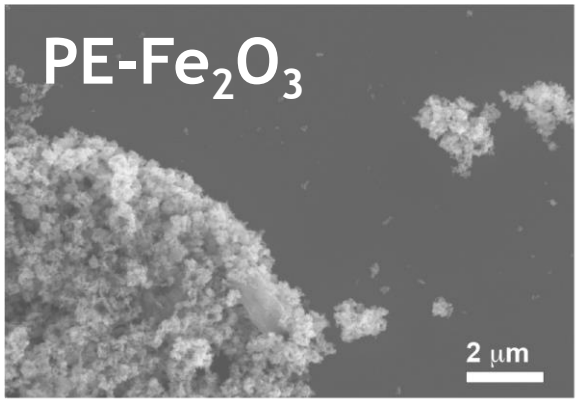

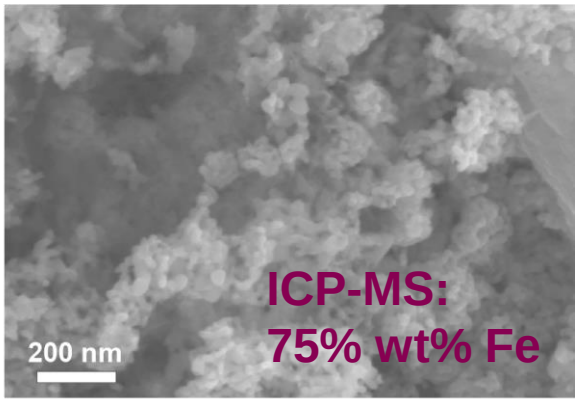

	500 ˚C	
	EC (%)	OC (%)
PE	78	22
PE-org	75	25
PE-Fe_2O_3	-	-

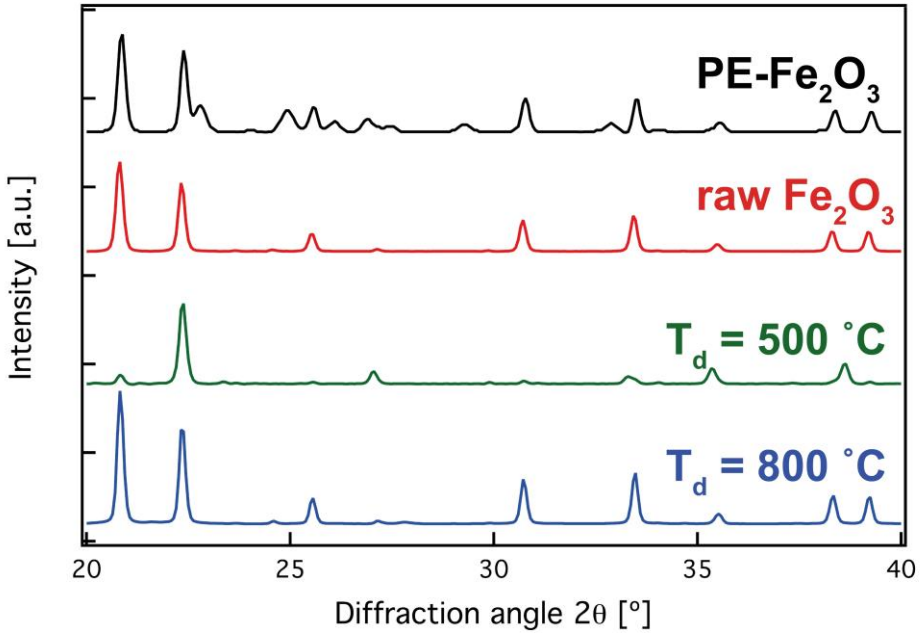

- Change of Fe_2O_3 crystal phase for final T = 500 ˚C (reduced from hematite to maghemite)

Summary

- Novel integrated exposure generation system for the end-of-life thermal decomposition of NEPs
- Main question: Is there any nanofiller-specific effect?
  - Released aerosol:
    - Not in released aerosol concentration and size
    - Yes in chemical composition
  - Residual ash:
    - Most nanofiller remains in ash
    - Physicochemical properties of remaining nanofiller might not be the same as in raw materials

Outlook

- Collect and extract enough PM for tox studies (in vitro and in vivo)

Acknowledgements

HSPH

Philip Demokritou

Dilpreet Singh

Fang Zhang

BASF

Wendel Wohlleben

Lutz Hoering

Univ Arkansas

Ilias G. Kavouras

Marie-Cecile Chalbot

Carnegie Mellon

Gregory V. Lowry

Eleanor Spielman-Sun

- NSF (grant nr. 1436450)
- BASF AG
- Swiss NSF

FONDS NATIONAL SUISSE
SCHWEIZERISCHER NATIONALFONDS
FONDO NAZIONALE SVIZZERO
SWISS NATIONAL SCIENCE FOUNDATION

Thank you for listening

More info:

[1] **G. A. Sotiriou**, D. Singh, F. Zhang, W. Wohlleben, M-C. G. Chalbot, I. G. Kavouras & P. Demokritou*. "An integrated methodology for the assessment of environmental health implications during thermal decomposition of nano-enabled products" *Environ. Sci.: Nano* **2**, 262-272 (2015).

[2] **G. A. Sotiriou**, D. Singh, F. Zhang, M-C. G. Chalbot, L. Hoering, I. G. Kavouras W. Wohlleben & P. Demokritou*. "Thermal decomposition of nano-enabled thermoplastics: Possible environmental health and safety implications" *J. Hazard. Mater.* **305**, 87-95 (2016).

[3] D. Singh, **G. A. Sotiriou**, F. Zhang, J. Mead, D. Bello, W. Wohlleben & P. Demokritou*. "End-of-life thermal decomposition of nano-enabled polymers: effect of nanofiller loading and polymer matrix on by-products" *Environ. Sci.: Nano* **in press** DOI: 10.1039/C6EN00252H (2016).

Open PhD student position in our lab
visit: www.sotirioulab.net
for more info

sotirioulab

Released aerosol concentration and size (PU-CNT)

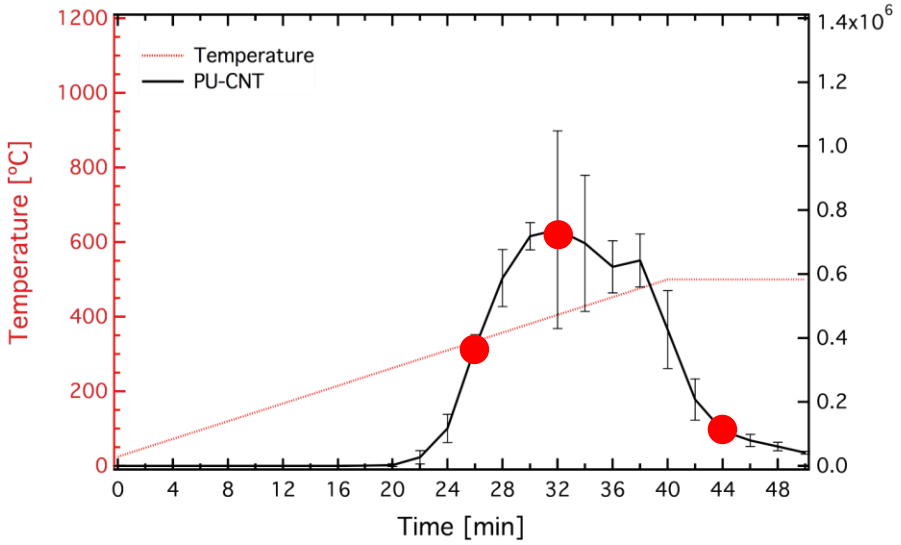

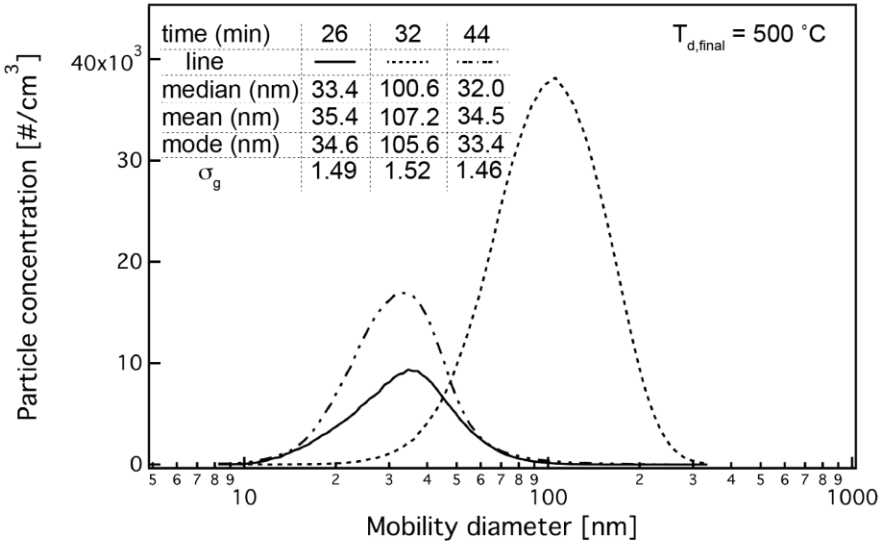

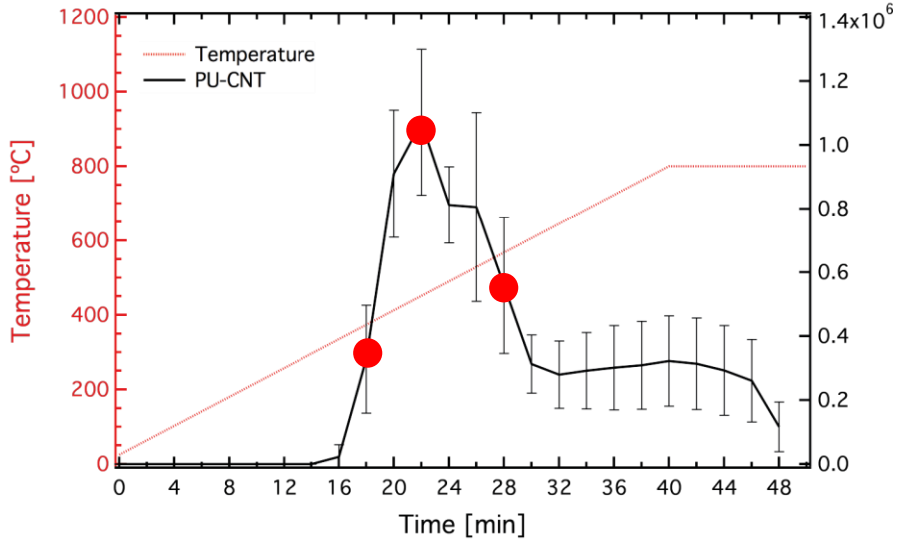

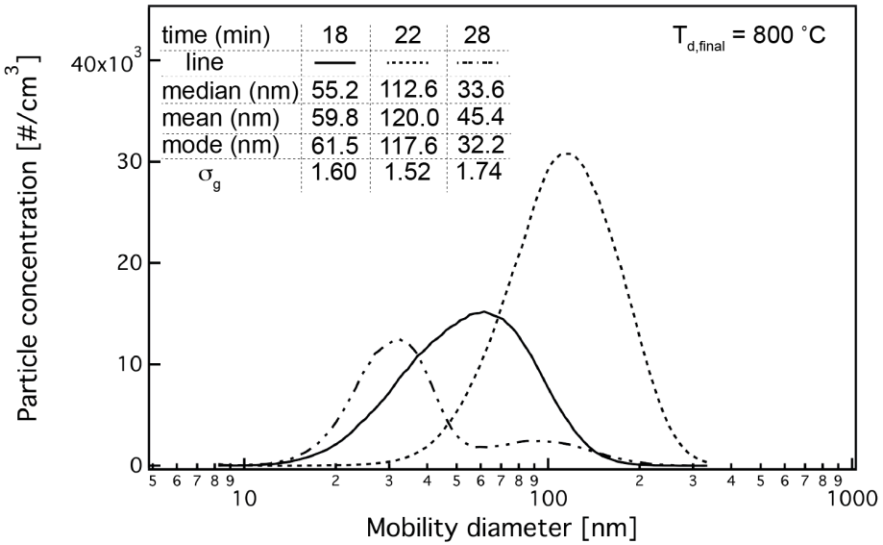

- route 1 (no treatment)

$T_{d,final}$: final thermal decomposition temperature

NANOTOX 2012

G.A. Sotiriou, E. Diaz, M. S. Long, J. Godleski, J. Brain, S.E. Pratsinis, P. Demokritou, "A Novel Platform for Pulmonary and Cardiovascular Toxicological Characterization of Inhaled Engineered Nanomaterials", *Nanotoxicology* **6**, 680-690 (2012).

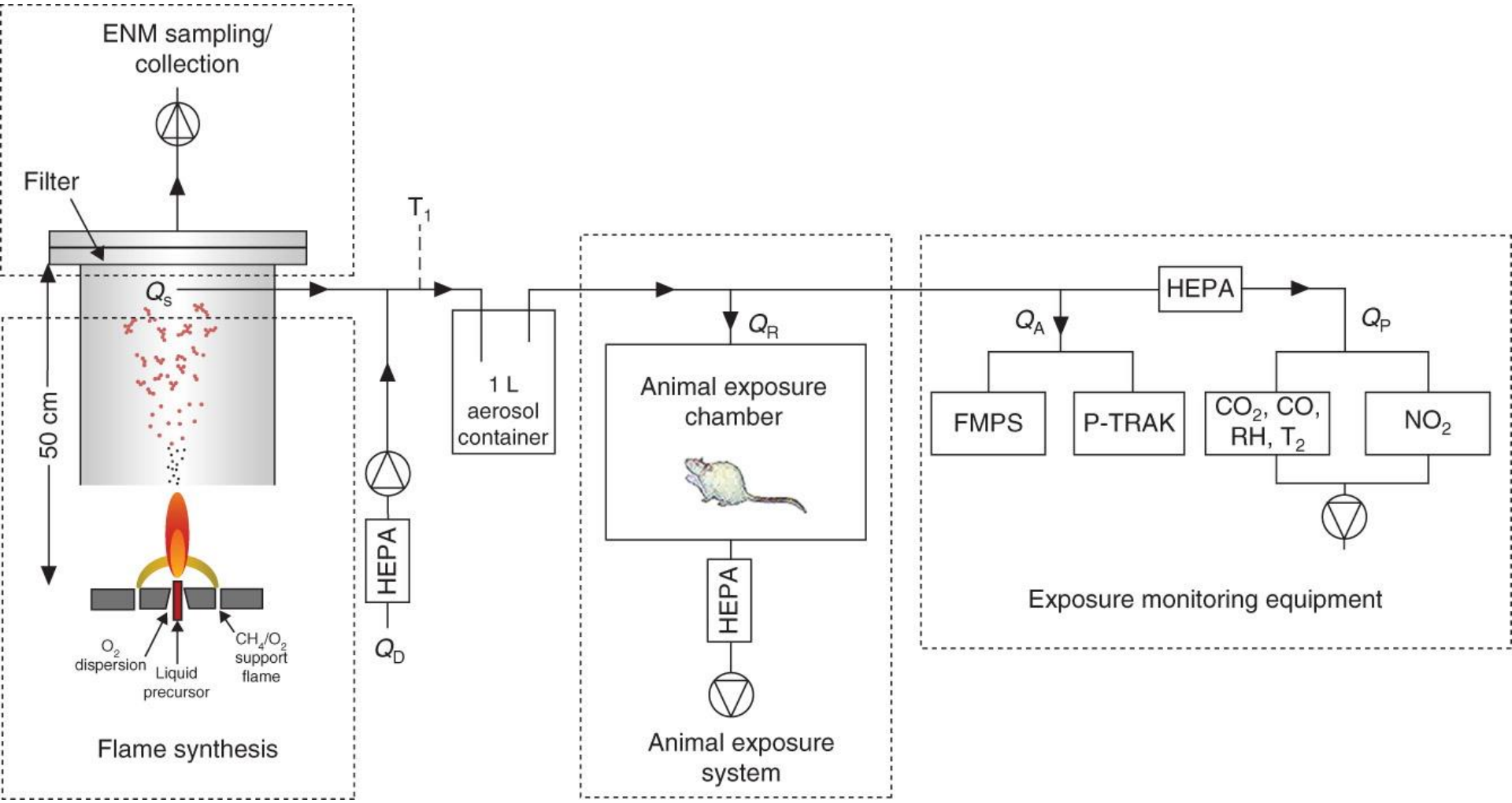
ENM sampling/
collection
Filter
Q_S
50 cm
O_2
dispersion
Liquid
precursor
CH_4/O_2
support
flame
Flame synthesis
T_1
HEPA
Q_D
1 L
aerosol
container
Q_R
Animal exposure
chamber
HEPA
Animal exposure
system
HEPA
Q_A
Q_P
FMPS
P-TRAK
CO_2, CO,
RH, T_2
NO_2
Exposure monitoring equipment

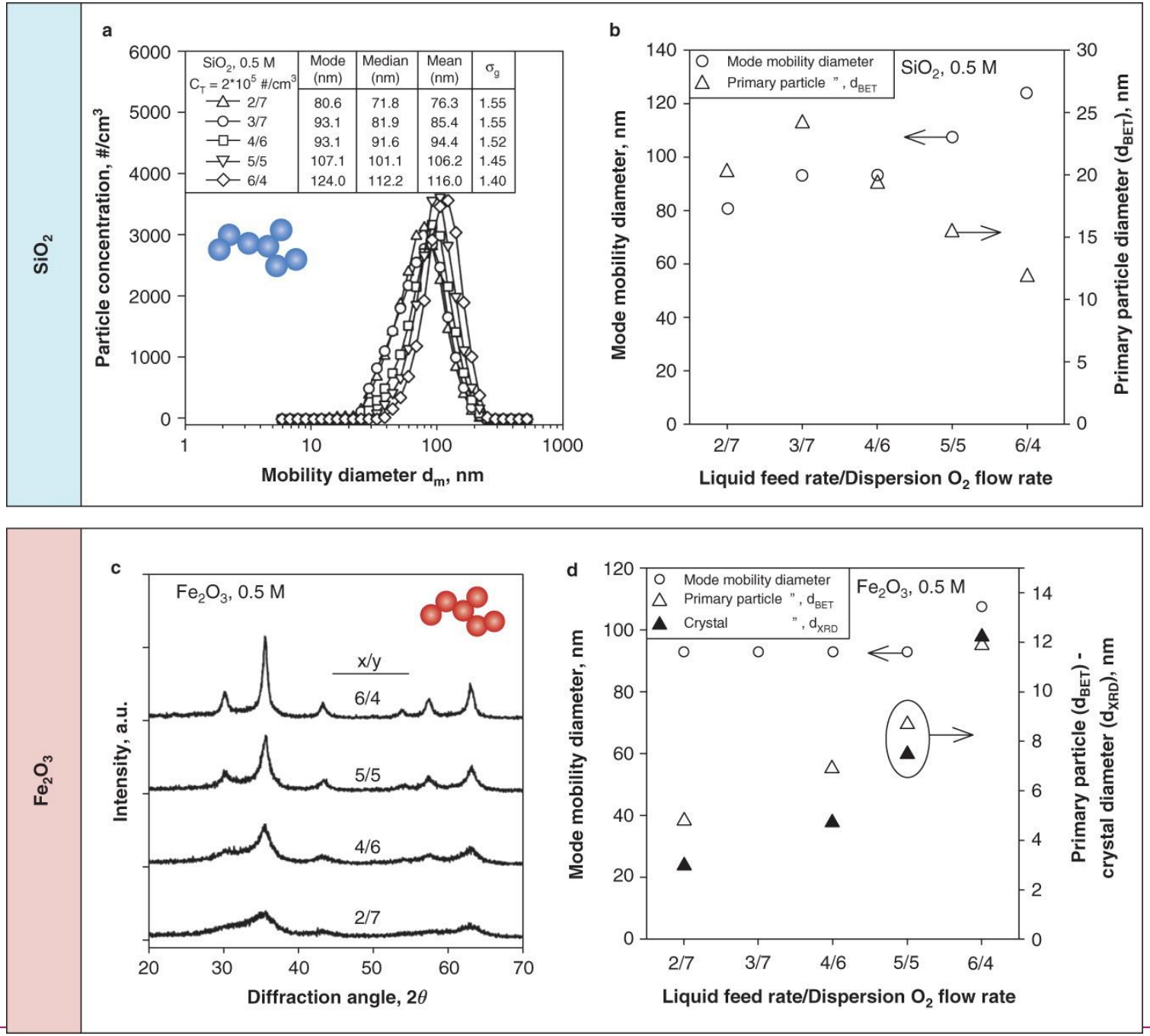
SiO2
a
SiO2, 0.5 M
CT = 2*10^5 #/cm^3
Mode (nm)
Median (nm)
Mean (nm)
σg
2/7 80.6 71.8 76.3 1.55
3/7 93.1 81.9 85.4 1.55
4/6 93.1 91.6 94.4 1.52
5/5 107.1 101.1 106.2 1.45
6/4 124.0 112.2 116.0 1.40
Particle concentration, #/cm3
Mobility diameter dm, nm
b
Mode mobility diameter
Primary particle ", dBET
SiO2, 0.5 M
Mode mobility diameter, nm
Primary particle diameter (dBET), nm
Liquid feed rate/Dispersion O2 flow rate
Fe2O3
c
Fe2O3, 0.5 M
x/y
6/4
5/5
4/6
2/7
Intensity, a.u.
Diffraction angle, 2θ
d
Mode mobility diameter
Primary particle ", dBET
Crystal ", dXRD
Fe2O3, 0.5 M
Mode mobility diameter, nm
Primary particle (dBET) - crystal diameter (dXRD), nm
Liquid feed rate/Dispersion O2 flow rate

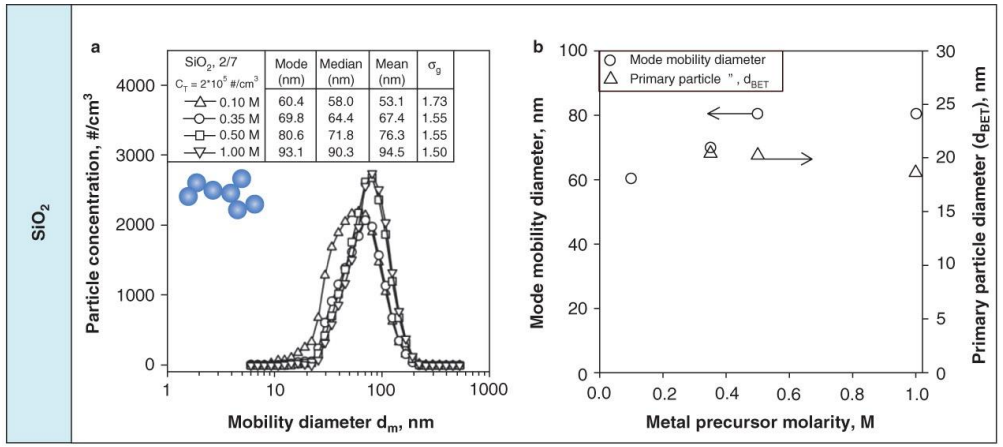
SiO2
a
SiO2, 2/7
CT = 2*10^5 #/cm^3
Mode (nm)
Median (nm)
Mean (nm)
σg
0.10 M 60.4 58.0 53.1 1.73
0.35 M 69.8 64.4 67.4 1.55
0.50 M 80.6 71.8 76.3 1.55
1.00 M 93.1 90.3 94.5 1.50
Particle concentration, #/cm3
Mobility diameter dm, nm
b
Mode mobility diameter
Primary particle ", dBET
Mode mobility diameter, nm
Primary particle diameter (dBET), nm
Metal precursor molarity, M

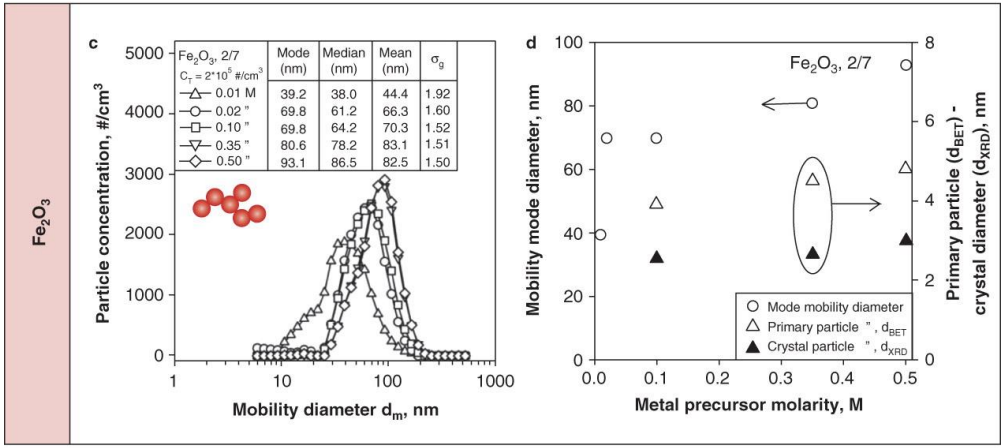
Fe2O3
c
Fe2O3, 2/7
CT = 2*10^5 #/cm^3
Mode (nm)
Median (nm)
Mean (nm)
σg
0.01 M 39.2 38.0 44.4 1.92
0.02 " 69.8 61.2 66.3 1.60
0.10 " 69.8 64.2 70.3 1.52
0.35 " 80.6 78.2 83.1 1.51
0.50 " 93.1 86.5 82.5 1.50
Particle concentration, #/cm3
Mobility diameter dm, nm
d
Fe2O3, 2/7
Mode mobility diameter
Primary particle ", dBET
Crystal particle ", dXRD
Mobility mode diameter, nm
Primary particle (dBET) - crystal diameter (dXRD), nm
Metal precursor molarity, M

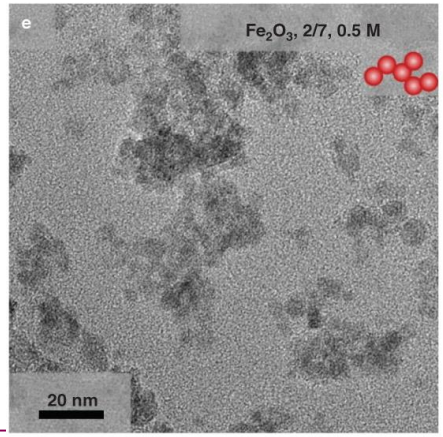
e
Fe2O3, 2/7, 0.5 M
20 nm

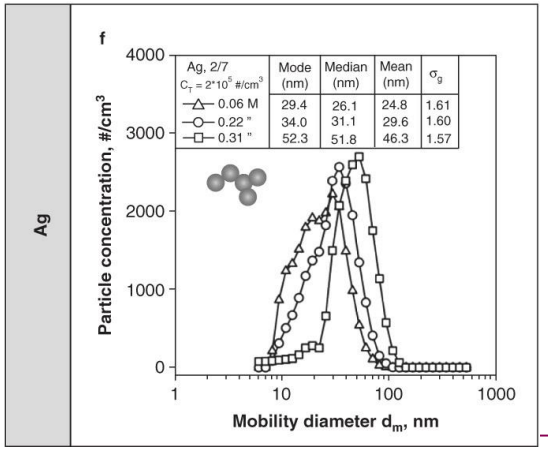
Ag
f
Ag, 2/7
CT = 2*10^5 #/cm^3
Mode (nm)
Median (nm)
Mean (nm)
σg
0.06 M 29.4 26.1 24.8 1.61
0.22 " 34.0 31.1 29.6 1.60
0.31 " 52.3 51.8 46.3 1.57
Particle concentration, #/cm3
Mobility diameter dm, nm

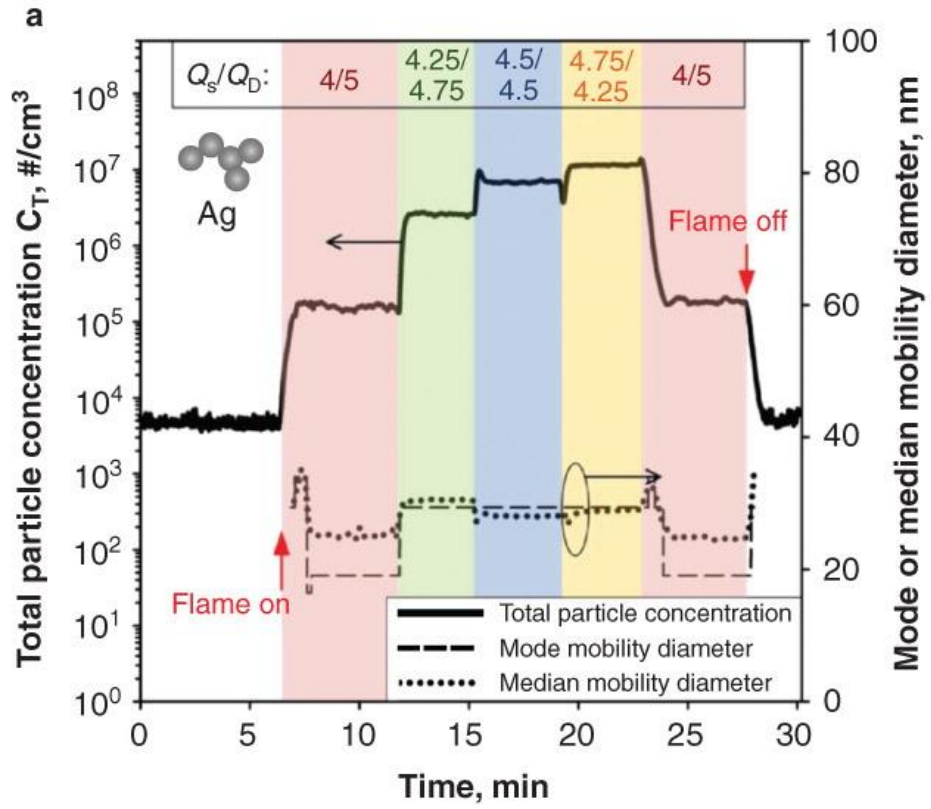
a
Q_s/Q_D:
4/5
4.25/ 4.75
4.5/ 4.5
4.75/ 4.25
4/5
Ag
Flame on
Flame off
Total particle concentration
Mode mobility diameter
Median mobility diameter
Total particle concentration C_T, #/cm^3
Mode or median mobility diameter, nm
Time, min

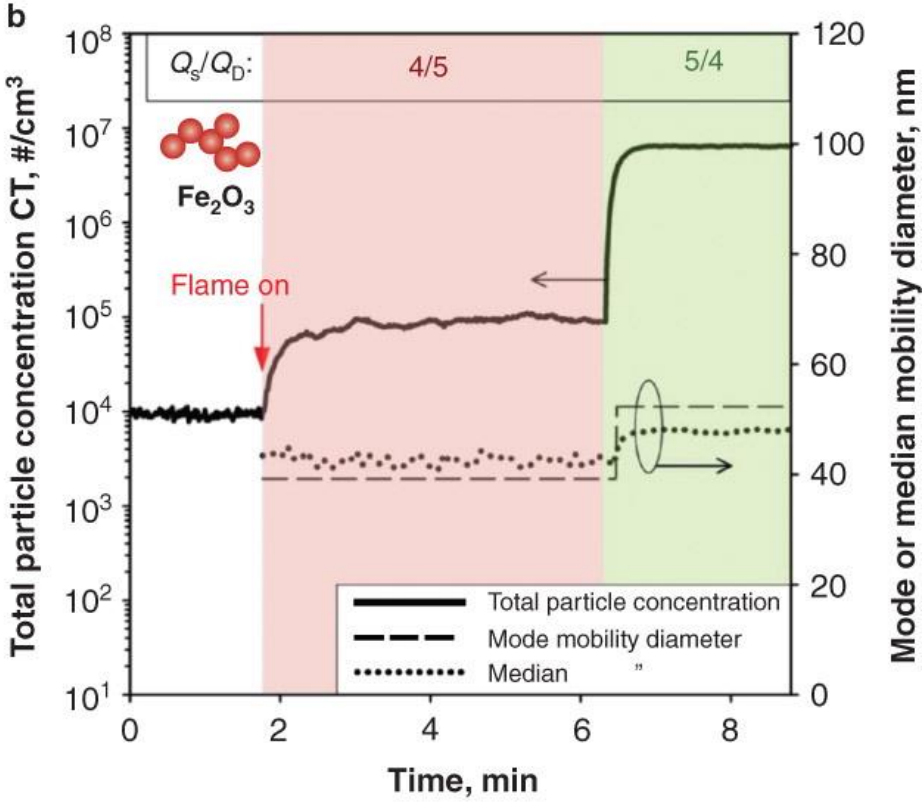
b
Q_s/Q_D:
4/5
5/4
Fe_2O_3
Flame on
Total particle concentration
Mode mobility diameter
Median
Total particle concentration CT, #/cm^3
Mode or median mobility diameter, nm
Time, min

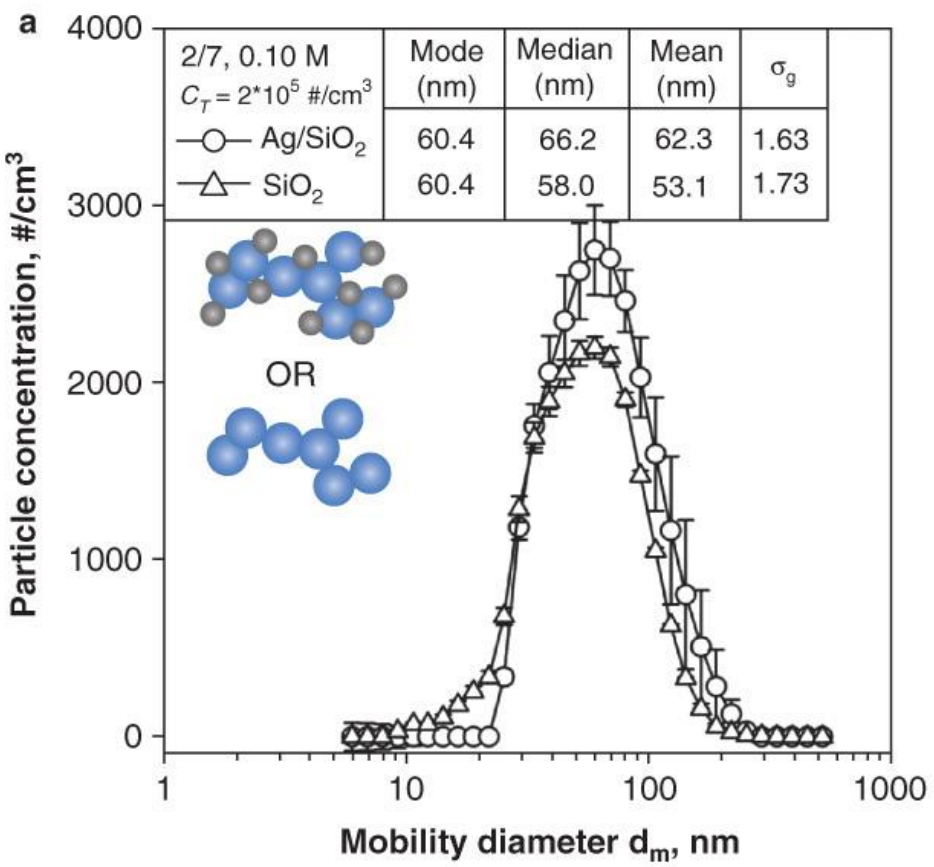
a
2/7, 0.10 M
C_T = 2*10^5 #/cm^3
Ag/SiO$_2$
SiO$_2$
Mode (nm)
Median (nm)
Mean (nm)
σ_g
60.4
66.2
62.3
1.63
60.4
58.0
53.1
1.73
OR
Particle concentration, #/cm^3
Mobility diameter d$_m$, nm
4000
3000
2000
1000
0
1
10
100
1000

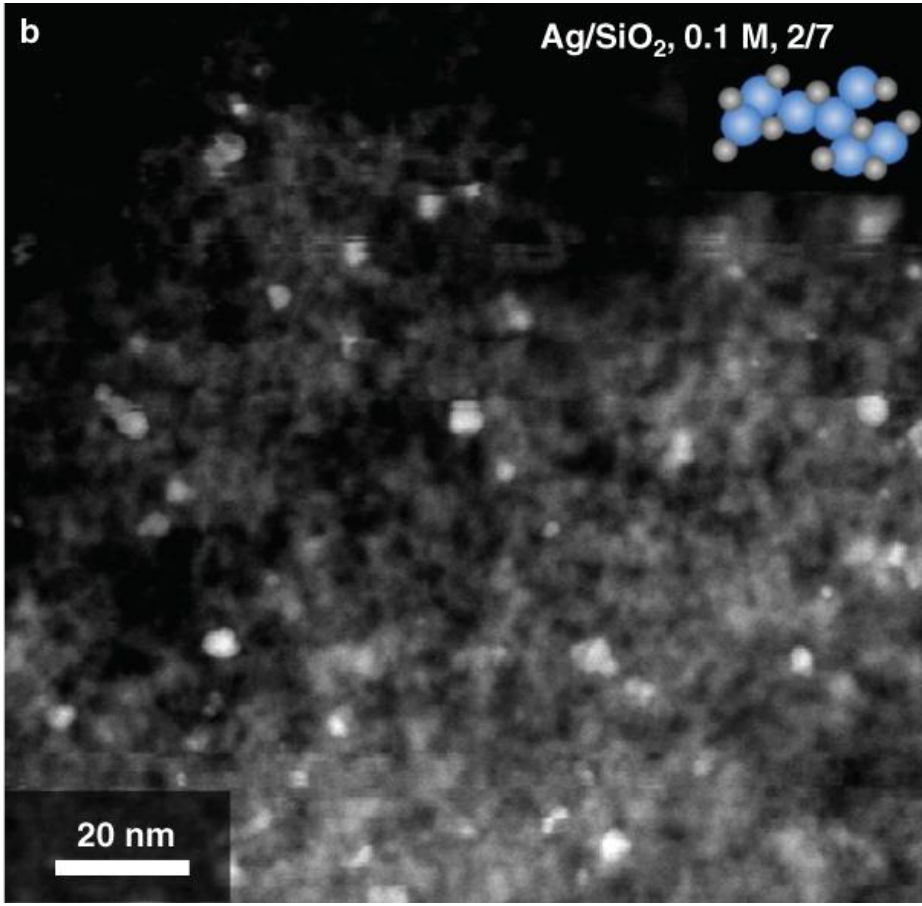
b
Ag/SiO$_2$, 0.1 M, 2/7
20 nm

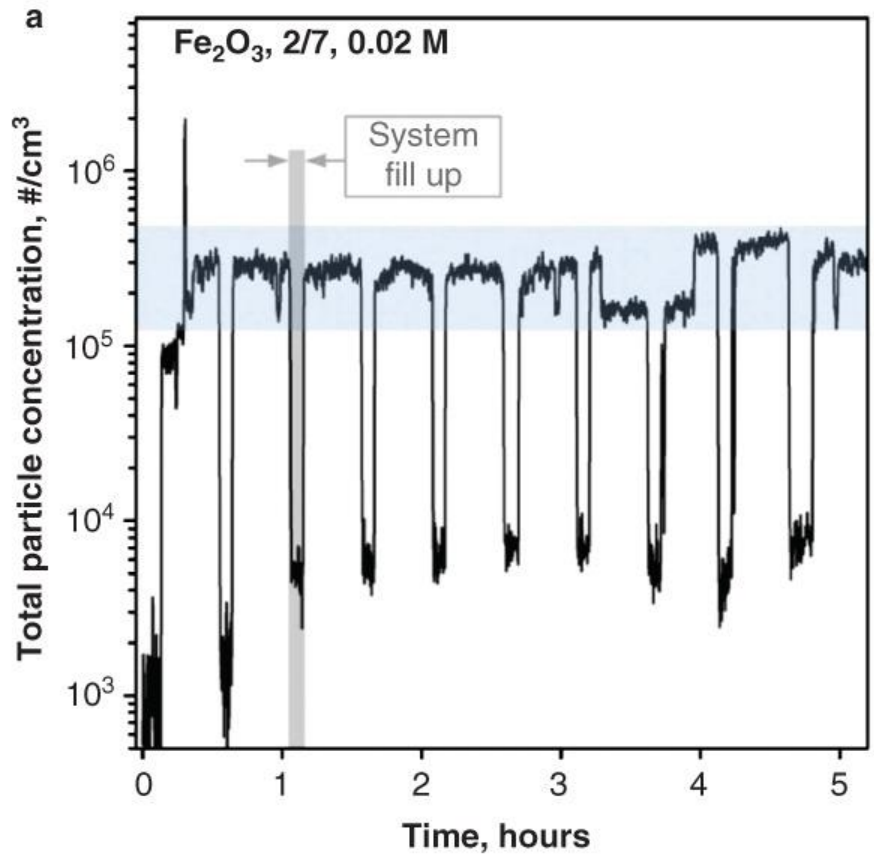
a
Fe_2O_3, 2/7, 0.02 M
System fill up
Total particle concentration, #/cm³
10^6
10^5
10^4
10^3
0
1
2
3
4
5
Time, hours

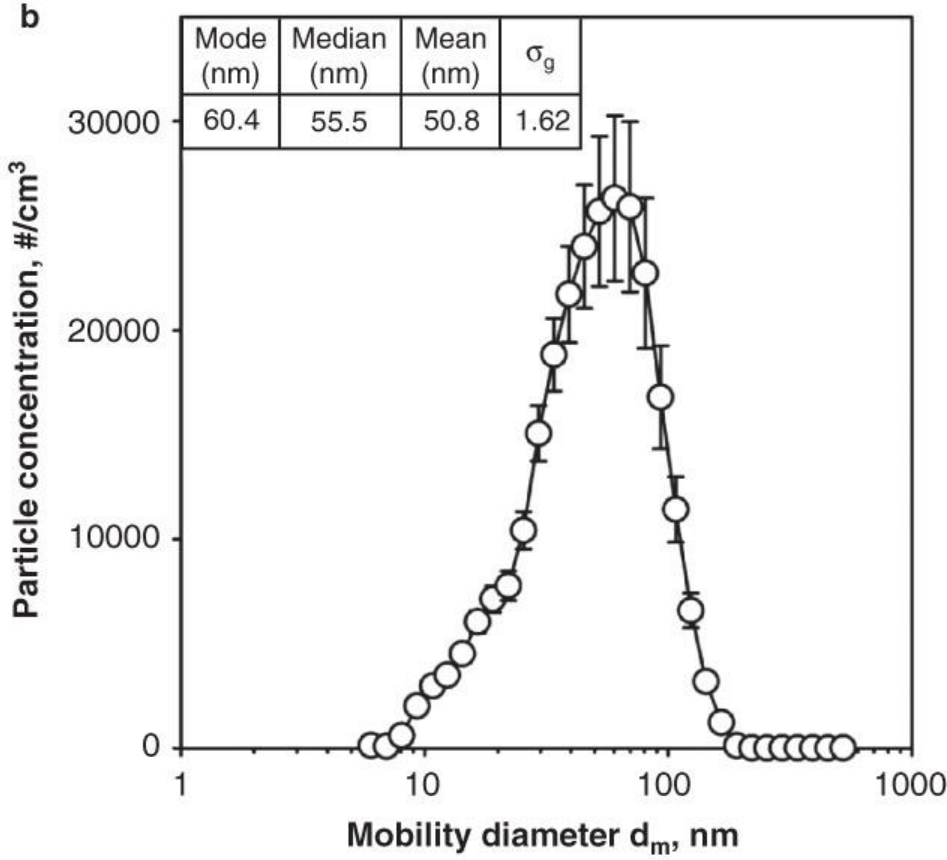
b
Mode (nm)
Median (nm)
Mean (nm)
σ_g
60.4
55.5
50.8
1.62
Particle concentration, #/cm³
30000
20000
10000
0
1
10
100
1000
Mobility diameter d_m, nm

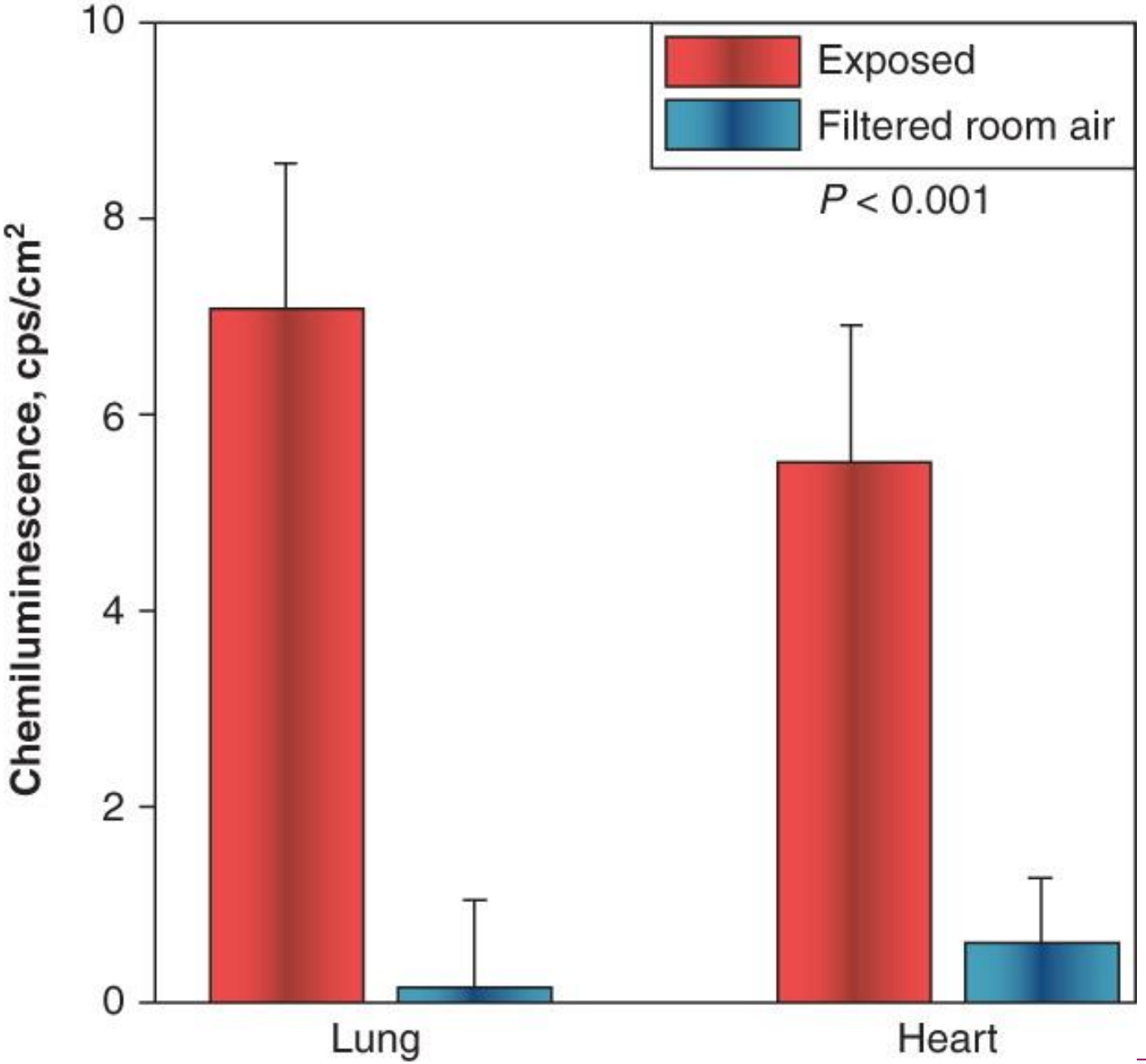
10
8
6
4
2
0
Chemiluminescence, cps/cm²
Exposed
Filtered room air
P < 0.001
Lung
Heart

SMALL 2013

A. Pratsinis, P. Hervella, J-C. Leroux, S.E. Pratsinis, **G.A. Sotiriou**, "Toxicity of Silver Nanoparticles in Macrophages", *Small* **9**, 2576-2584 (2013).

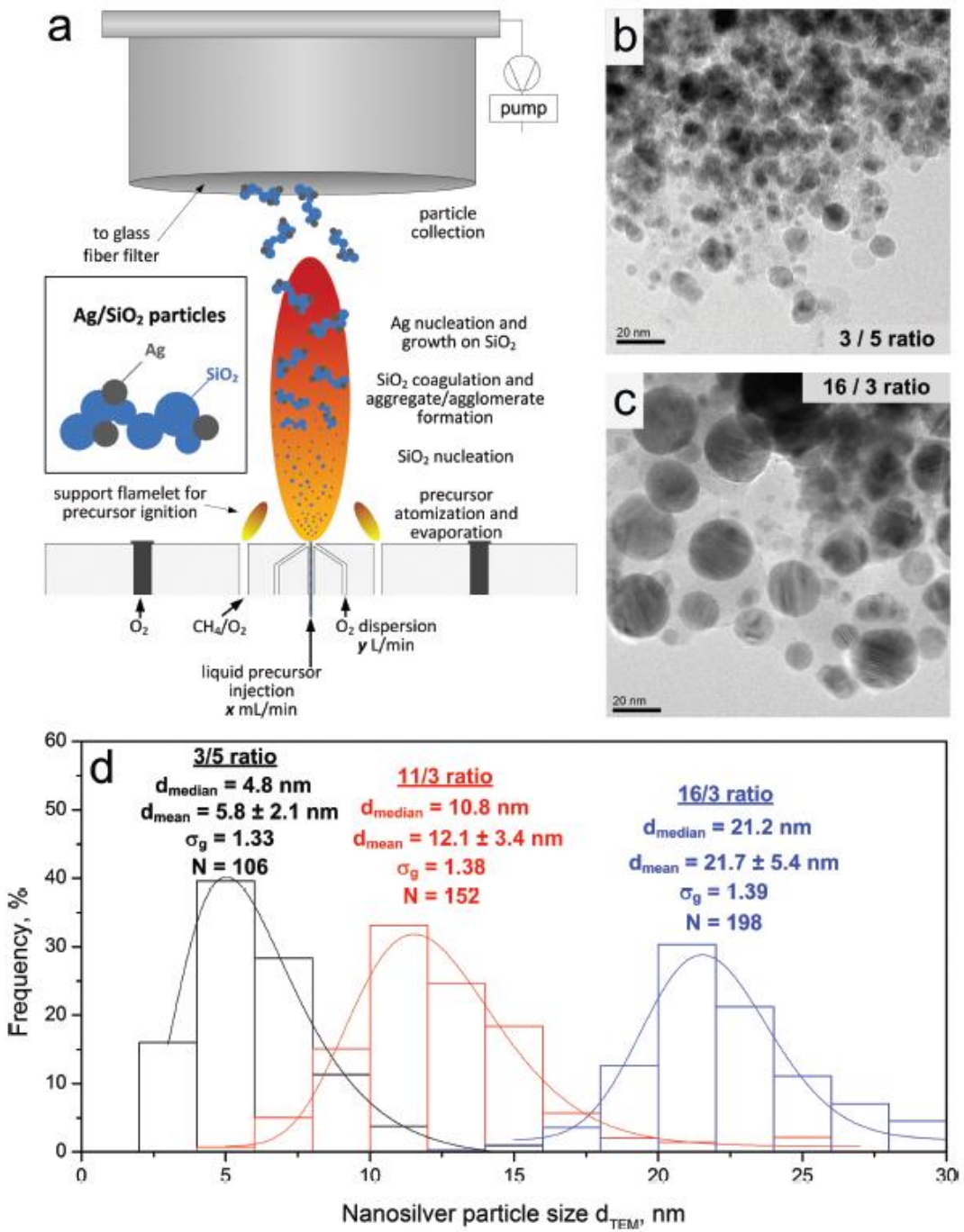
a
pump
to glass fiber filter
particle collection
Ag/SiO2 particles
Ag
SiO2
Ag nucleation and growth on SiO2
SiO2 coagulation and aggregate/agglomerate formation
SiO2 nucleation
support flamelet for precursor ignition
precursor atomization and evaporation
O2
CH4/O2
O2 dispersion y L/min
liquid precursor injection x mL/min
b
20 nm
3 / 5 ratio
c
16 / 3 ratio
20 nm
d
3/5 ratio
dmedian = 4.8 nm
dmean = 5.8 ± 2.1 nm
σg = 1.33
N = 106
11/3 ratio
dmedian = 10.8 nm
dmean = 12.1 ± 3.4 nm
σg = 1.38
N = 152
16/3 ratio
dmedian = 21.2 nm
dmean = 21.7 ± 5.4 nm
σg = 1.39
N = 198
Frequency, %
Nanosilver particle size dTEM, nm

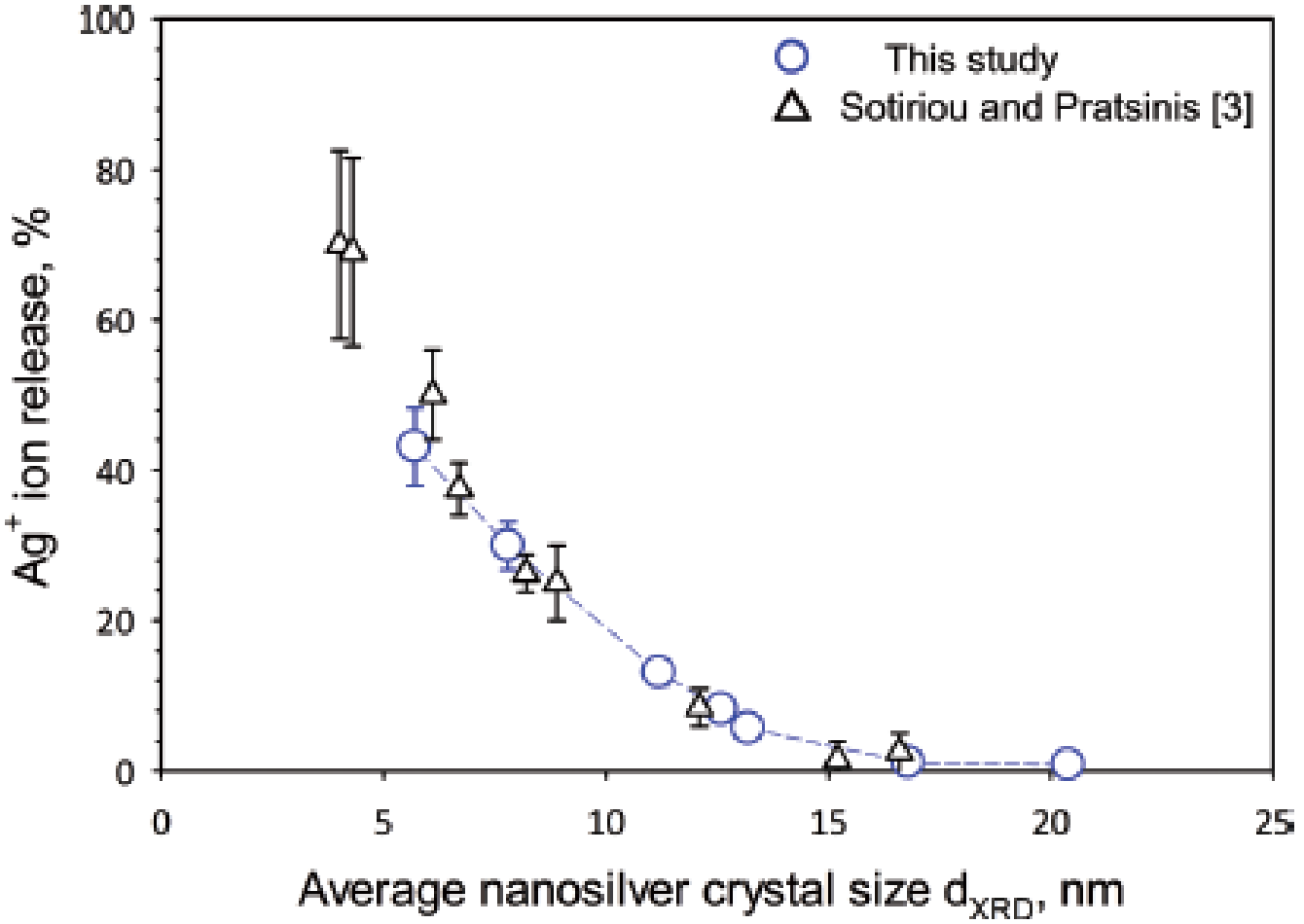

[3] Sotiriou, Pratsinis, *Environ. Sci. Technol.* **44**, 5649 (2010).

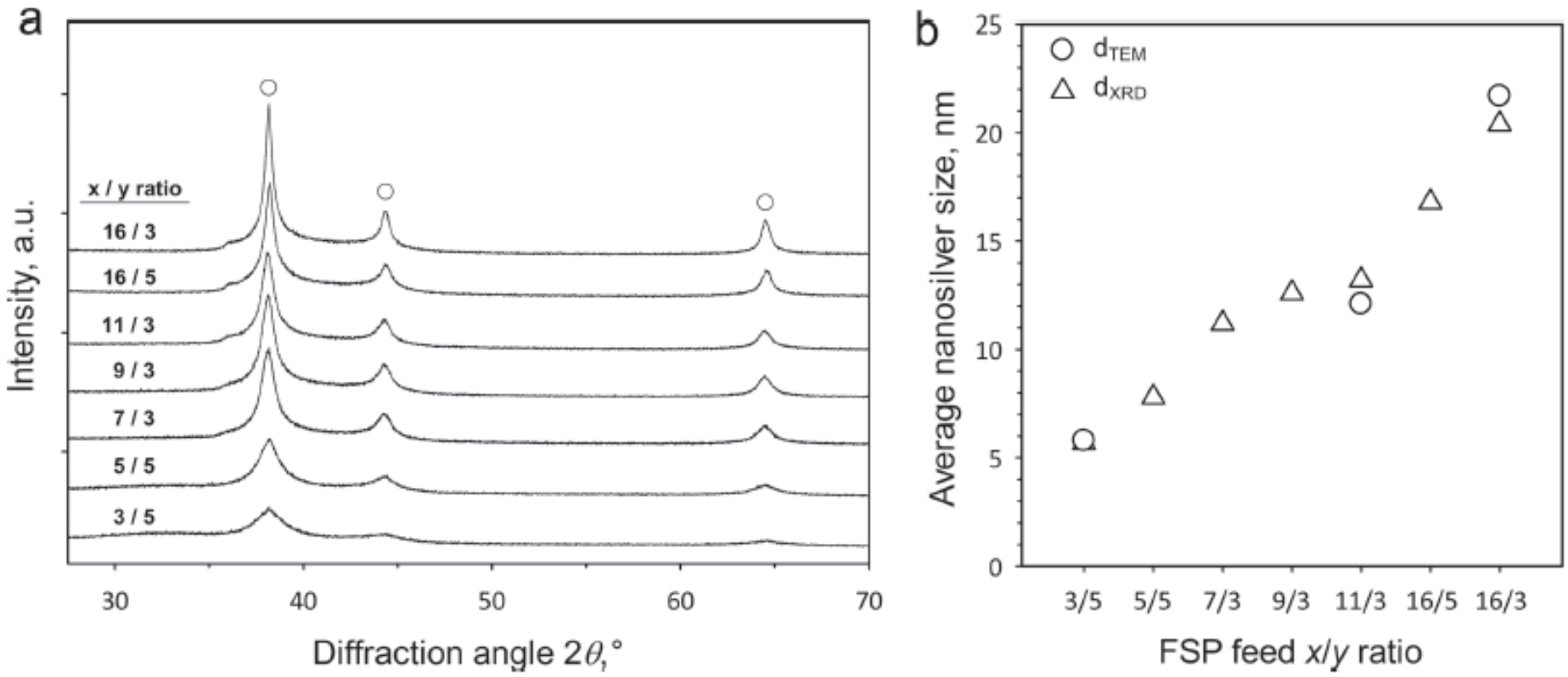
a
Intensity, a.u.
x / y ratio
16 / 3
16 / 5
11 / 3
9 / 3
7 / 3
5 / 5
3 / 5
30
40
50
60
70
Diffraction angle 2θ, °
b
Average nanosilver size, nm
dTEM
dXRD
0
5
10
15
20
25
3/5
5/5
7/3
9/3
11/3
16/5
16/3
FSP feed x/y ratio

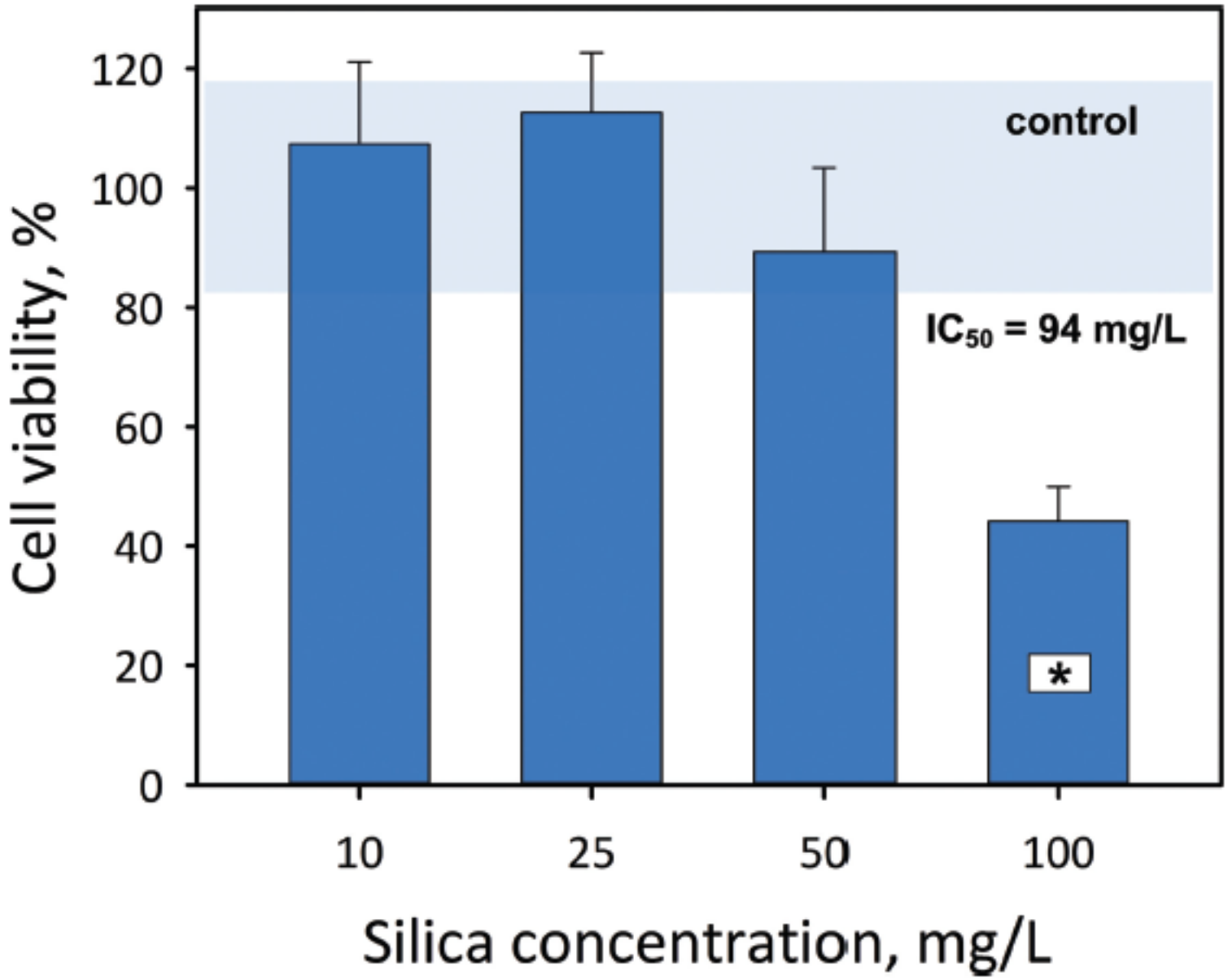
Cell viability, %
120
100
80
60
40
20
0
control
IC50 = 94 mg/L
*
10
25
50
100
Silica concentration, mg/L

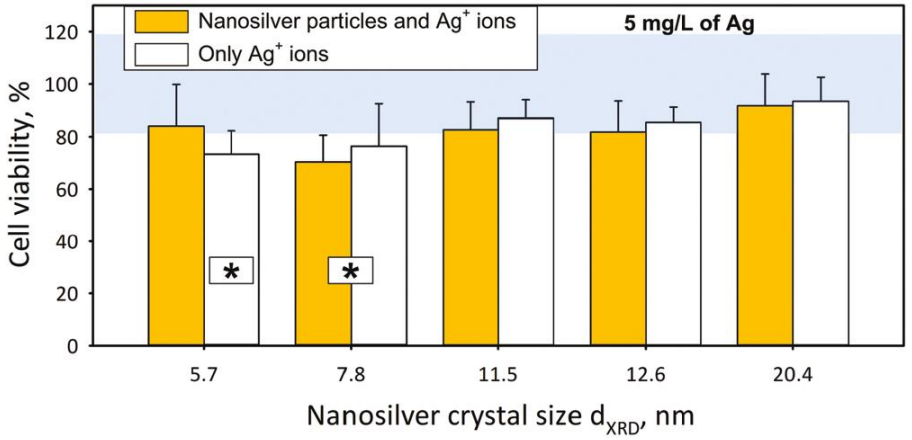
Nanosilver particles and Ag+ ions
Only Ag+ ions
5 mg/L of Ag
Cell viability, %
120
100
80
60
40
20
0
*
*
5.7
7.8
11.5
12.6
20.4
Nanosilver crystal size dXRD, nm

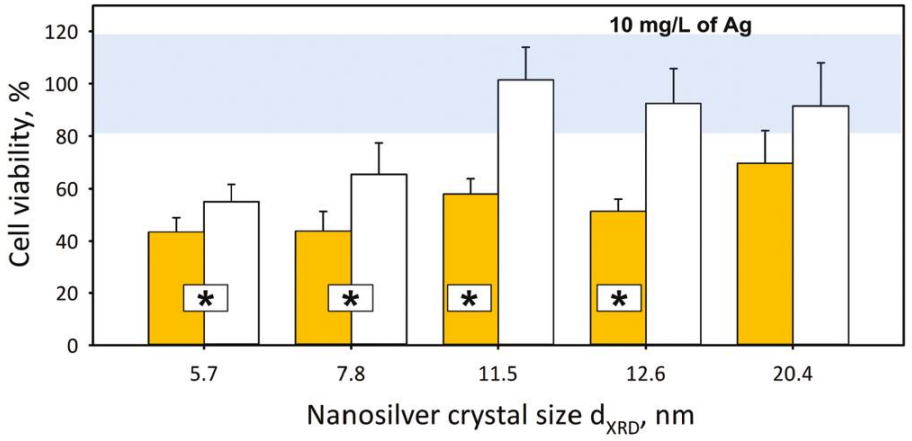
10 mg/L of Ag
Cell viability, %
120
100
80
60
40
20
0
*
*
*
*
5.7
7.8
11.5
12.6
20.4
Nanosilver crystal size dXRD, nm

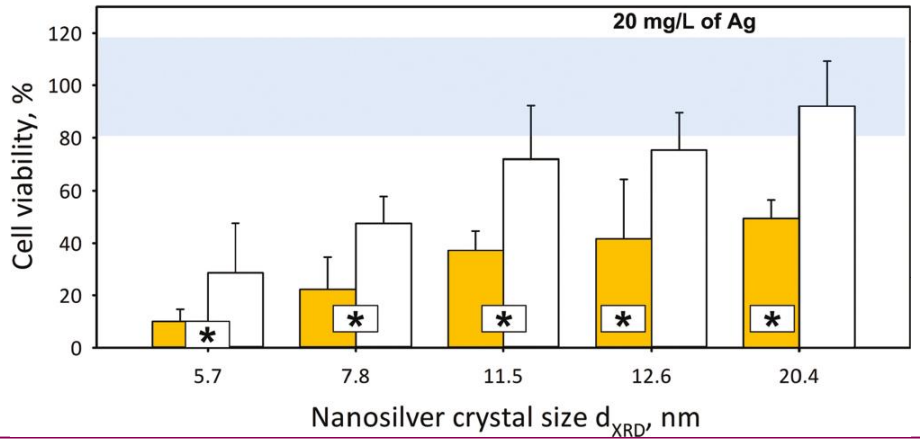
20 mg/L of Ag
Cell viability, %
120
100
80
60
40
20
0
*
*
*
*
*
5.7
7.8
11.5
12.6
20.4
Nanosilver crystal size dXRD, nm

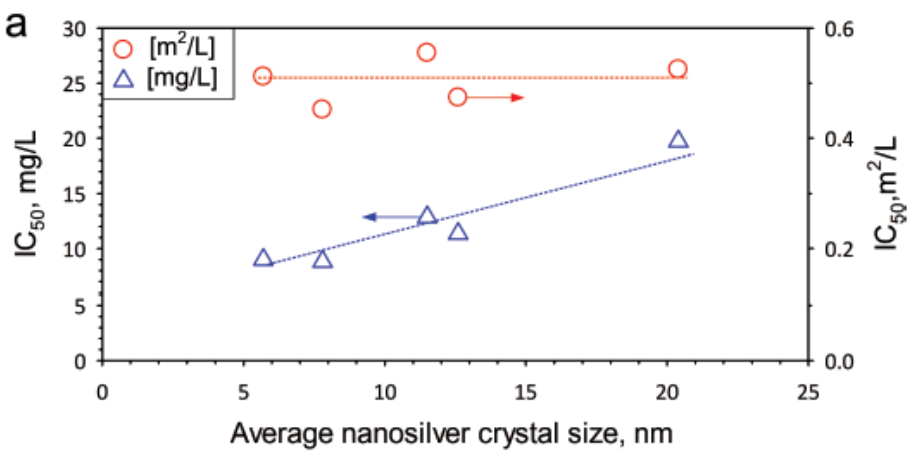
a
[m²/L]
[mg/L]
IC50, mg/L
IC50,m²/L
Average nanosilver crystal size, nm

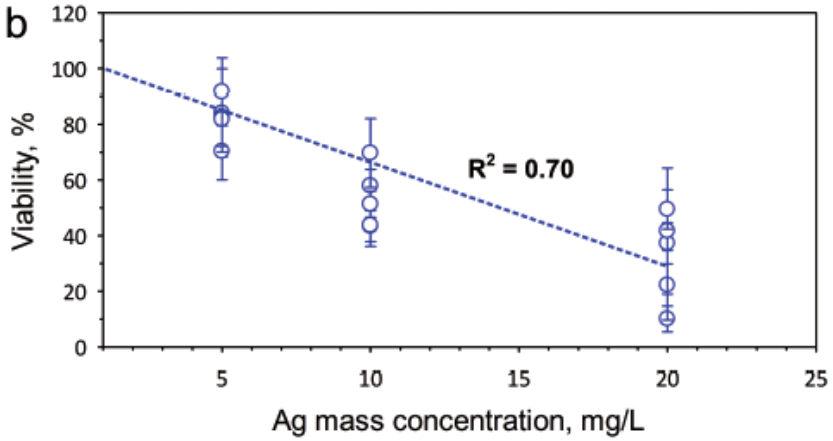
b
Viability, %
R² = 0.70
Ag mass concentration, mg/L

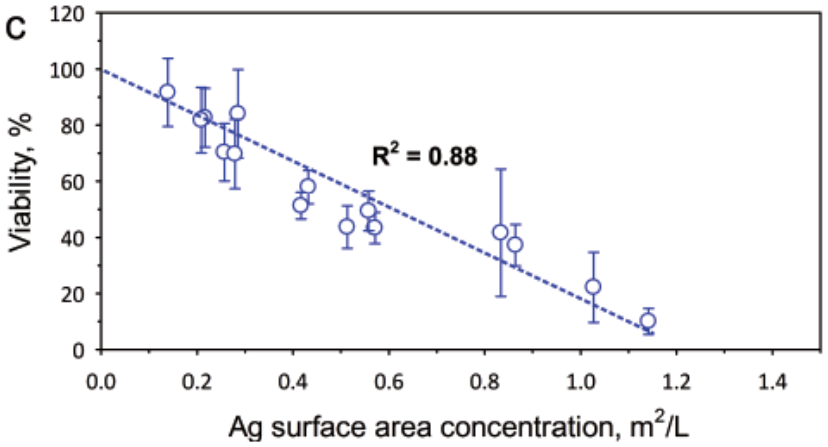
c
Viability, %
R² = 0.88
Ag surface area concentration, m²/L

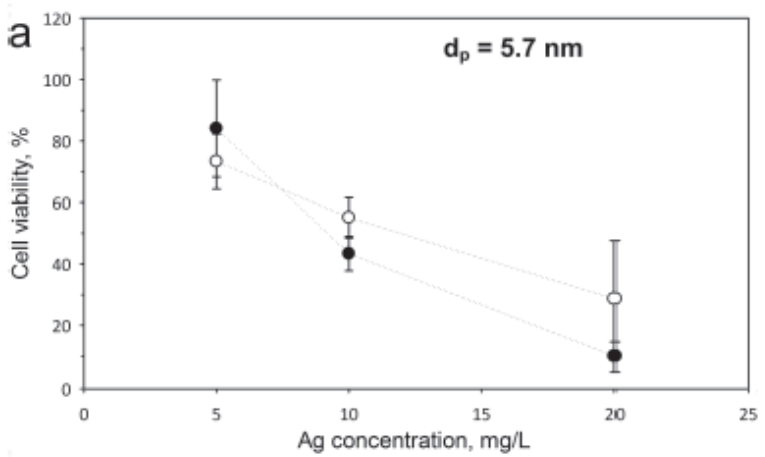
a
dp = 5.7 nm
Cell viability, %
Ag concentration, mg/L

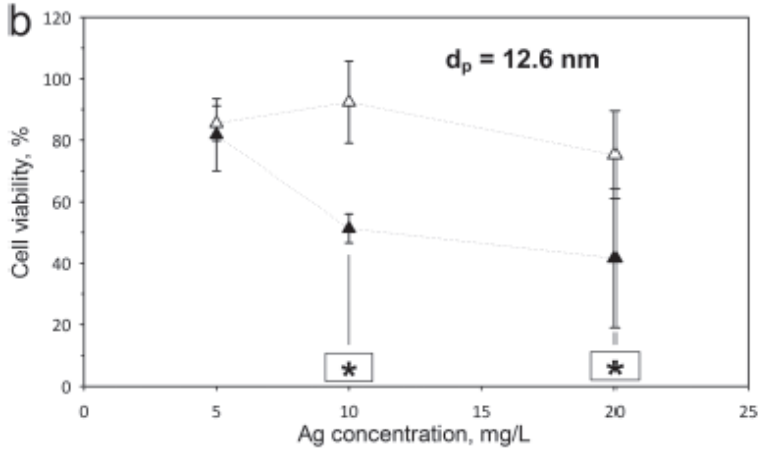
b
dp = 12.6 nm
Cell viability, %
Ag concentration, mg/L

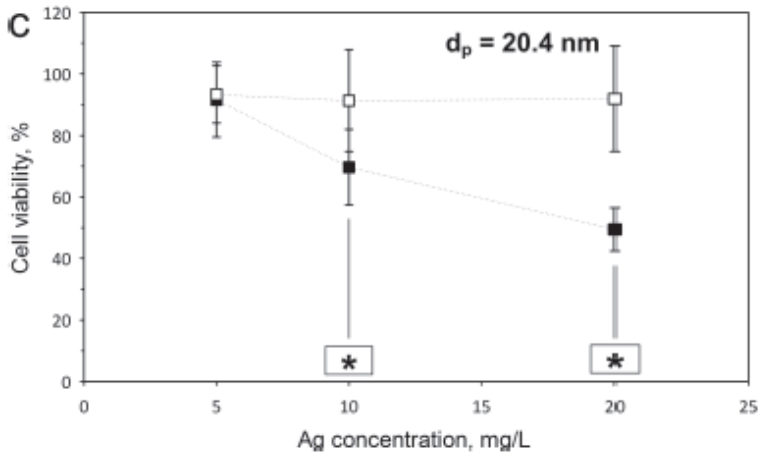
c
dp = 20.4 nm
Cell viability, %
Ag concentration, mg/L

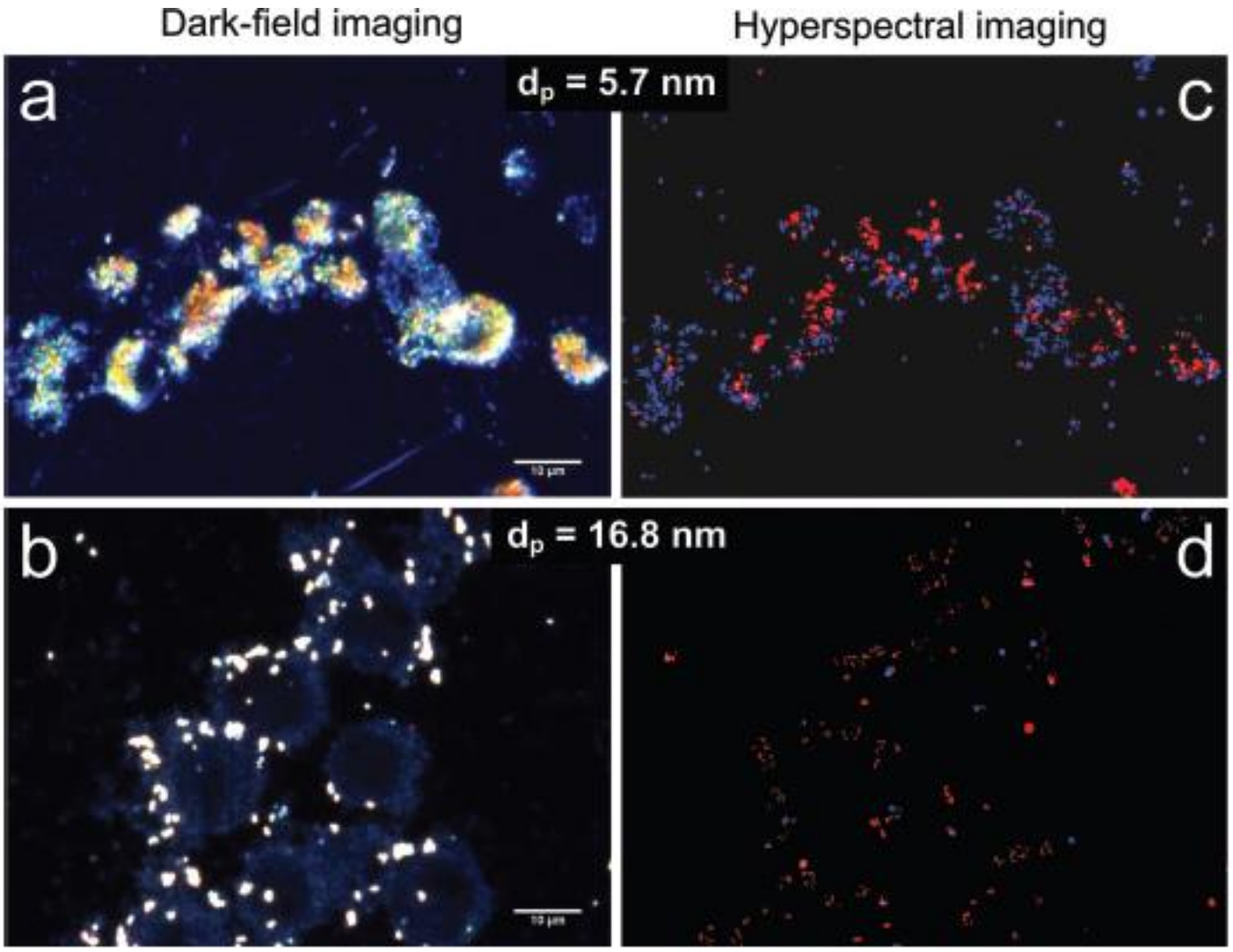
Dark-field imaging
Hyperspectral imaging
a
d_p = 5.7 nm
c
b
d_p = 16.8 nm
d

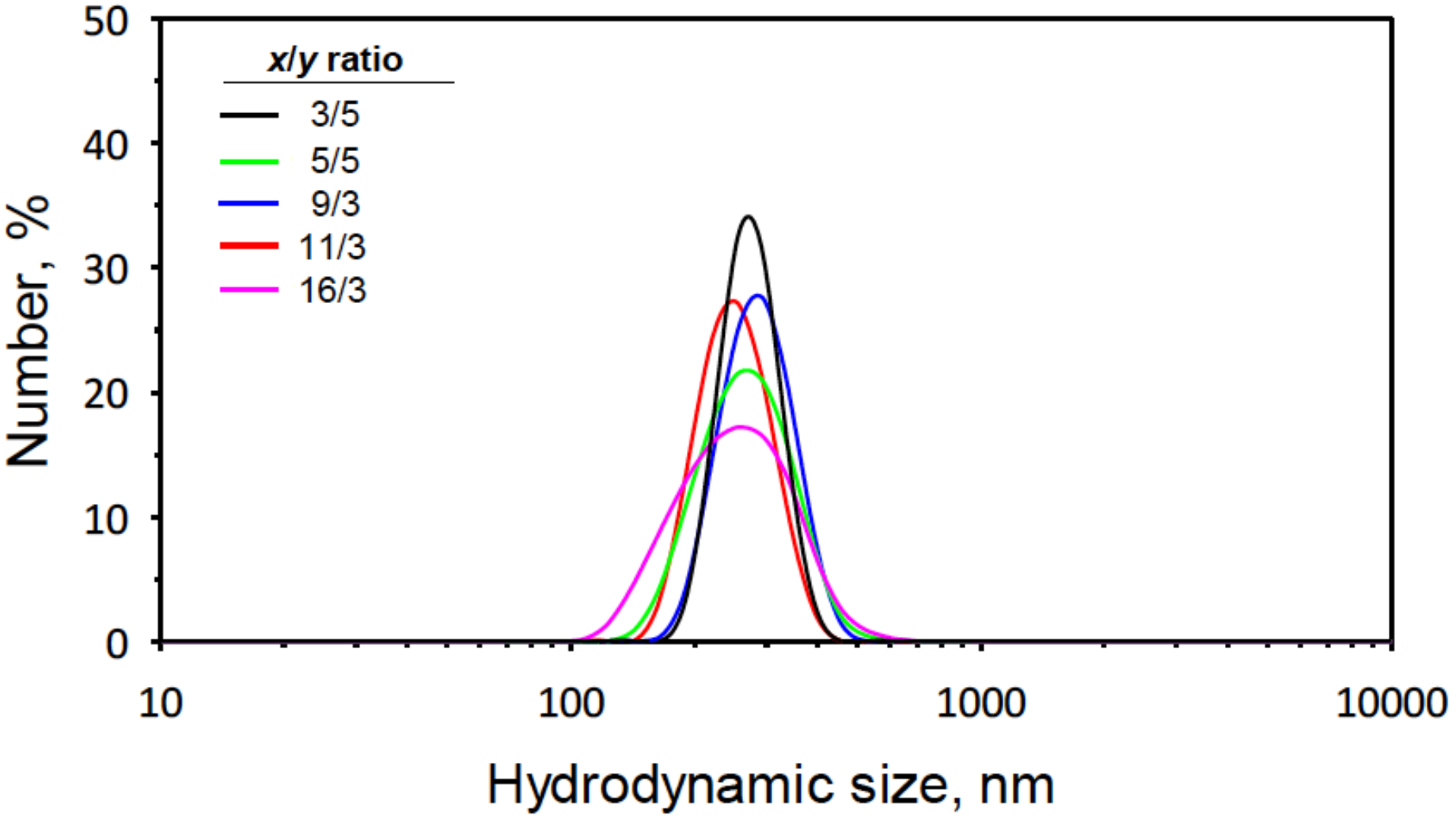
x/y ratio
3/5
5/5
9/3
11/3
16/3
Number, %
0
10
20
30
40
50
10
100
1000
10000
Hydrodynamic size, nm

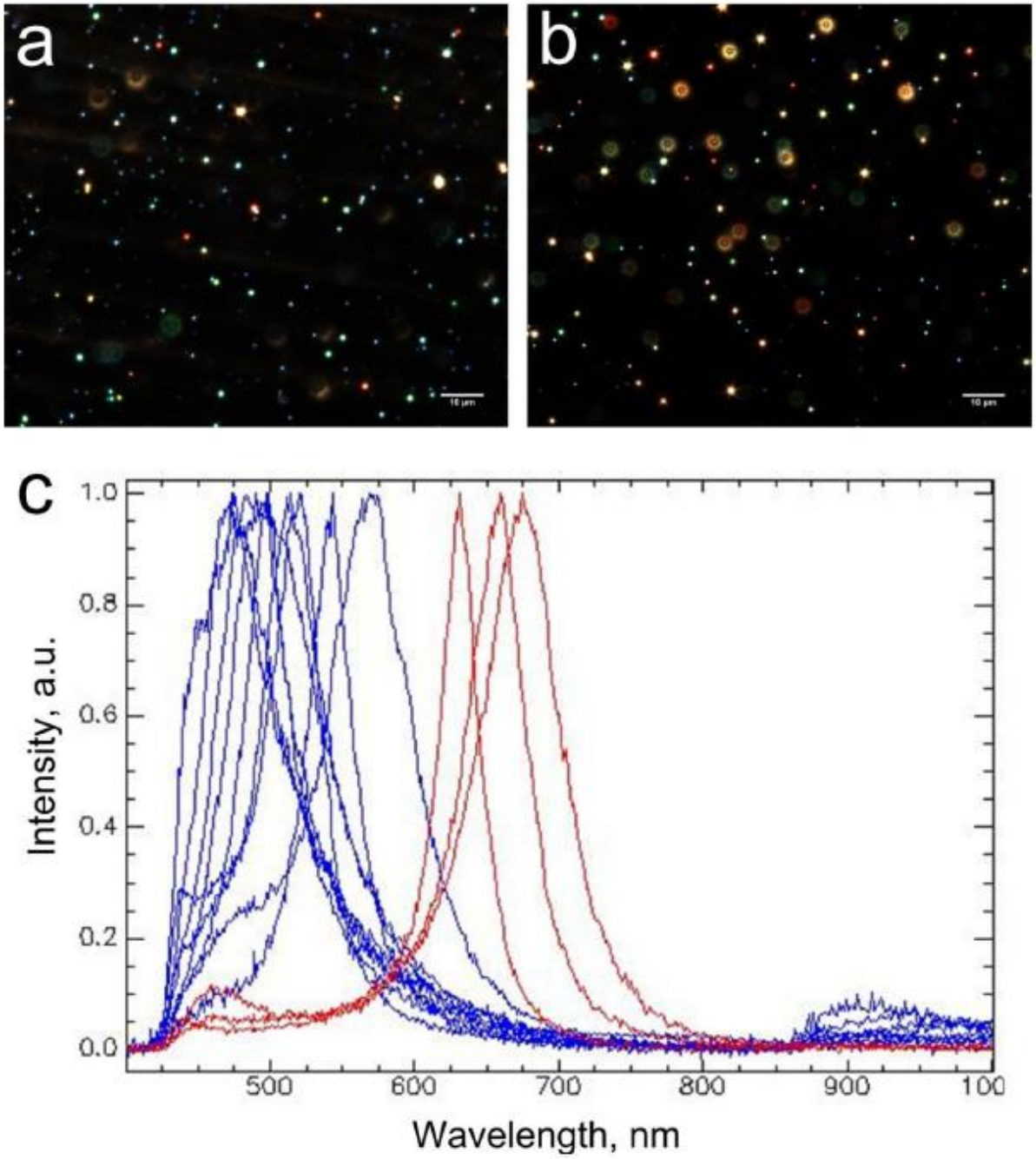
a
b
c
Intensity, a.u.
1.0
0.8
0.6
0.4
0.2
0.0
500
600
700
800
900
100
Wavelength, nm

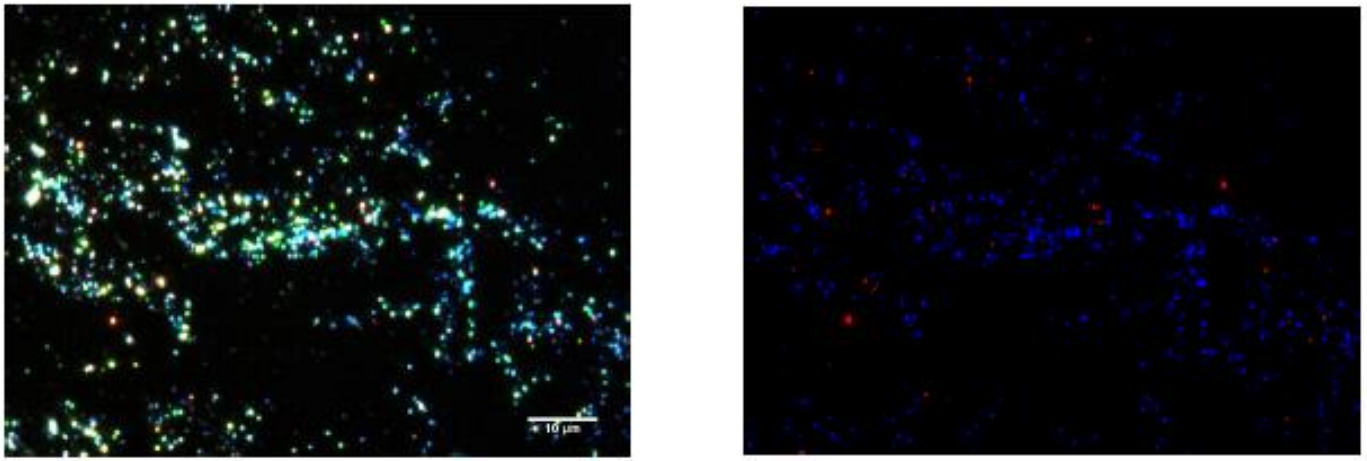

Figure S3. Dark-field images of 5.7 nm dispersed nanosilver in water and its corresponding hyperspectral image after the filtering of the acquired library.

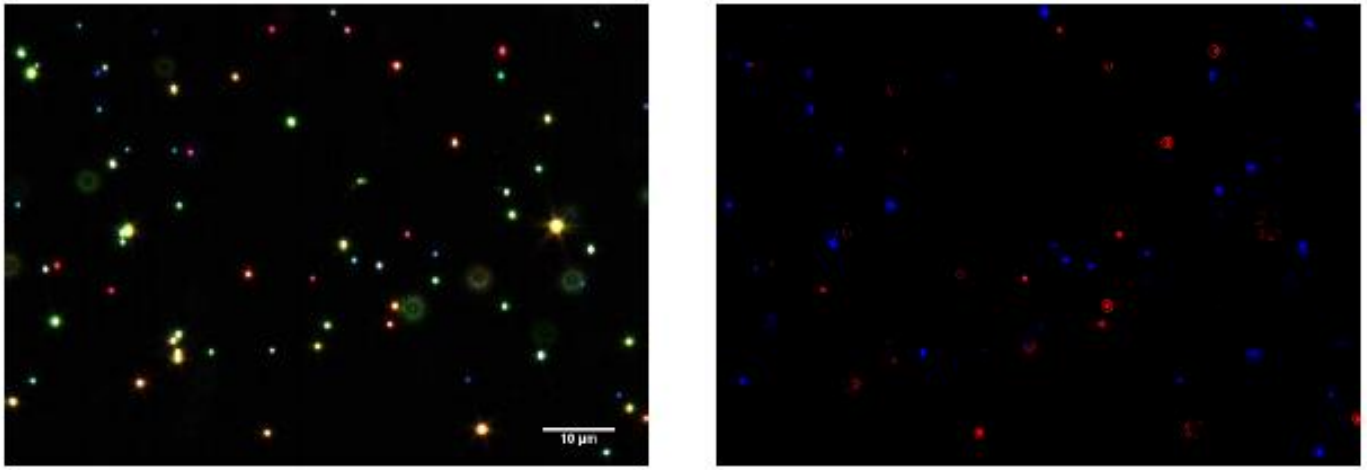

Figure S4. Dark-field images of 16.8 nm dispersed nanosilver in water and its corresponding hyperspectral image after the filtering of the acquired library.

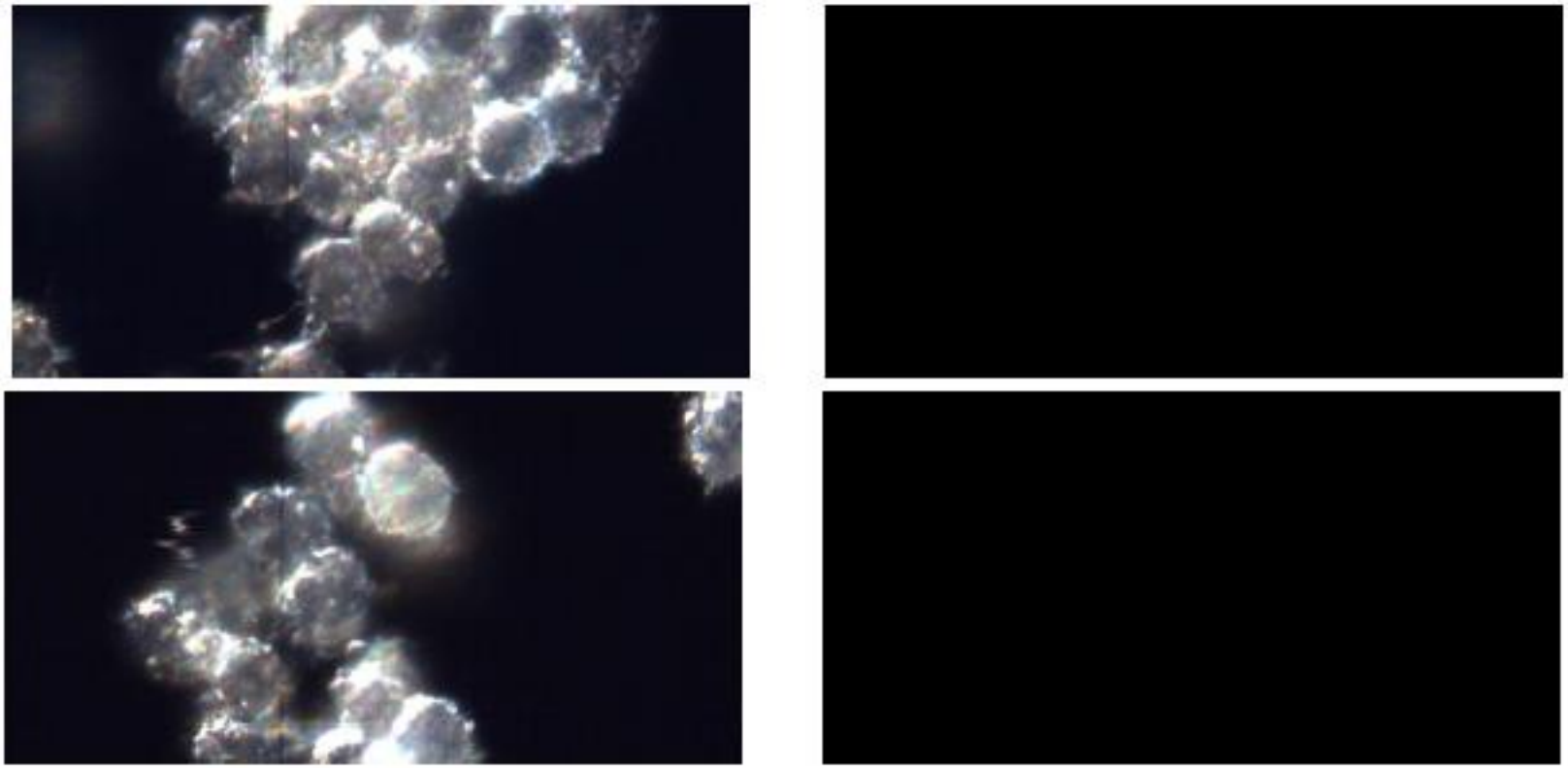

Figure S5. Dark-field images of the murine macrophages and the corresponding hyperspectral image after the filtering of the acquired library. No signal is detected, as expected, verifying that there is no nanosilver signal present.

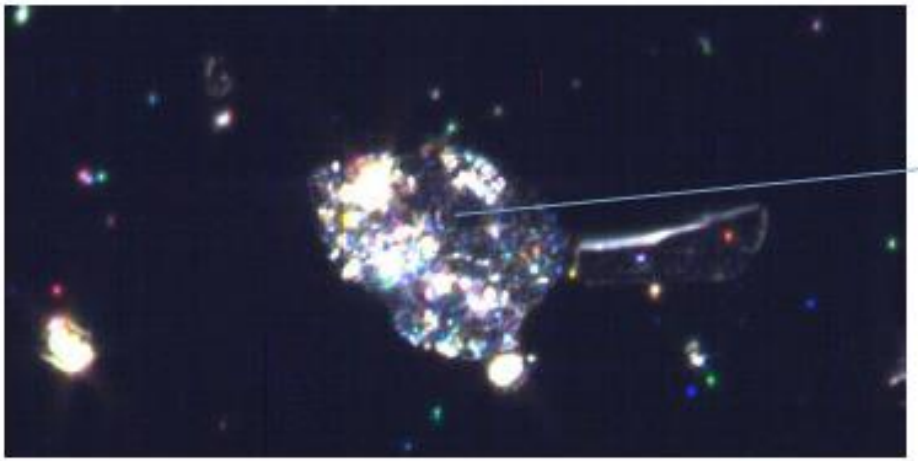

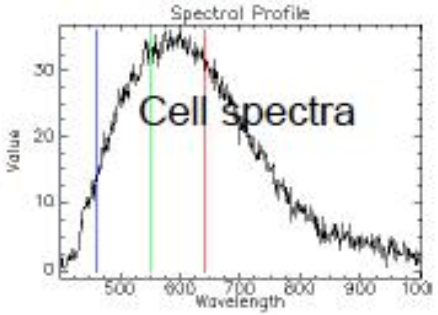

Blue particles:

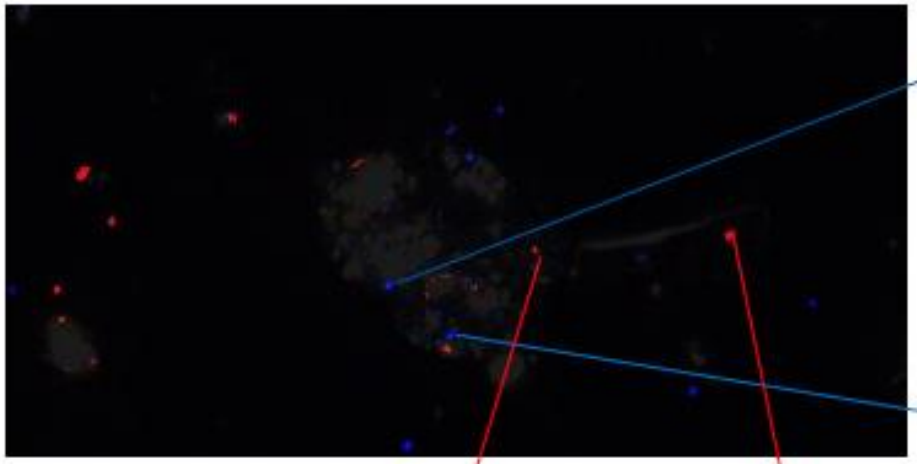

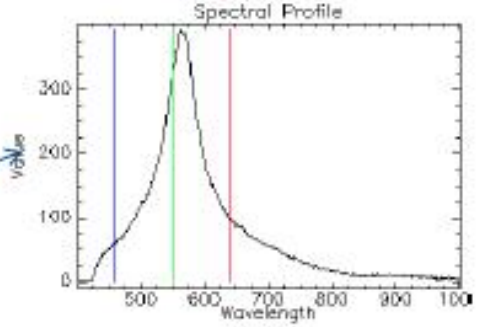

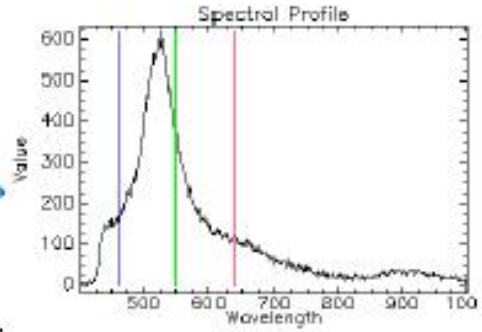

Red particles:

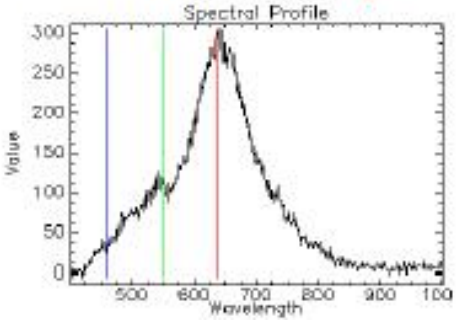

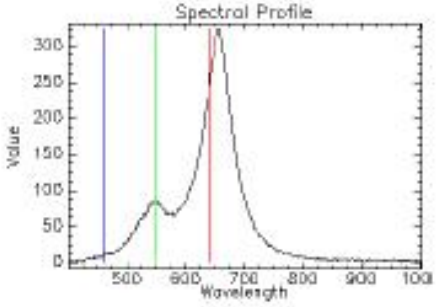

ACS SUST CHEM 2013

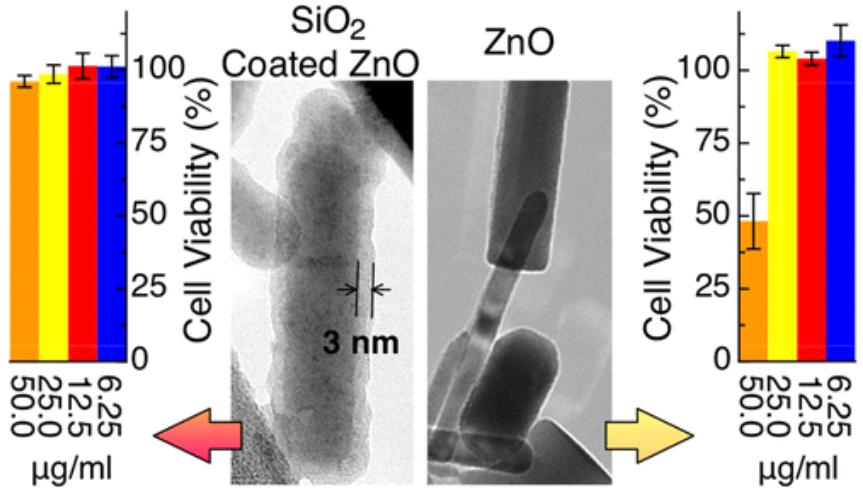

S. Gass, J. Cohen, G. Pyrgiotakis, **G.A. Sotiriou**, S.E. Pratsinis, P. Demokritou, "Safer Formulation Concept for Flame-Generated Engineered Nanomaterials", *ACS Sustainable Chem. Eng.* **1**, 843-857 (2013).

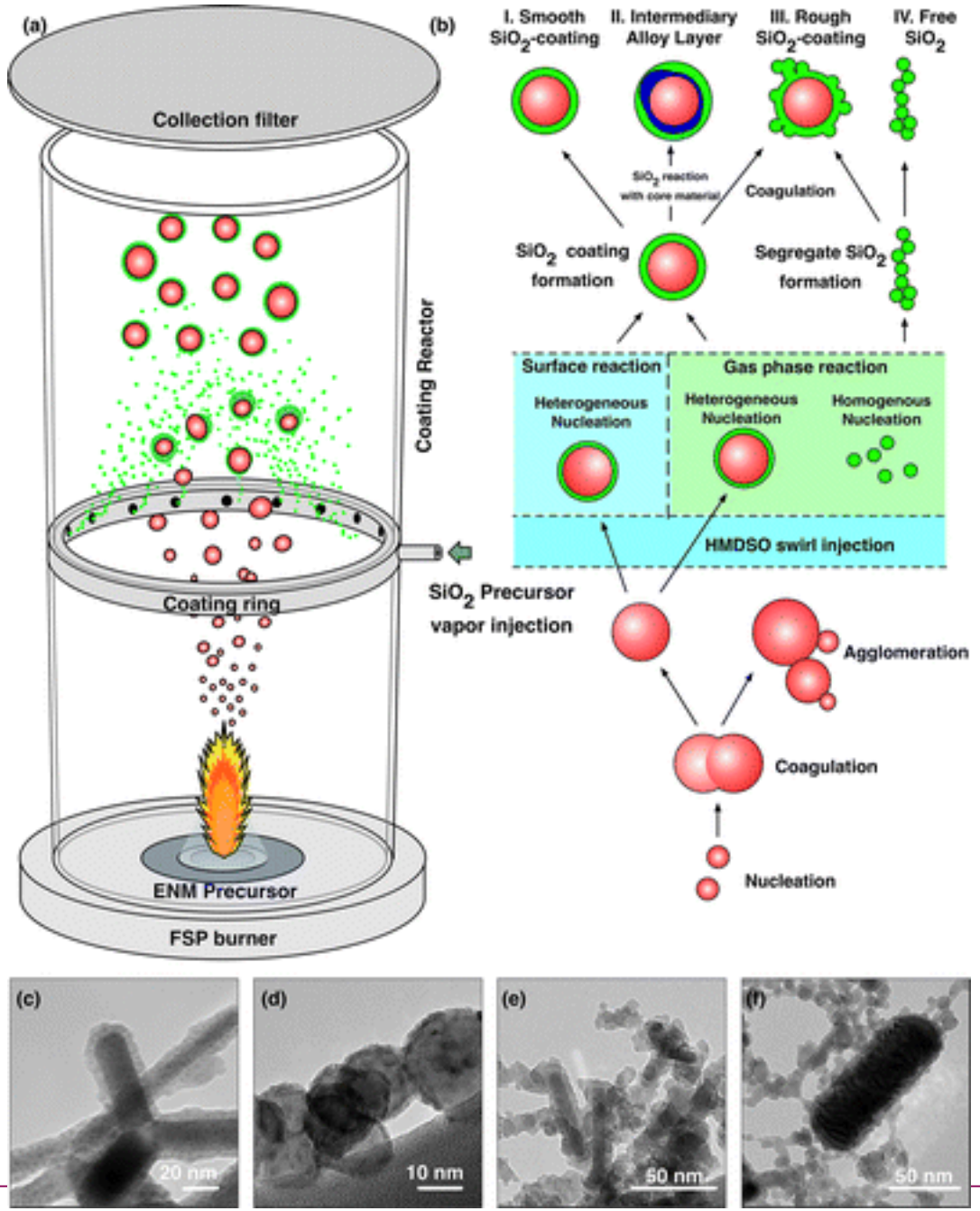
(a)
Collection filter
Coating Reactor
Coating ring
ENM Precursor
FSP burner
(b)
I. Smooth SiO_2-coating
II. Intermediary Alloy Layer
III. Rough SiO_2-coating
IV. Free SiO_2
SiO_2 reaction with core material
Coagulation
SiO_2 coating formation
Segregate SiO_2 formation
Surface reaction
Gas phase reaction
Heterogeneous Nucleation
Heterogeneous Nucleation
Homogenous Nucleation
HMDSO swirl injection
SiO_2 Precursor vapor injection
Agglomeration
Coagulation
Nucleation

(c)
20 nm
(d)
10 nm
(e)
50 nm
(f)
50 nm

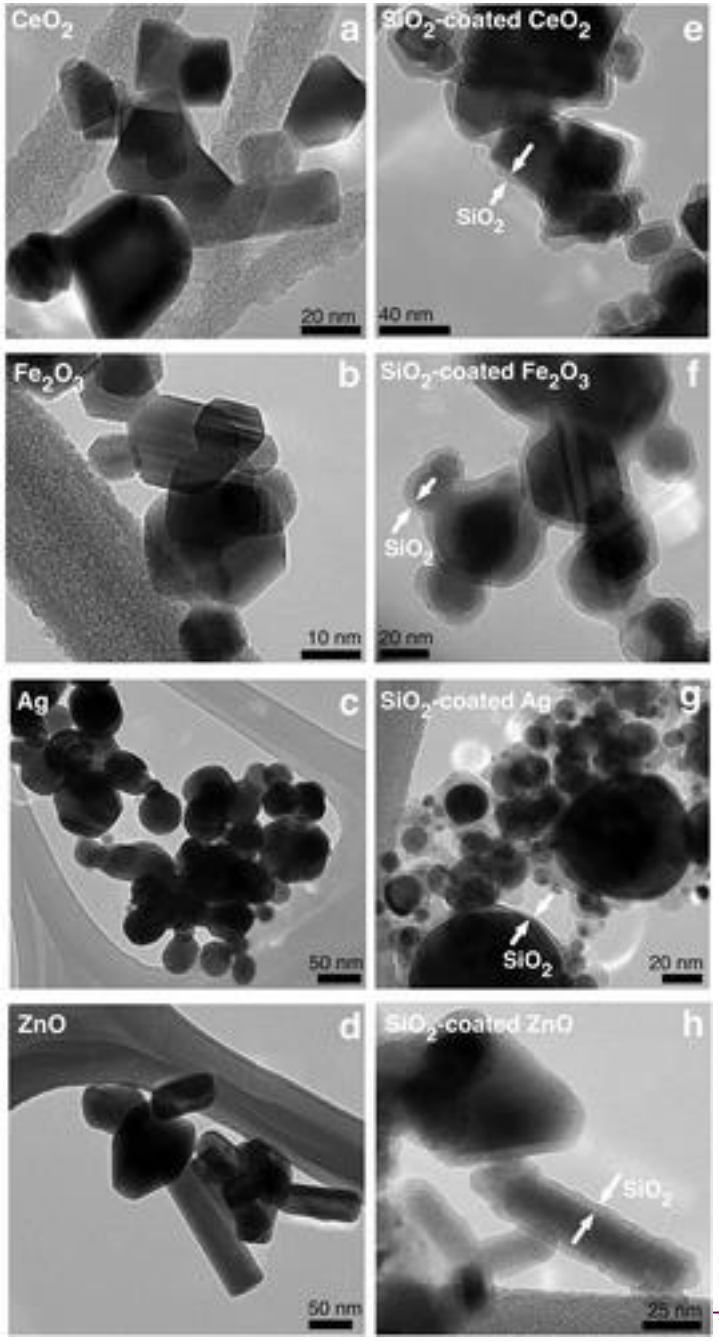
CeO_2
a
20 nm
SiO_2-coated CeO_2
e
SiO_2
40 nm
Fe_2O_3
b
10 nm
SiO_2-coated Fe_2O_3
f
SiO_2
20 nm
Ag
c
50 nm
SiO_2-coated Ag
g
SiO_2
20 nm
ZnO
d
50 nm
SiO_2-coated ZnO
h
SiO_2
25 nm

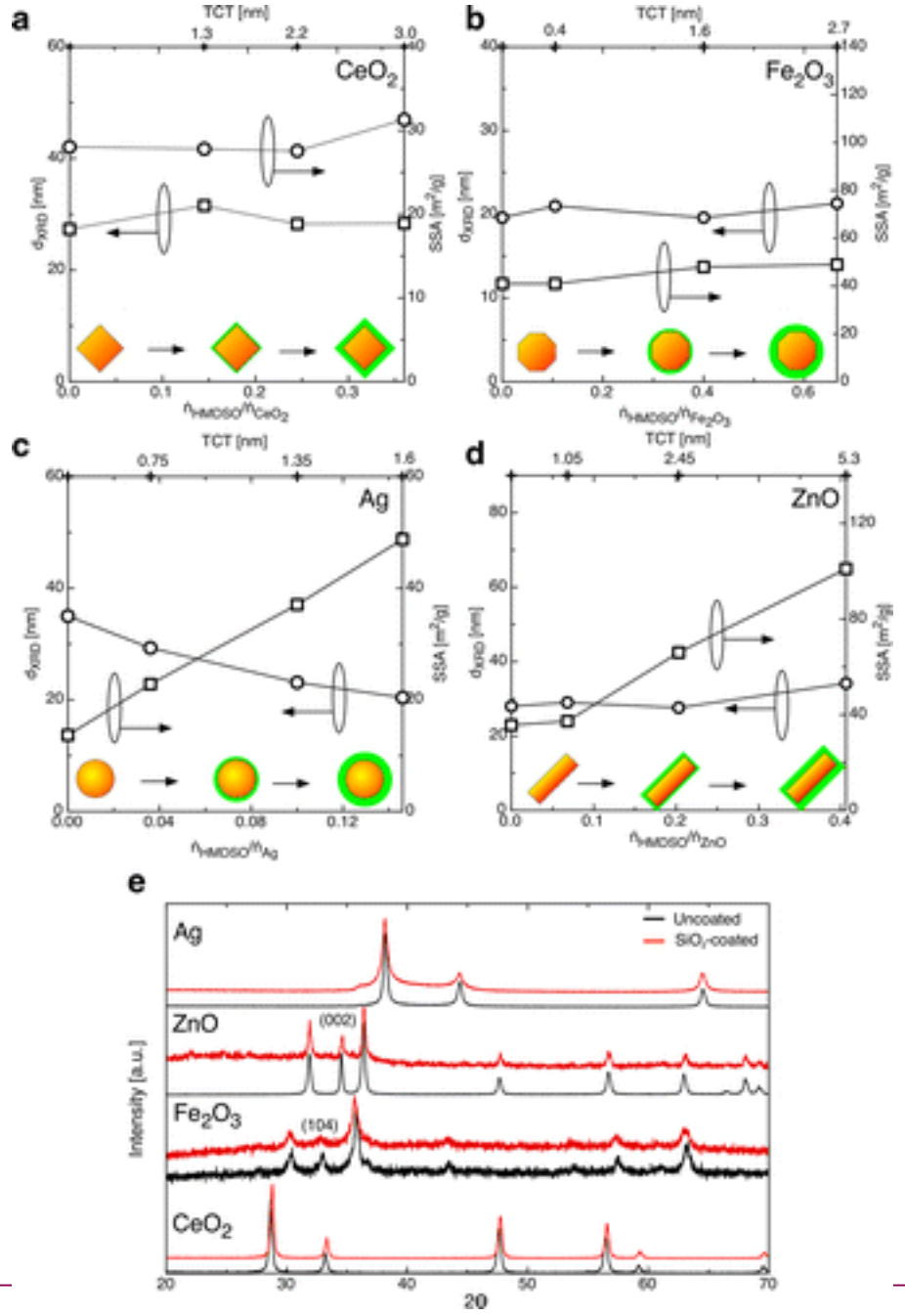
a
TCT [nm]
1.3
2.2
3.0
CeO_2
d_{XRD} [nm]
SSA [m^2/g]
n_{HMDSO}/n_{CeO_2}
b
TCT [nm]
0.4
1.6
2.7
Fe_2O_3
d_{XRD} [nm]
SSA [m^2/g]
$n_{HMDSO}/n_{Fe_2O_3}$
c
TCT [nm]
0.75
1.35
1.6
Ag
d_{XRD} [nm]
SSA [m^2/g]
n_{HMDSO}/n_{Ag}
d
TCT [nm]
1.05
2.45
5.3
ZnO
d_{XRD} [nm]
SSA [m^2/g]
n_{HMDSO}/n_{ZnO}
e
Uncoated
SiO_x-coated
Ag
ZnO
(002)
Fe_2O_3
(104)
CeO_2
Intensity [a.u.]
2θ

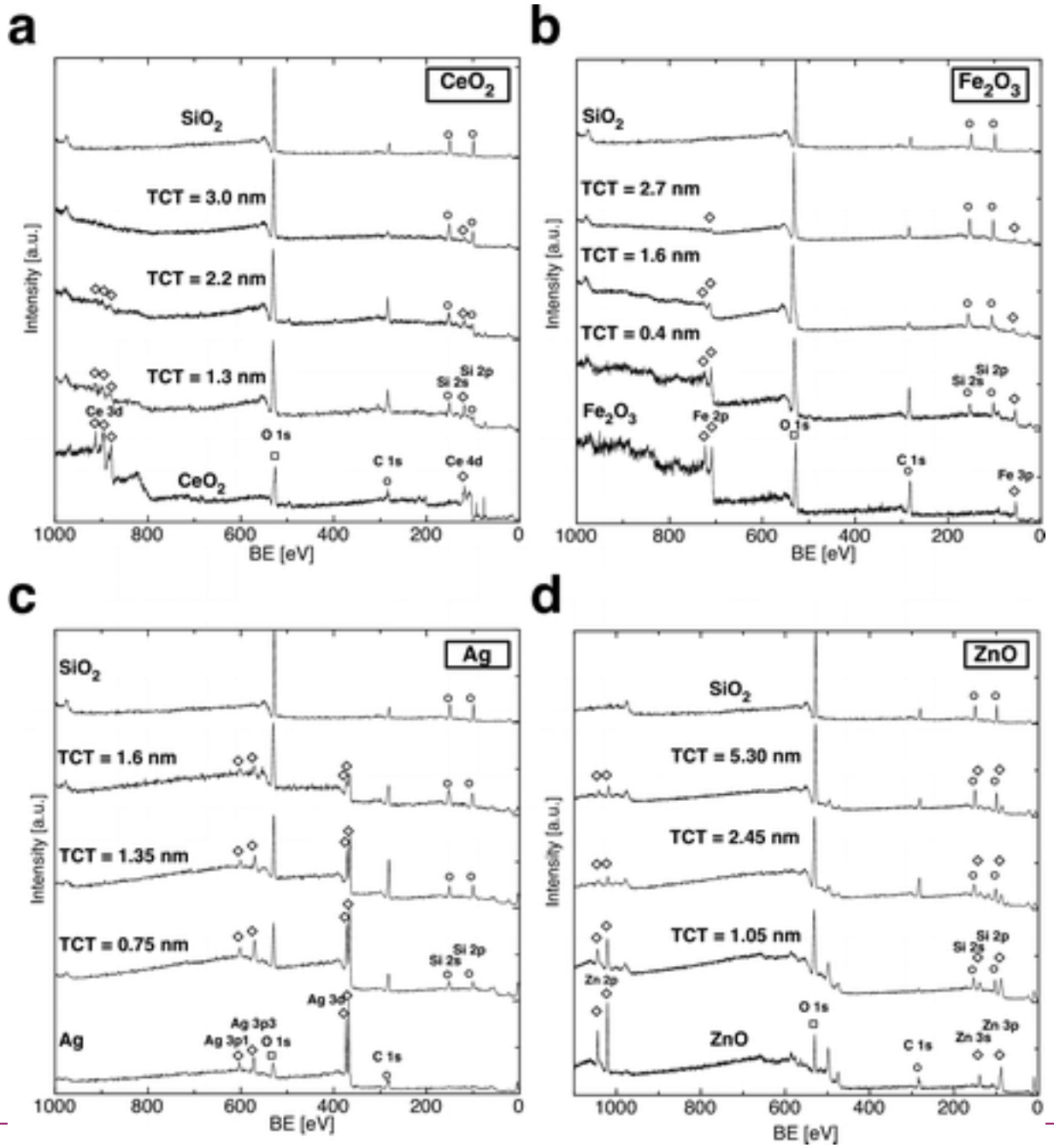
a
CeO2
SiO2
TCT = 3.0 nm
TCT = 2.2 nm
TCT = 1.3 nm
Ce 3d
O 1s
C 1s
Ce 4d
Si 2s
Si 2p
CeO2
Intensity [a.u.]
1000 800 600 400 200 0
BE [eV]
b
Fe2O3
SiO2
TCT = 2.7 nm
TCT = 1.6 nm
TCT = 0.4 nm
Fe2O3
Fe 2p
O 1s
Si 2s
Si 2p
C 1s
Fe 3p
Intensity [a.u.]
1000 800 600 400 200 0
BE [eV]
c
Ag
SiO2
TCT = 1.6 nm
TCT = 1.35 nm
TCT = 0.75 nm
Ag
Ag 3p3
Ag 3p1
O 1s
Ag 3d
C 1s
Si 2s
Si 2p
Intensity [a.u.]
1000 800 600 400 200 0
BE [eV]
d
ZnO
SiO2
TCT = 5.30 nm
TCT = 2.45 nm
TCT = 1.05 nm
Zn 2p
ZnO
O 1s
C 1s
Zn 3s
Zn 3p
Si 2s
Si 2p
Intensity [a.u.]
1000 800 600 400 200 0
BE [eV]

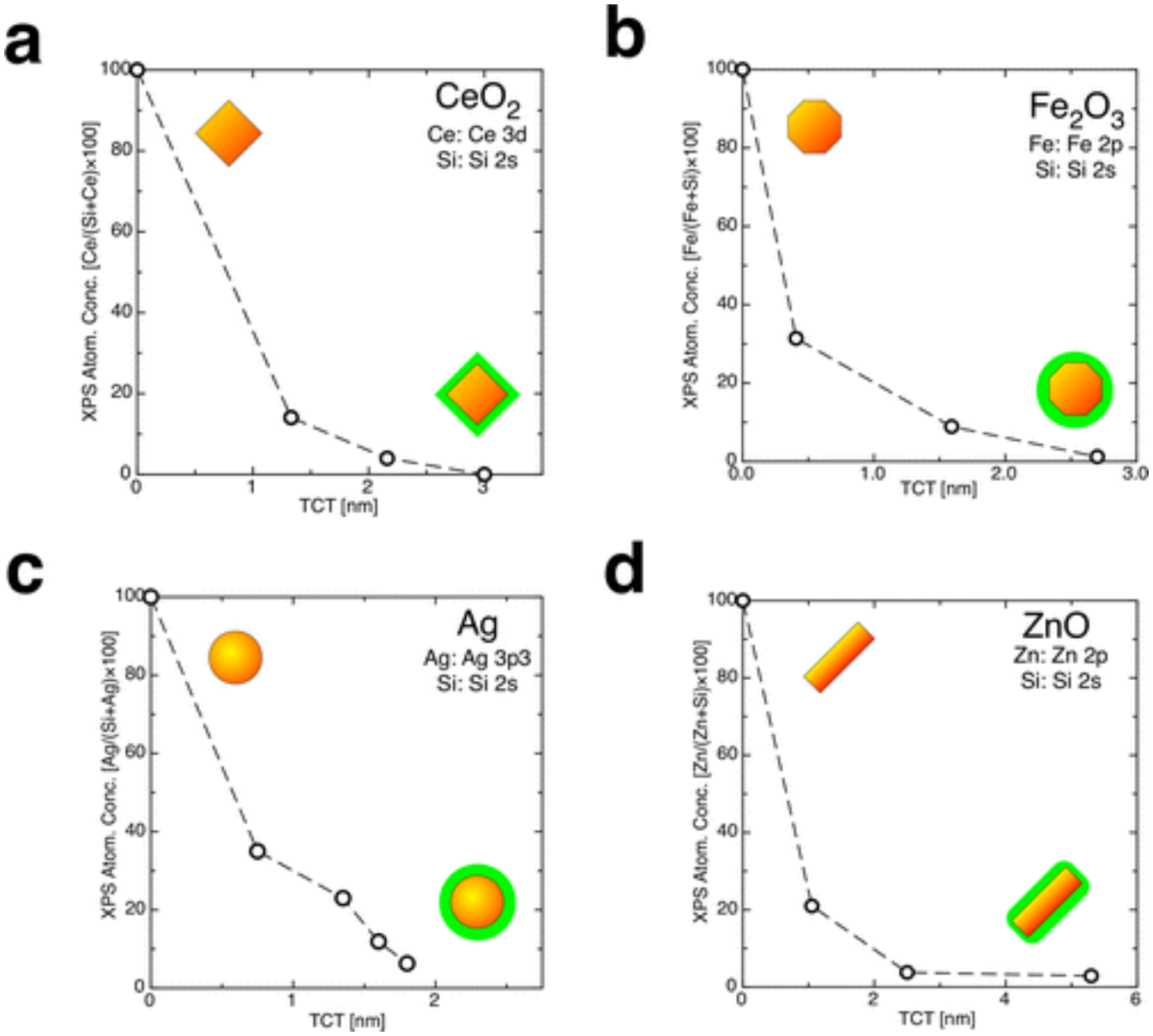
a
CeO2
Ce: Ce 3d
Si: Si 2s
XPS Atom. Conc. [Ce/(Si+Ce)x100]
TCT [nm]
b
Fe2O3
Fe: Fe 2p
Si: Si 2s
XPS Atom. Conc. [Fe/(Fe+Si)x100]
TCT [nm]
c
Ag
Ag: Ag 3p3
Si: Si 2s
XPS Atom. Conc. [Ag/(Si+Ag)x100]
TCT [nm]
d
ZnO
Zn: Zn 2p
Si: Si 2s
XPS Atom. Conc. [Zn/(Zn+Si)x100]
TCT [nm]

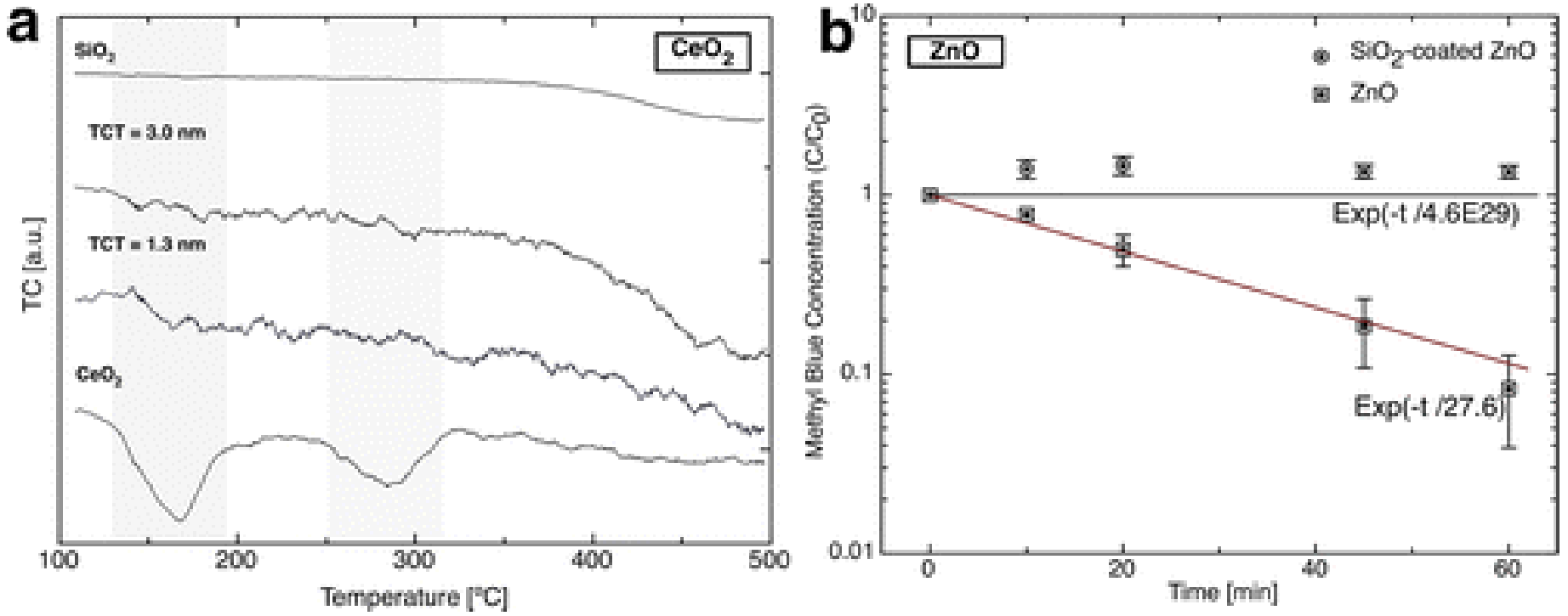
a
SiO2
CeO2
TCT = 3.0 nm
TCT = 1.3 nm
CeO2
TC [a.u.]
100
200
300
400
500
Temperature [°C]
b
ZnO
SiO2-coated ZnO
ZnO
Exp(-t /4.6E29)
Exp(-t /27.6)
Methyl Blue Concentration (C/C0)
10
1
0.1
0.01
0
20
40
60
Time [min]

ES:NANO 2014

G.A. Sotiriou, C. Watson, K.M. Murdaugh, T.H. Darrah, G. Pyrgiotakis, A. Elder, J.D. Brain & P. Demokritou. "Engineering Safer-by-Design, Transparent, Silica-coated ZnO Nanorods with Reduced DNA Damage Potential", *Environ. Sci.: Nano* **1**, 144-153 (2014).

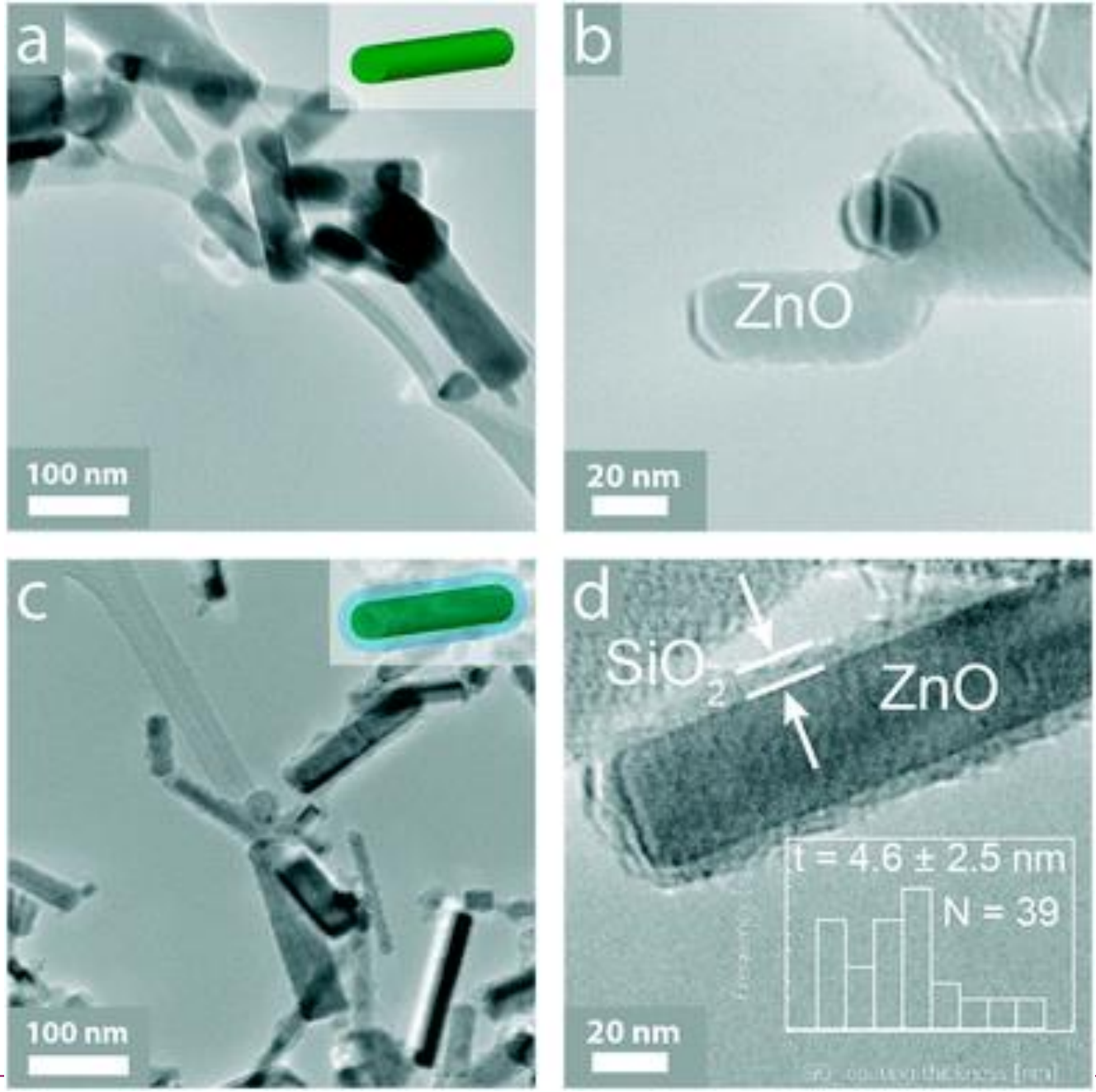
a
100 nm
b
ZnO
20 nm
c
100 nm
d
SiO2
ZnO
t = 4.6 ± 2.5 nm
N = 39
20 nm

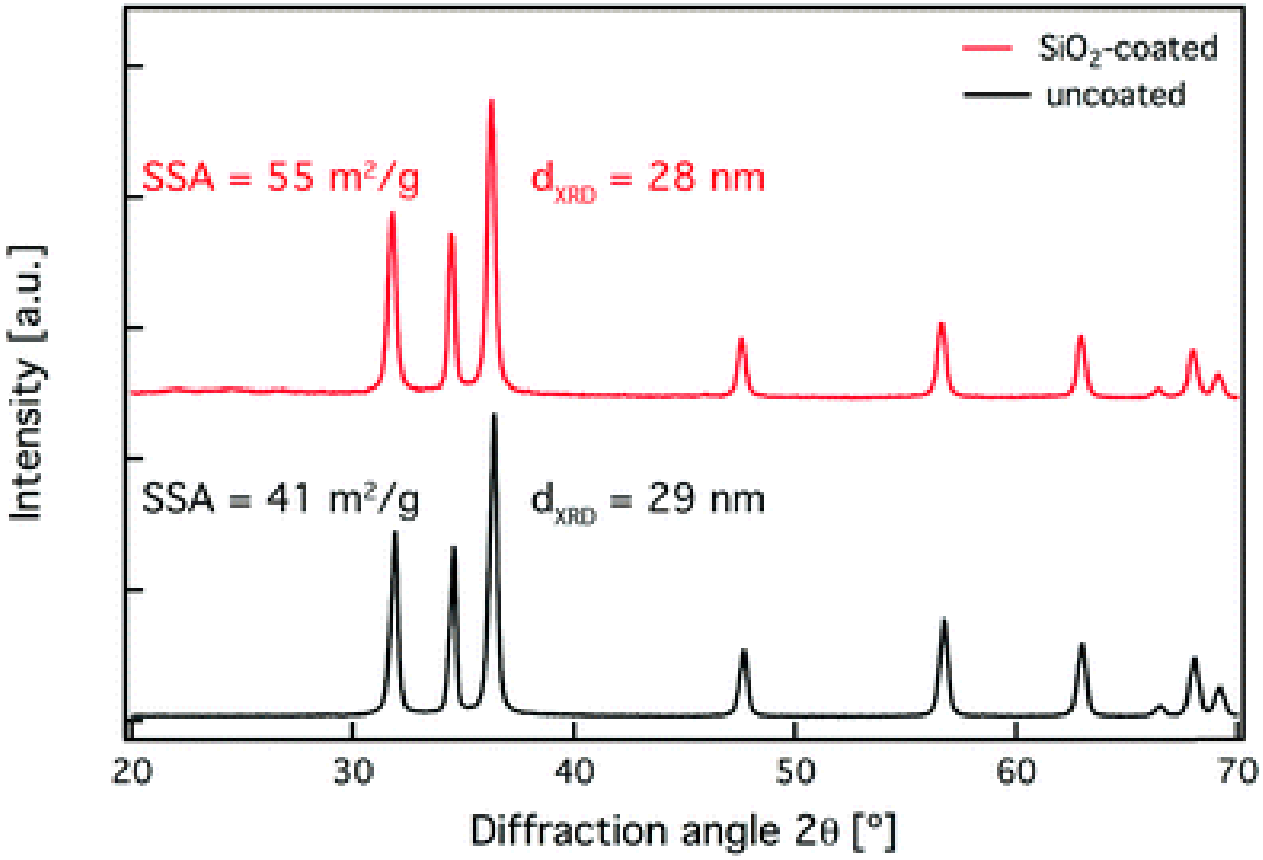
SiO2-coated
uncoated
SSA = 55 m²/g
dXRD = 28 nm
SSA = 41 m²/g
dXRD = 29 nm
Intensity [a.u.]
20
30
40
50
60
70
Diffraction angle 2θ [°]

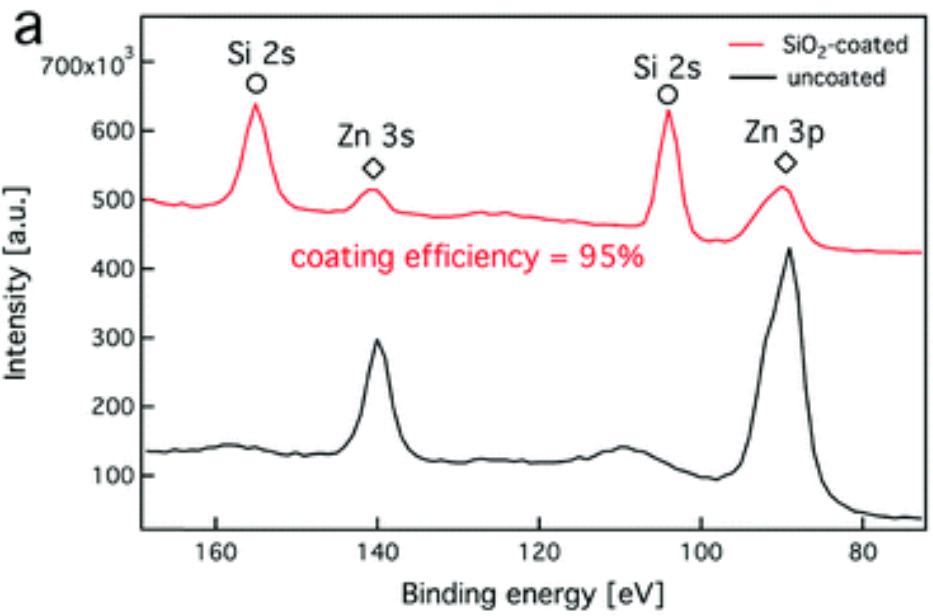
a
700x10^3
600
500
400
300
200
100
Intensity [a.u.]
Si 2s
Zn 3s
Si 2s
Zn 3p
SiO2-coated
uncoated
coating efficiency = 95%
160
140
120
100
80
Binding energy [eV]

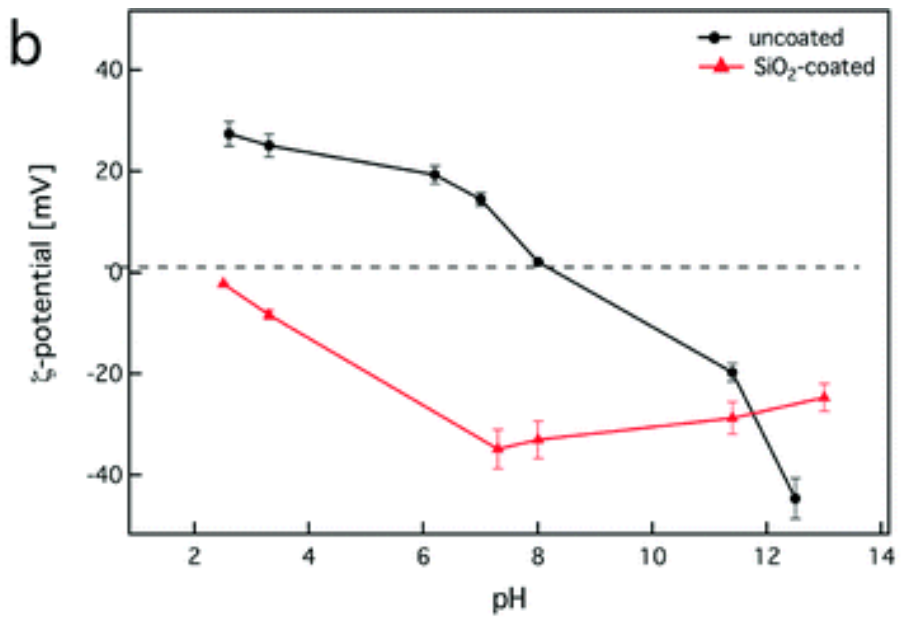
b
uncoated
SiO2-coated
40
20
0
-20
-40
ζ-potential [mV]
2
4
6
8
10
12
14
pH

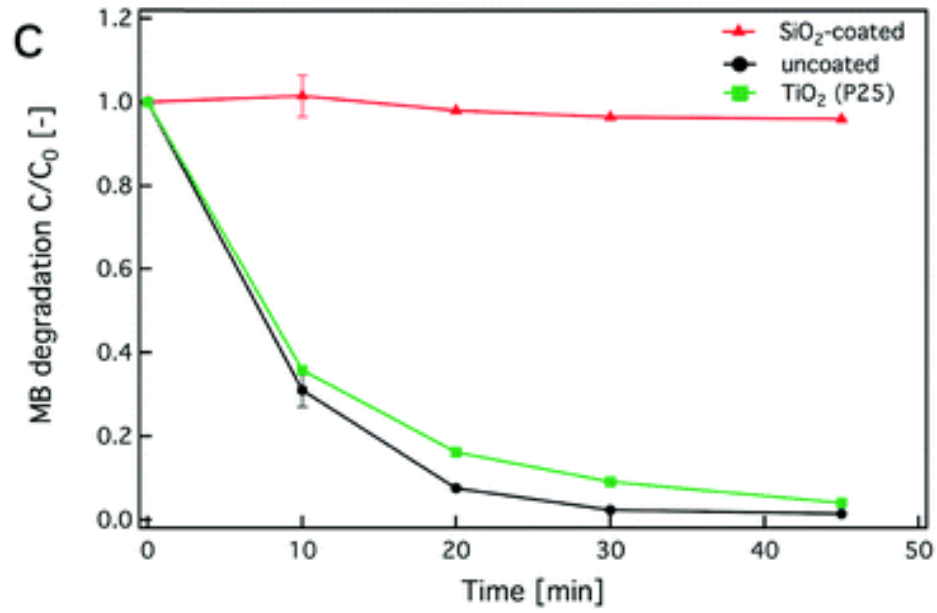
c
SiO2-coated
uncoated
TiO2 (P25)
1.2
1.0
0.8
0.6
0.4
0.2
0.0
MB degradation C/C0 [-]
0
10
20
30
40
50
Time [min]

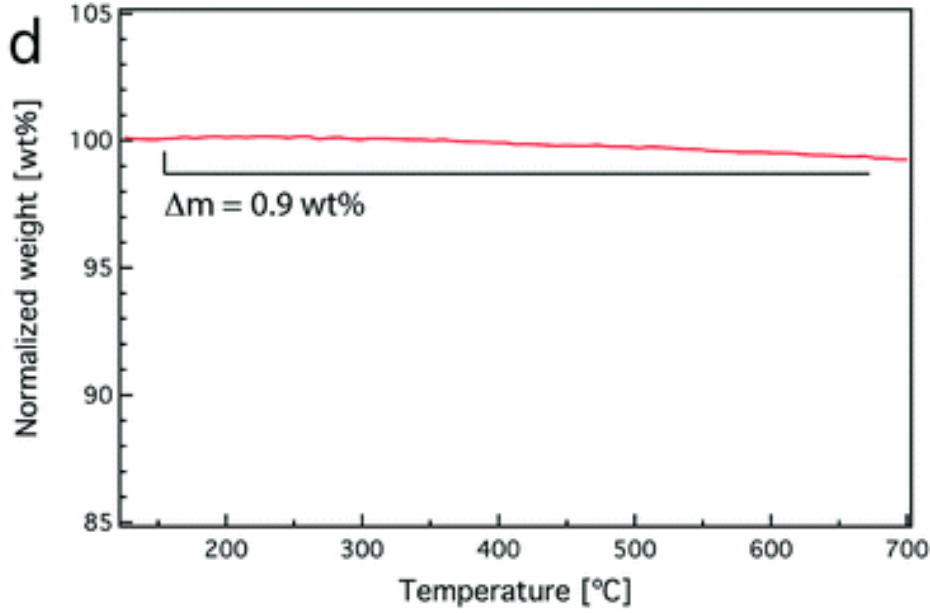
d
105
100
95
90
85
Normalized weight [wt%]
Δm = 0.9 wt%
200
300
400
500
600
700
Temperature [°C]

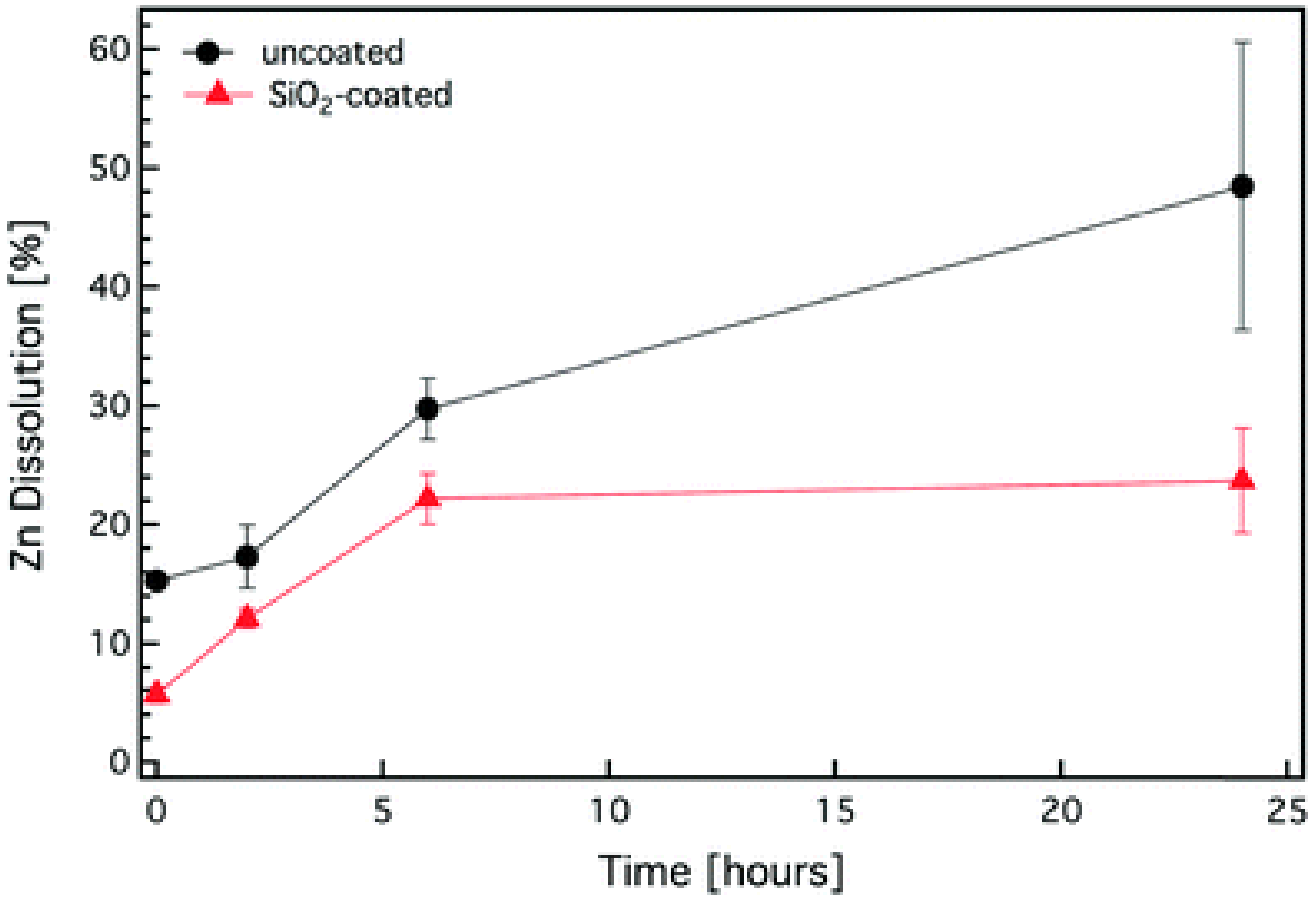
uncoated
SiO2-coated
Zn Dissolution [%]
Time [hours]
0
10
20
30
40
50
60
0
5
10
15
20
25

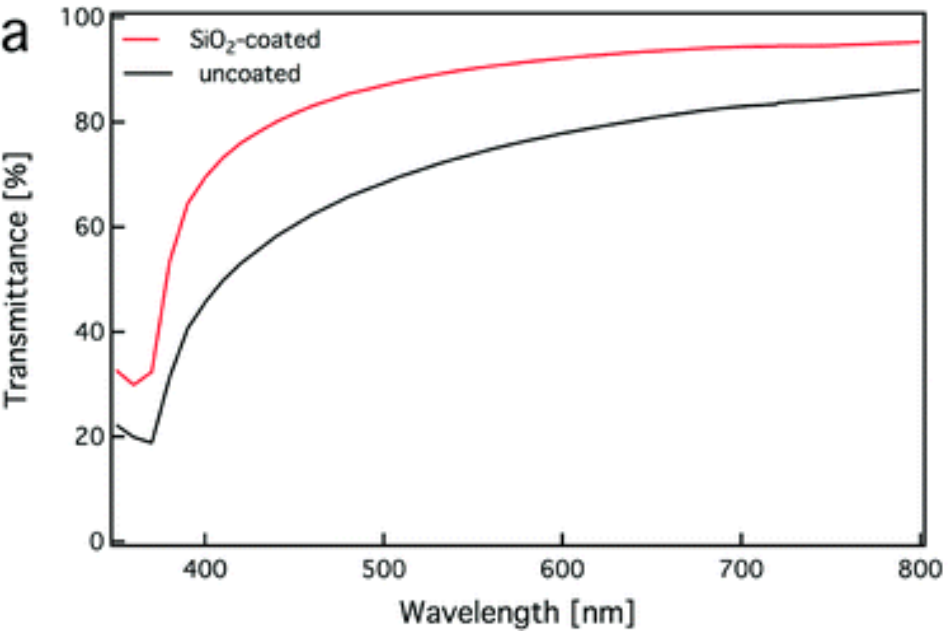
a
SiO2-coated
uncoated
Transmittance [%]
Wavelength [nm]
0
20
40
60
80
100
400
500
600
700
800

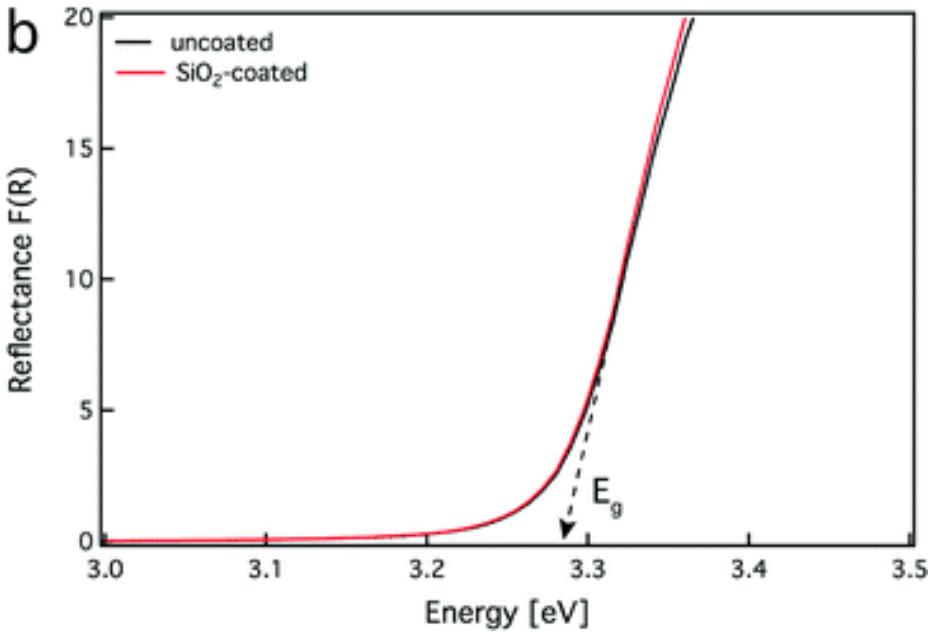
b
uncoated
SiO2-coated
Reflectance F(R)
Energy [eV]
Eg
0
5
10
15
20
3.0
3.1
3.2
3.3
3.4
3.5

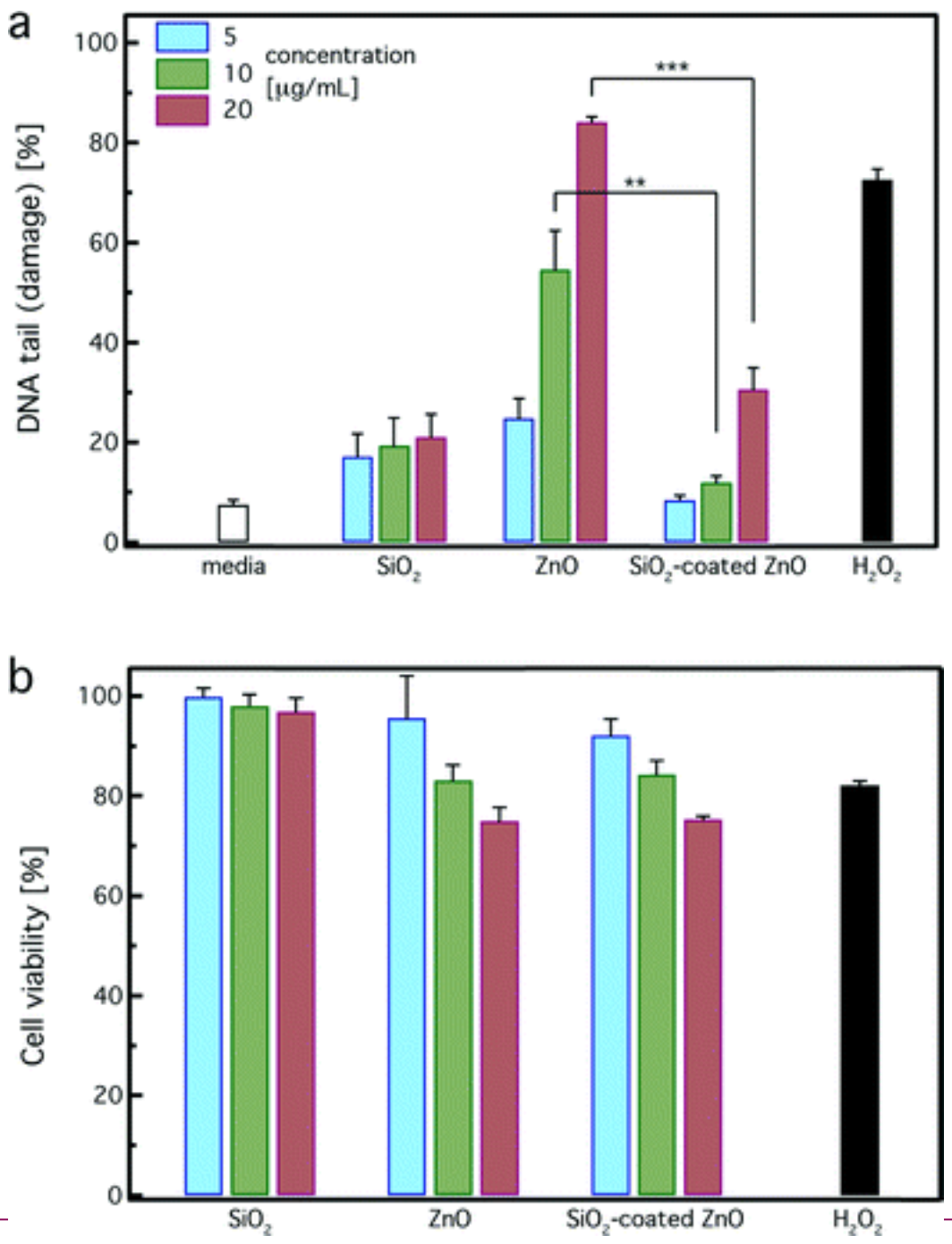
a
DNA tail (damage) [%]
100
80
60
40
20
0
5
10
20
concentration
[µg/mL]
***
**
media
SiO2
ZnO
SiO2-coated ZnO
H2O2
b
Cell viability [%]
100
80
60
40
20
0
SiO2
ZnO
SiO2-coated ZnO
H2O2

P&FT 2014

N.V. Konduru, K.M. Murdaugh, **G.A. Sotiriou**, T.C. Donaghey, P. Demokritou, J.D. Brain & R.M. Molina. "Bioavailability, distribution and clearance of tracheally-instilled and gavaged uncoated or silica-coated zinc oxide nanoparticles", *Part. Fibre Toxicol.* **11**:44 (2014).

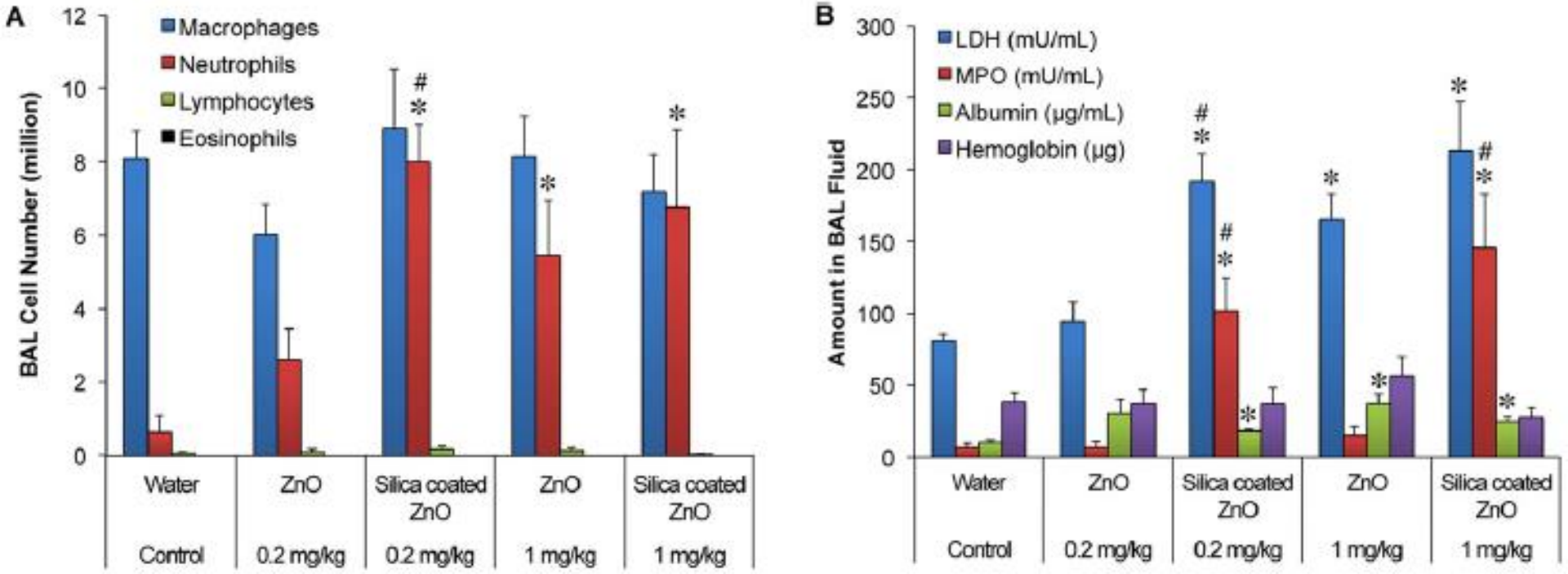

Figure 2 Cellular and biochemical parameters of lung injury and inflammation in bronchoalveolar lavage (BAL). Tracheally instilled ZnO and SiO_2-coated ZnO induced a dose-dependent lung injury and inflammation at 24 hours. **(A)** Significant increases in BAL neutrophils were observed at 1 mg/kg of both NPs (n = 6/group). At the lower dose of 0.2 mg/kg (n = 4-6/group), only the SiO_2-coated ZnO (n = 4) induced significant neutrophil influx in the lungs. **(B)** Similarly, significant increases in LDH, myeloperoxidase and albumin were observed at 1 mg/kg of both NPs, and at 0.2 mg of SiO_2-coated ZnO. (*$P < 0.05$, vs. control, #$P < 0.05$, SiO_2-coated ZnO versus ZnO).

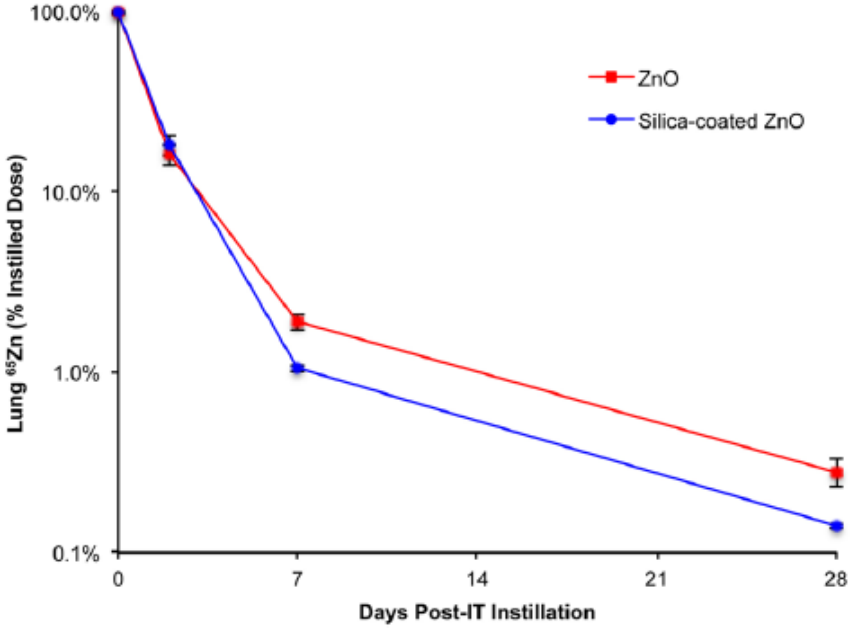

Figure 3 Lung clearance of ^{65}Zn post-IT instillation of ^{65}ZnO and SiO_2-coated ^{65}ZnO NPs. The percentages of instilled ^{65}Zn measured in the whole lungs are shown over a period of 28 days. The clearance of ^{65}Zn was rapid with only 16-18% of dose remaining at 2 days. By day 7, only 1.1% (SiO_2-coated ^{65}ZnO NPs) and 1.9% (^{65}ZnO NPs) were measured in the lungs. And by the end of experiment, ^{65}Zn was nearly gone (less than 0.3% of dose). Although statistically higher levels of ^{65}ZnO NPs than of SiO_2-coated ^{65}ZnO NPs remained in the lungs at 7 and 28 days, the graphs show nearly identical clearance kinetics. (n = 8 rats at 5 minutes, 2 days, and 7 days, n = 5 at 28 days).

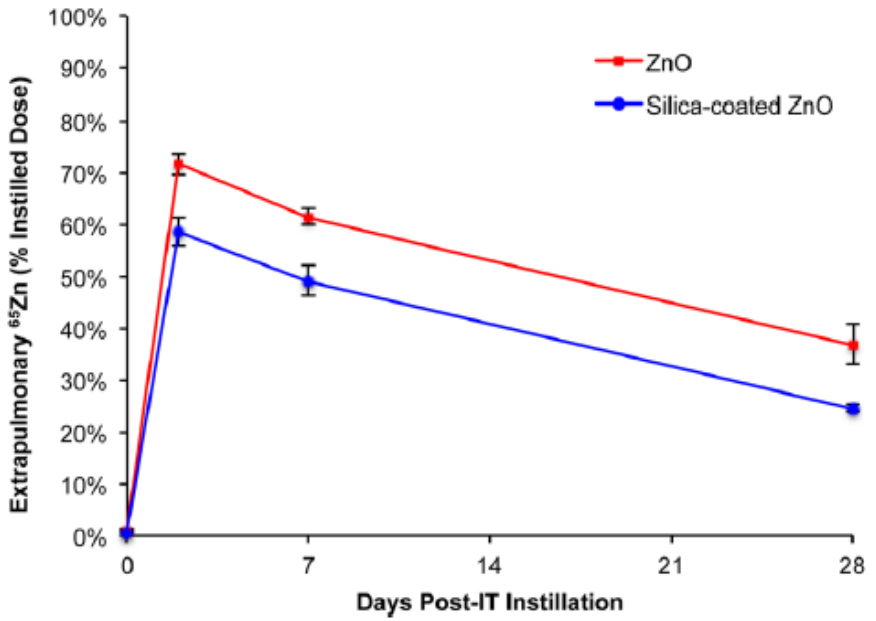

Figure 4 Extrapulmonary distribution of ^{65}Zn post-IT instillation of ^{65}ZnO and SiO_2-coated ^{65}ZnO NPs. Data are % of instilled dose recovered in all secondary tissues examined. It included blood, thoracic lymph nodes, bone, bone marrow, skin, brain, skeletal muscle, testes, kidneys, heart, liver, and the gastrointestinal tract. There was a rapid absorption and accumulation of ^{65}Zn in secondary tissues. At day 2, 59-72% of the dose was detected in extrapulmonary organs. Then, ^{65}Zn levels decreased over time to 25-37% by day 28. Significantly more ^{65}Zn was detected in secondary organs at all time points in rats instilled with uncoated ^{65}ZnO NPs.

Table 1 Tissue distribution of ^{65}Zn at 2 days after intratracheal instillation of ^{65}ZnO or SiO_2-coated ^{65}ZnO NPs in rats

	ZnO	SiO_2-coated ZnO
	Mean ± SE	Mean ± SE
Lungs	16.08 ± 2.00	18.09 ± 2.17
Blood	2.54 ± 0.07*	2.22 ± 0.08
Lymph nodes	0.63 ± 0.23	0.49 ± 0.04
Bone marrow	3.37 ± 0.32	2.89 ± 0.15
Bone	9.59 ± 0.46	9.25 ± 0.29
Skin	11.30 ± 1.00	12.52 ± 0.77
Brain	0.17 ± 0.01	0.19 ± 0.01 #
Skeletal muscle	14.22 ± 0.77*	6.39 ± 2.44
Testes	0.84 ± 0.05	0.78 ± 0.04
Kidneys	2.05 ± 0.07*	1.74 ± 0.03
Spleen	0.50 ± 0.02	0.44 ± 0.02
Heart	0.47 ± 0.04*	0.36 ± 0.01
Liver	12.23 ± 0.24*	9.88 ± 0.38
Stomach	1.01 ± 0.14	0.78 ± 0.02
Small intestine	7.37 ± 0.32	6.89 ± 0.20
Large intestine	2.08 ± 0.21	1.91 ± 0.12
Cecum	3.42 ± 0.22*	2.35 ± 0.25
Total recovered	87.78 ± 2.35*	76.78 ± 2.84

Data are mean ± SE% instilled dose, n = 8/group.
Total recovered = sum of ^{65}Zn in analyzed organs, feces and urine.
*P < 0.05, ZnO > SiO_2-coated ZnO.
# P <0.05, SiO_2-coated ZnO > ZnO.

Table 2 Tissue distribution of ^{65}Zn at 7 days after intratracheal instillation of ^{65}ZnO or SiO_2-coated ^{65}ZnO NPs in rats

	^{65}ZnO	SiO_2-coated ^{65}ZnO
	Mean ± SE	Mean ± SE
Lungs	1.90 ± 0.18	1.05 ± 0.04
Blood	2.13 ± 0.05*	1.79 ± 0.07
Lymph nodes	0.18 ± 0.02	0.31 ± 0.05 #
Bone marrow	3.70 ± 0.28	3.38 ± 0.16
Bone	12.12 ± 0.53	12.21 ± 0.84
Skin	10.02 ± 0.49	10.55 ± 0.80
Brain	0.25 ± 0.01	0.27 ± 0.01
Skeletal muscle	19.81 ± 0.84*	8.34 ± 3.45
Testes	1.27 ± 0.06	1.23 ± 0.03
Kidneys	0.75 ± 0.03	0.69 ± 0.02
Spleen	0.21 ± 0.01	0.20 ± 0.01
Heart	0.27 ± 0.01*	0.23 ± 0.01
Liver	5.80 ± 0.13*	5.19 ± 0.25
Stomach	0.66 ± 0.02	0.66 ± 0.03
Small intestine	2.83 ± 0.10	2.53 ± 0.12
Large intestine	0.84 ± 0.07	0.83 ± 0.05
Cecum	1.15 ± 0.06	1.04 ± 0.09
Total recovered	81.33 ± 6.51*	69.91 ± 3.33

Data are mean ± SE% instilled dose, n = 8/group.
Total recovered = sum of ^{65}Zn in analyzed organs, feces and urine.
*P < 0.05, ZnO > SiO_2-coated ZnO.
# P <0.05, SiO_2-coated ZnO > ZnO.

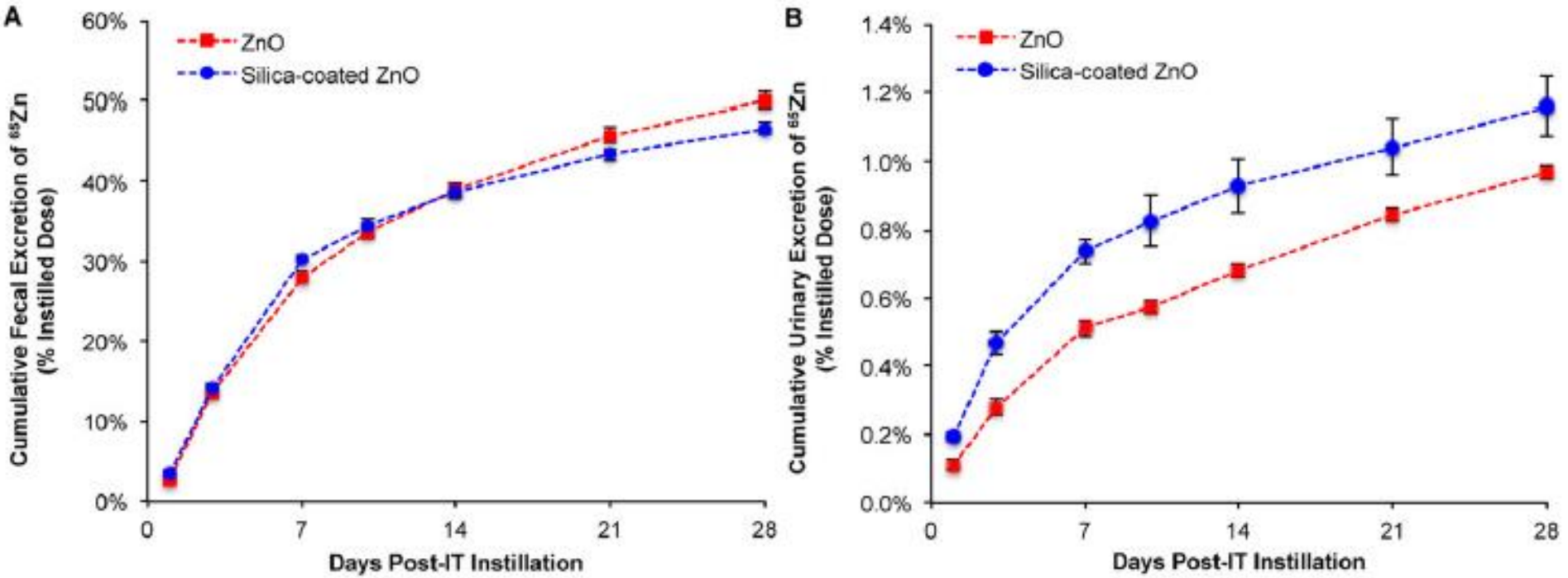

Figure 5 Fecal and urinary excretion of ^{65}Zn post-IT instillation of ^{65}ZnO and SiO_2-coated ^{65}ZnO NPs. Data are estimated cumulative urinary or fecal excretion of ^{65}Zn over 28 days. The predominant excretion pathway was via the feces. Approximately half of the instilled ^{65}Zn was excreted in the feces in both groups over 28 days **(A)**. Only about 1% of the ^{65}Zn dose was excreted in the urine **(B)**.

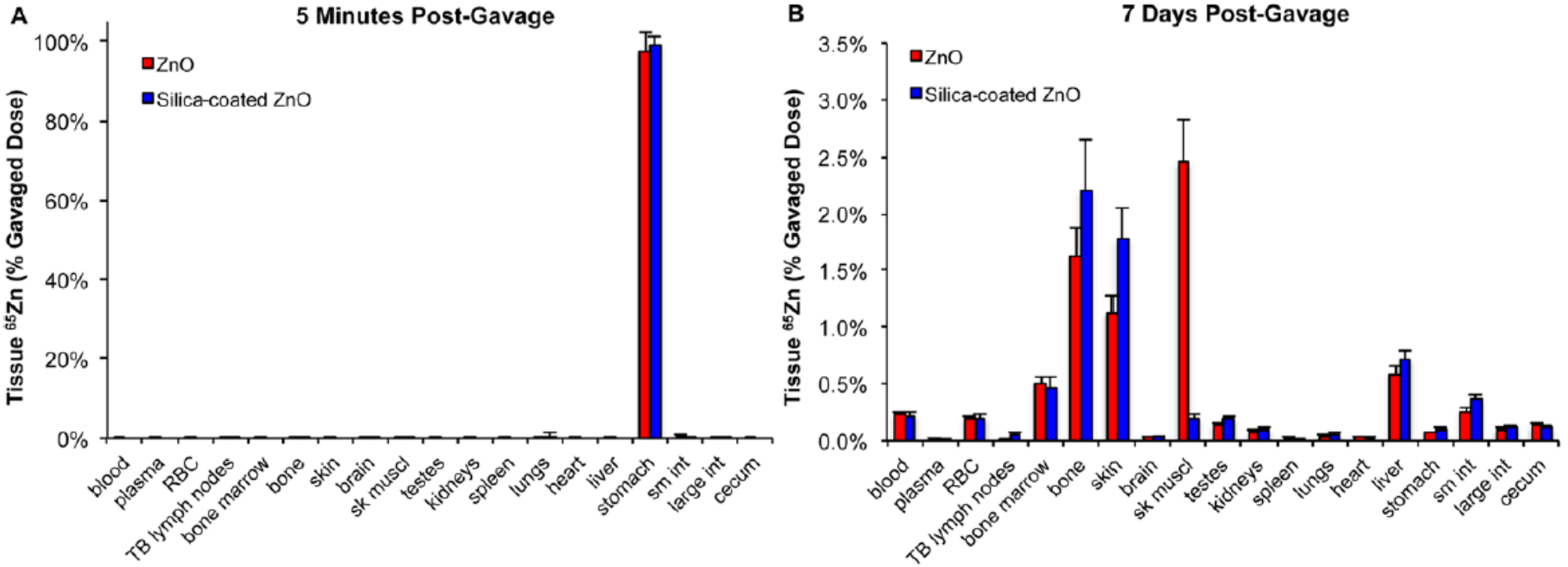

Figure 6 Tissue distribution of ^{65}Zn post-gavage of ^{65}ZnO and SiO_2-coated ^{65}ZnO NPs. Data are % dose of administered ^{65}Zn in different organs. **(A)** At 5 minutes post-gavage, the ^{65}Zn levels in tissues other than the gastrointestinal tract were much lower (0.3% for uncoated, 0.05% for coated ^{65}ZnO NPs). **(B)** At day 7, significantly more ^{65}Zn was absorbed and retained in non-GIT tissues (6.9% for uncoated, 6.0% for coated ^{65}ZnO NPs). Significantly more ^{65}Zn was measured in skeletal muscle in rat gavaged with uncoated versus coated ^{65}ZnO NPs. (Note: RBC: red blood cell; sk muscl: skeletal muscle; sm int: small intestine: large int: large intestine).

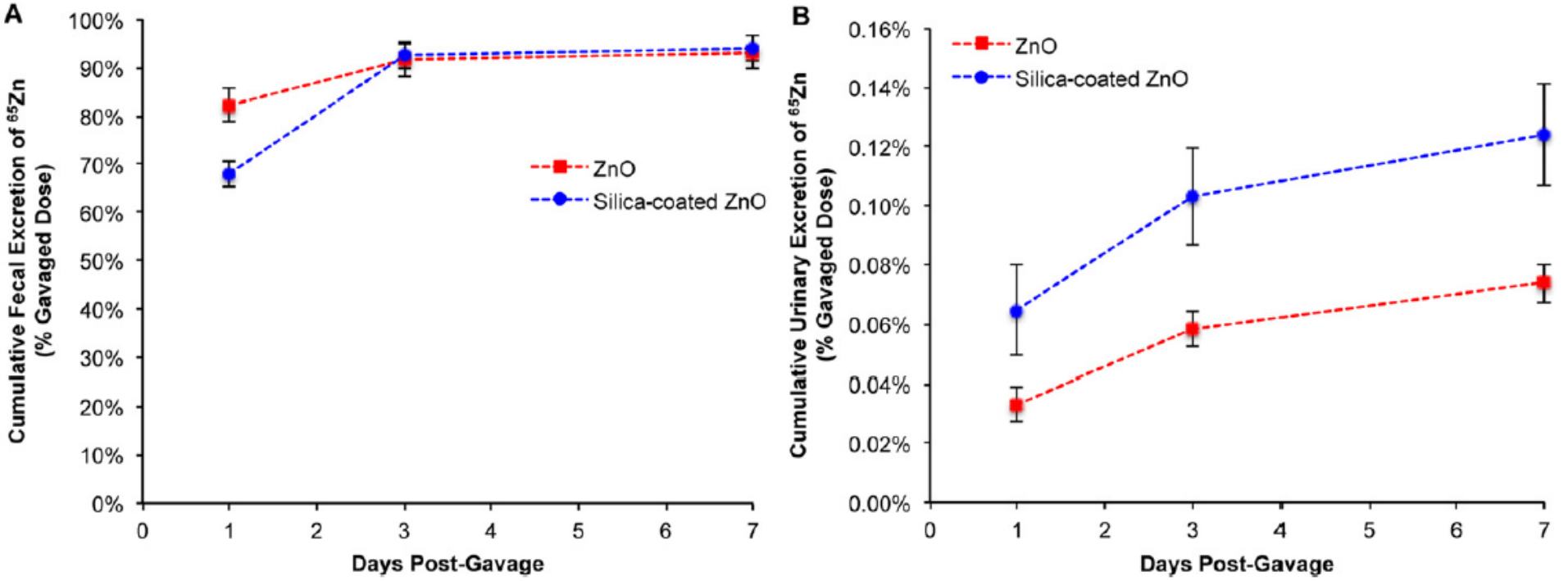

Figure 7 Fecal and urinary excretion of ^{65}Zn post-gavage of ^{65}ZnO and SiO_2-coated ^{65}ZnO NPs. Data are estimated cumulative urinary or fecal excretion of ^{65}Zn over 7 days. Similar to the IT-instilled groups, the predominant excretion pathway was via the feces. Ninety five % of the instilled ^{65}Zn was excreted in both groups by day 7 **(A)**. Only 0.1% of the ^{65}Zn dose was excreted in the urine **(B)**.

ES:NANO 2015

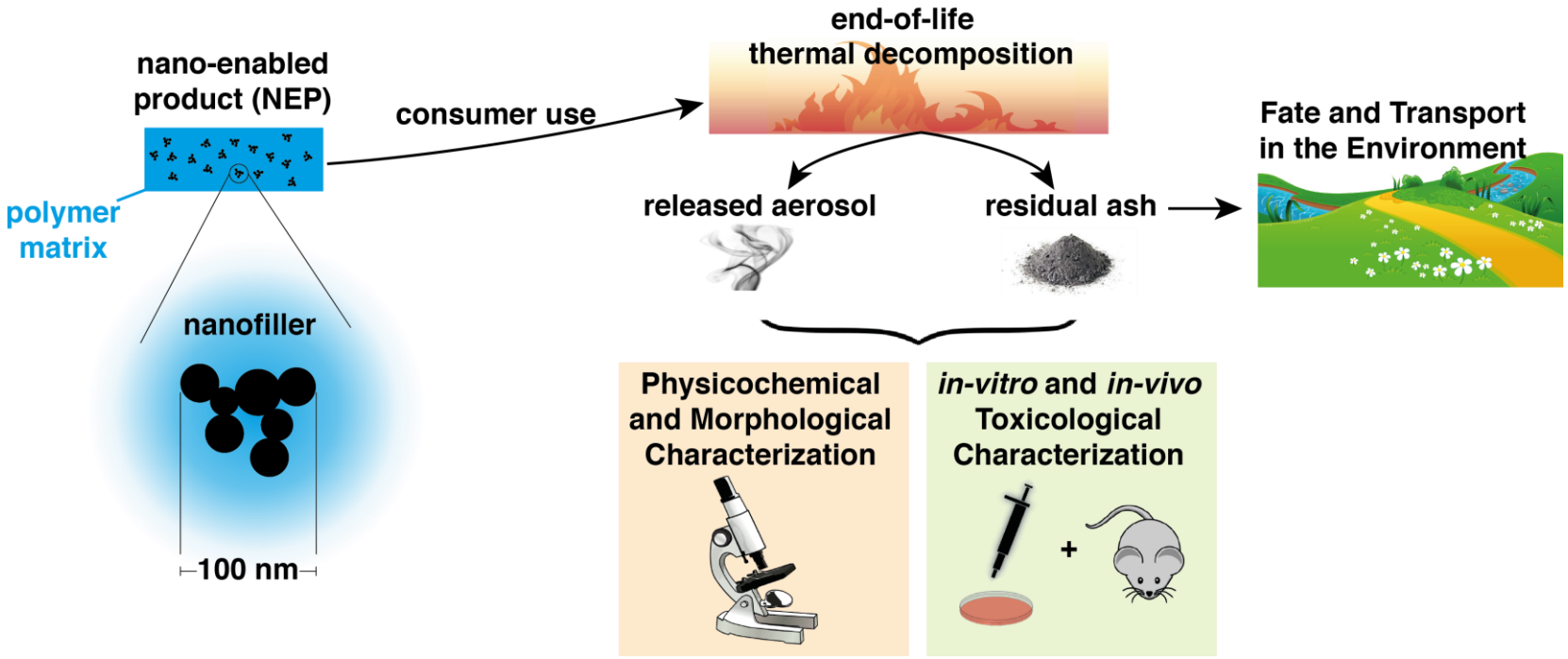

G. A. Sotiriou, D. Singh, F. Zhang, W. Wohlleben, M-C. G. Chalbot, I. G. Kavouras & P. Demokritou. "An integrated methodology for the assessment of environmental health implications during thermal decomposition of nano-enabled products" *Environ. Sci.: Nano* **2**, 262-272 (2015).

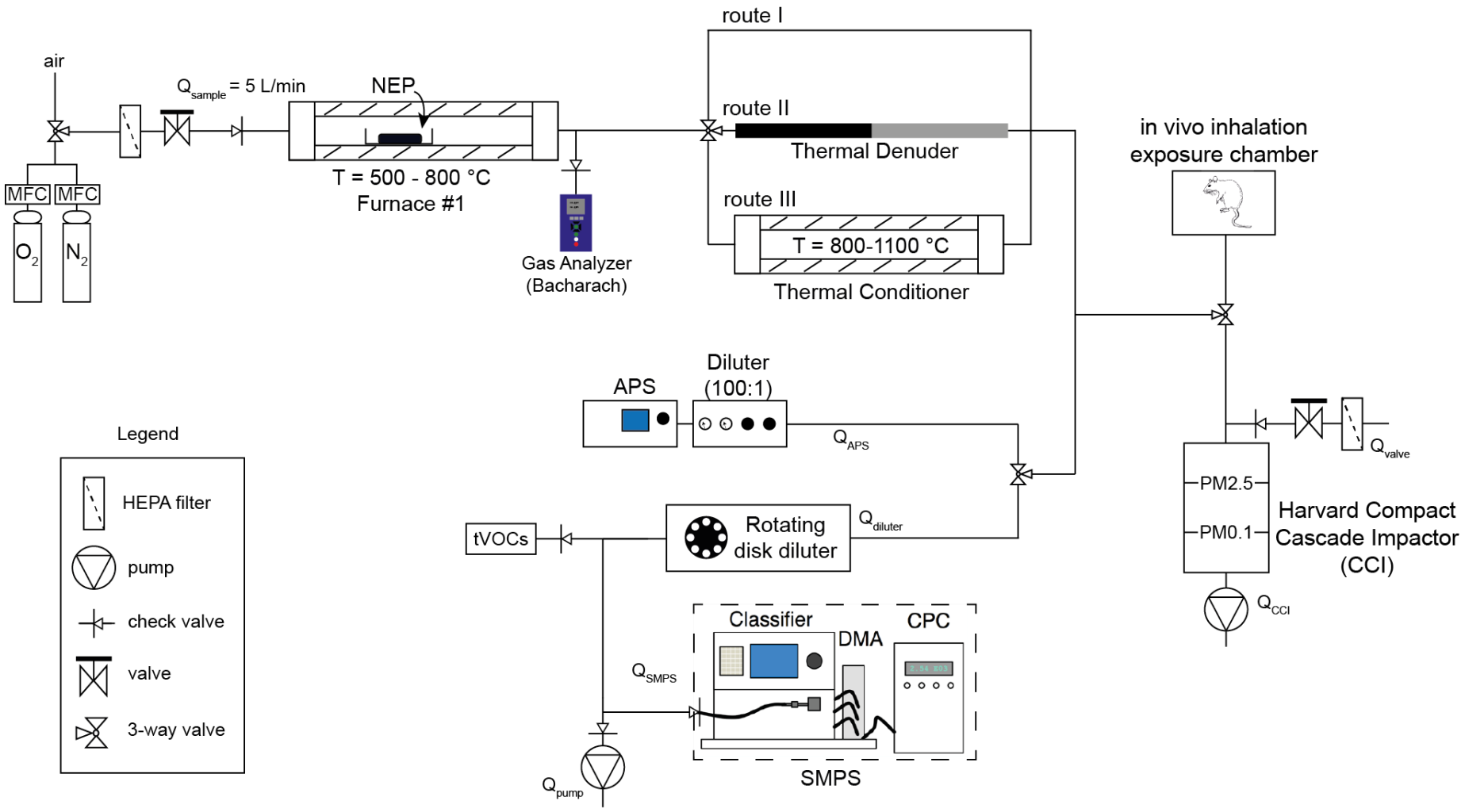
air
Q_{sample} = 5 L/min
NEP
T = 500 - 800 °C
Furnace #1
MFC
MFC
O_2
N_2
Gas Analyzer
(Bacharach)
route I
route II
Thermal Denuder
route III
T = 800-1100 °C
Thermal Conditioner
in vivo inhalation
exposure chamber
APS
Diluter
(100:1)
Q_{APS}
Q_{valve}
PM2.5
PM0.1
Harvard Compact
Cascade Impactor
(CCI)
Q_{CCI}
tVOCs
Rotating
disk diluter
$Q_{diluter}$
Classifier
DMA
CPC
Q_{SMPS}
SMPS
Q_{pump}
Legend
HEPA filter
pump
check valve
valve
3-way valve

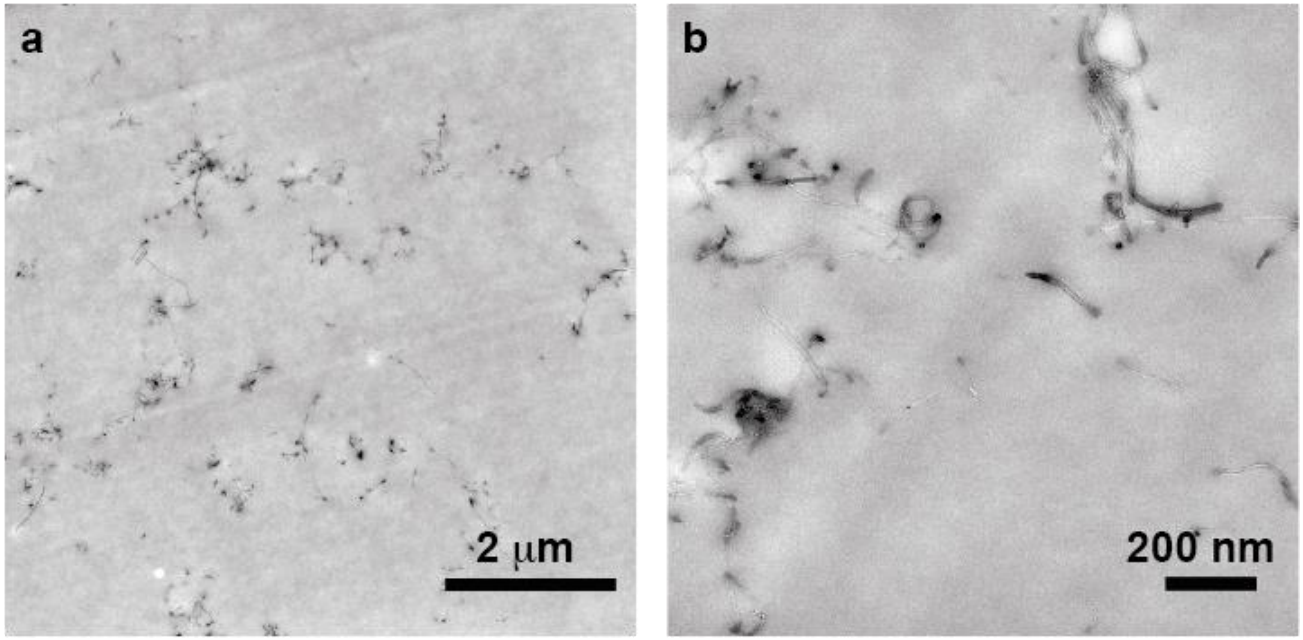
a
2 μm
b
200 nm

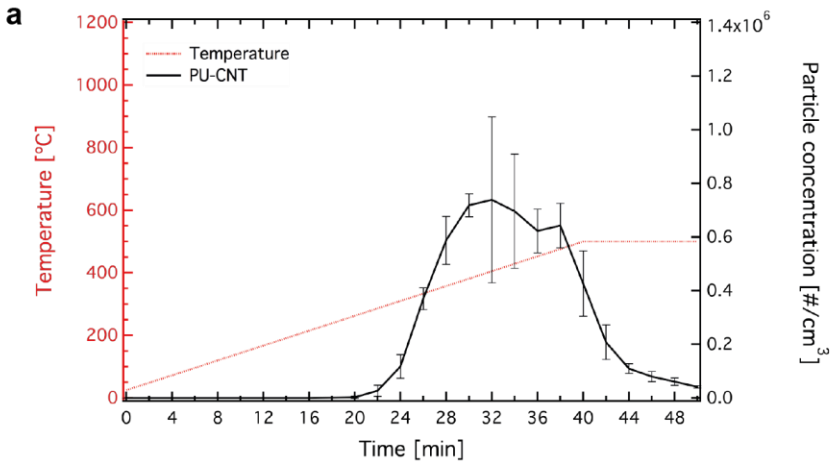
a
Temperature
PU-CNT
Temperature [°C]
Particle concentration [#/cm3]
Time [min]

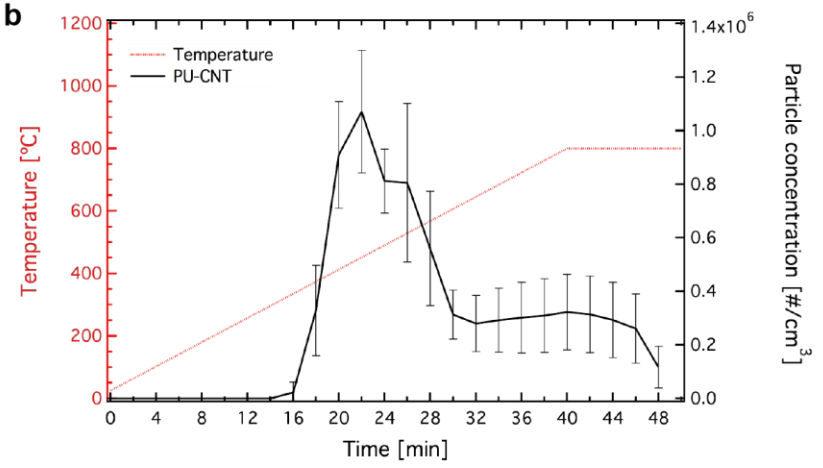
b
Temperature
PU-CNT
Temperature [°C]
Particle concentration [#/cm3]
Time [min]

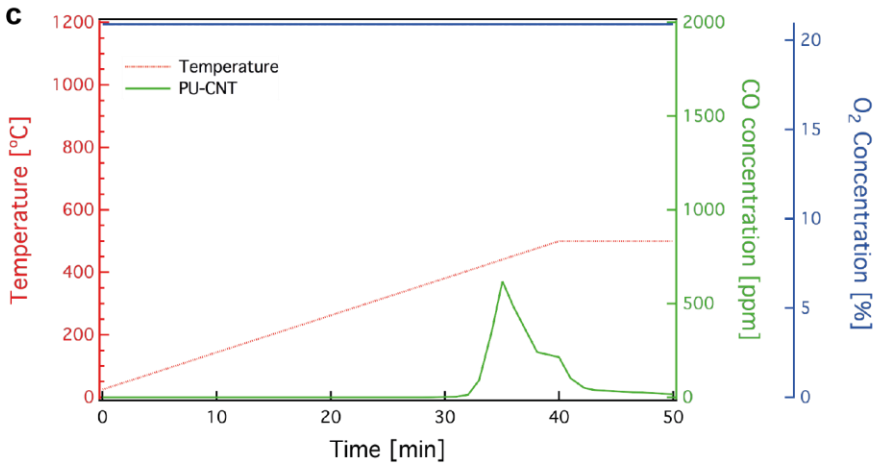
c
Temperature
PU-CNT
Temperature [°C]
CO concentration [ppm]
O2 Concentration [%]
Time [min]

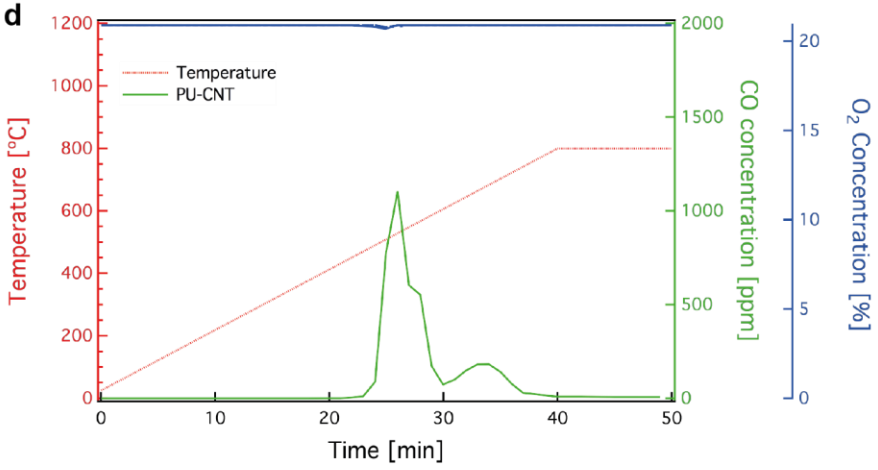
d
Temperature
PU-CNT
Temperature [°C]
CO concentration [ppm]
O2 Concentration [%]
Time [min]

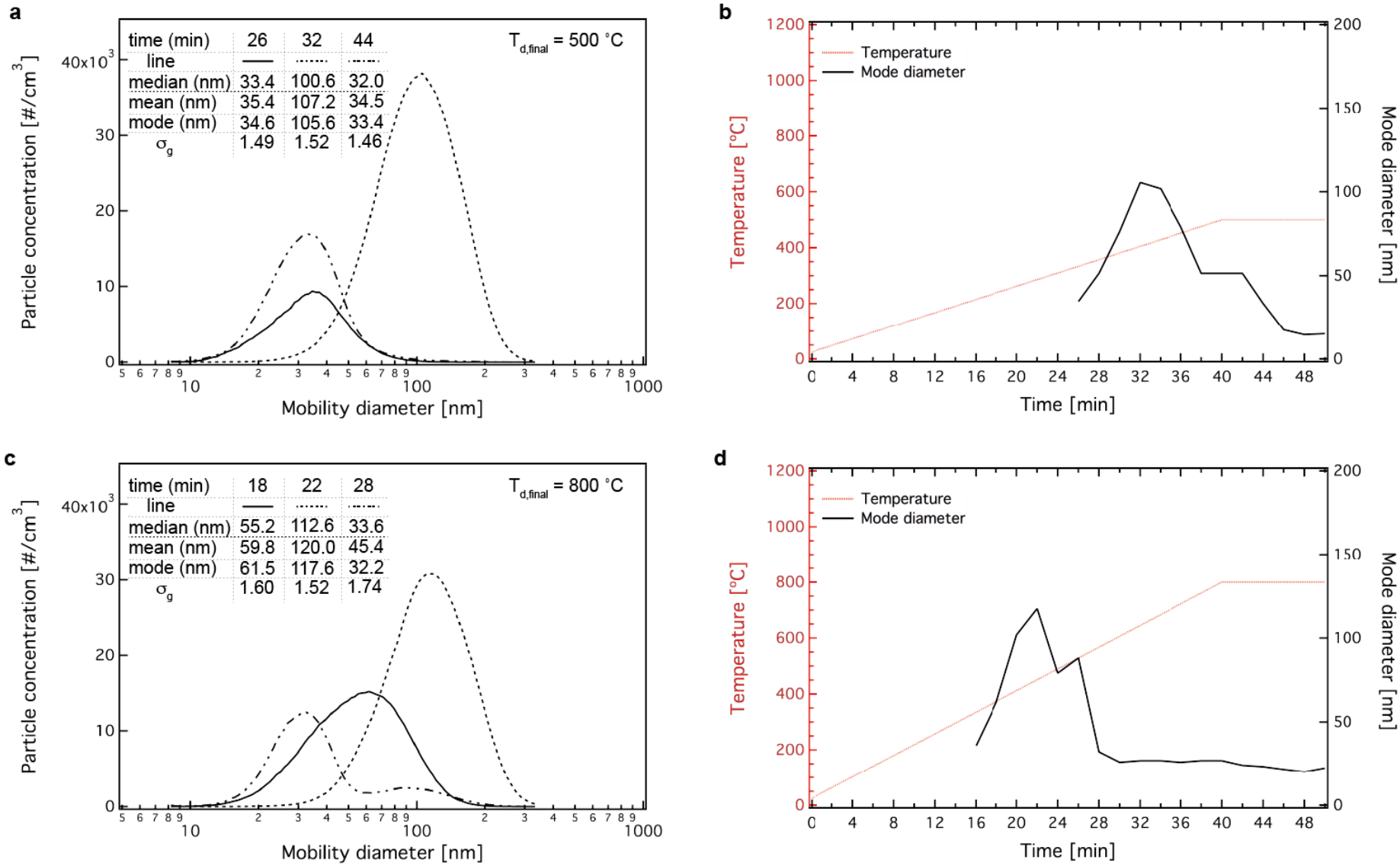
a
time (min) 26 32 44
line
median (nm) 33.4 100.6 32.0
mean (nm) 35.4 107.2 34.5
mode (nm) 34.6 105.6 33.4
σg 1.49 1.52 1.46
T d,final = 500 °C
Particle concentration [#/cm3]
Mobility diameter [nm]
b
Temperature
Mode diameter
Temperature [°C]
Mode diameter [nm]
Time [min]
c
time (min) 18 22 28
line
median (nm) 55.2 112.6 33.6
mean (nm) 59.8 120.0 45.4
mode (nm) 61.5 117.6 32.2
σg 1.60 1.52 1.74
T d,final = 800 °C
Particle concentration [#/cm3]
Mobility diameter [nm]
d
Temperature
Mode diameter
Temperature [°C]
Mode diameter [nm]
Time [min]

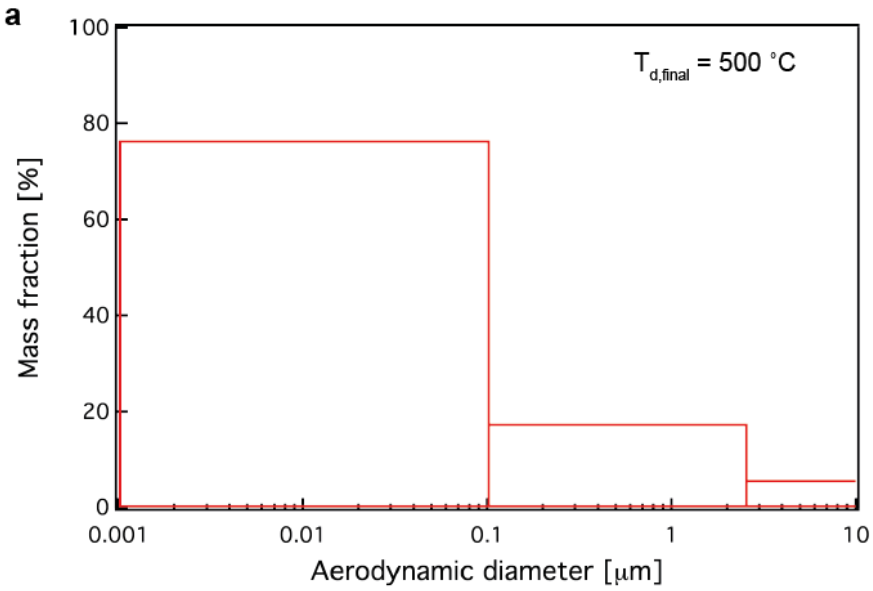
a
100
80
60
40
20
0
Mass fraction [%]
$T_{d,final}$ = 500 °C
0.001
0.01
0.1
1
10
Aerodynamic diameter [μm]

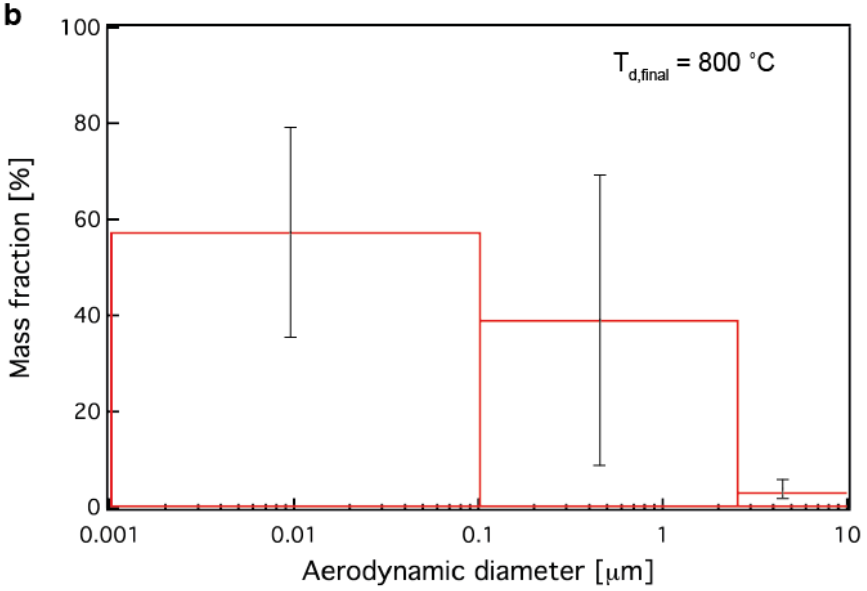
b
100
80
60
40
20
0
Mass fraction [%]
$T_{d,final}$ = 800 °C
0.001
0.01
0.1
1
10
Aerodynamic diameter [μm]

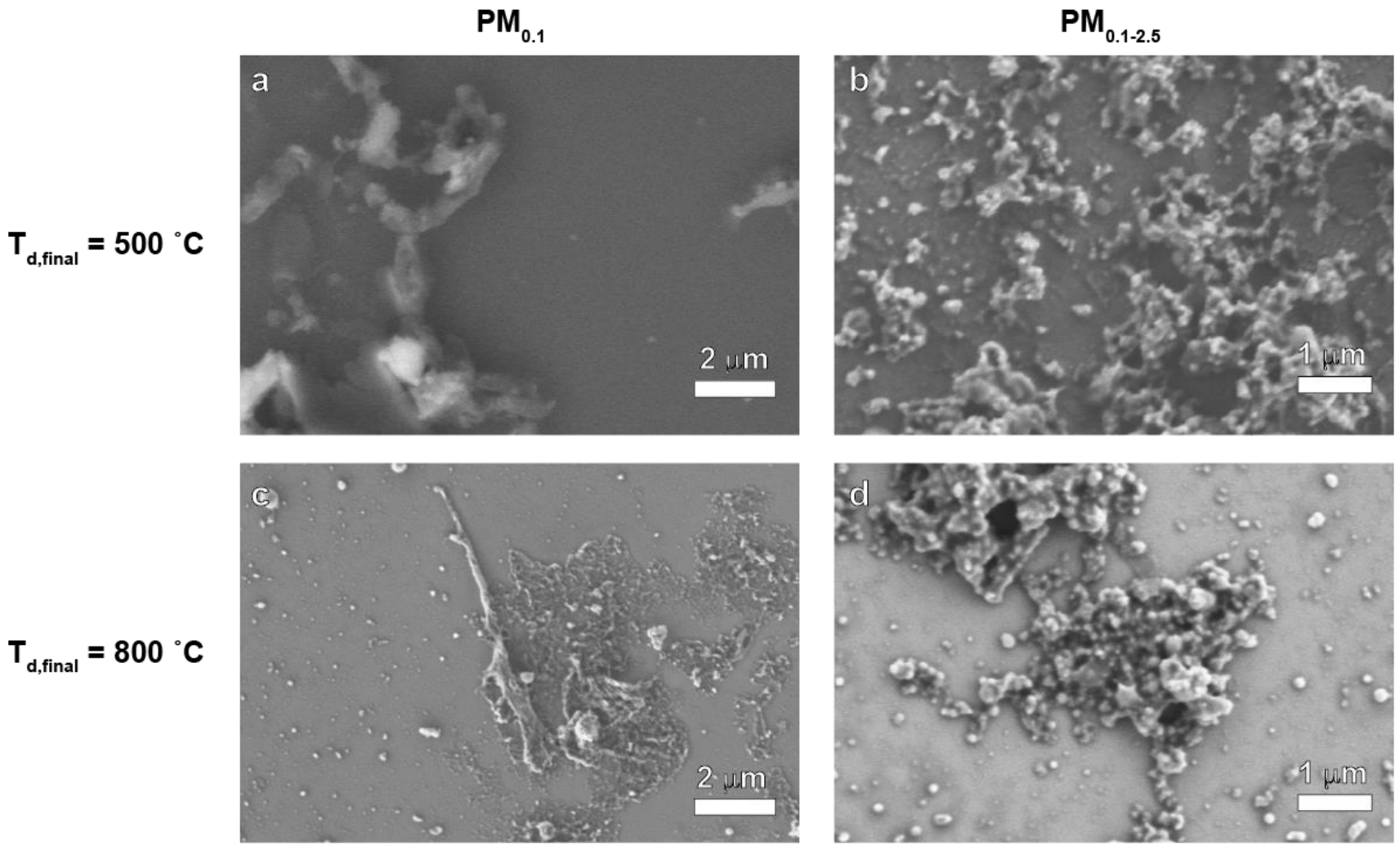
PM0.1
PM0.1-2.5
Td,final = 500 ˚C
Td,final = 800 ˚C
a
b
c
d
2 μm
1 μm
2 μm
1 μm

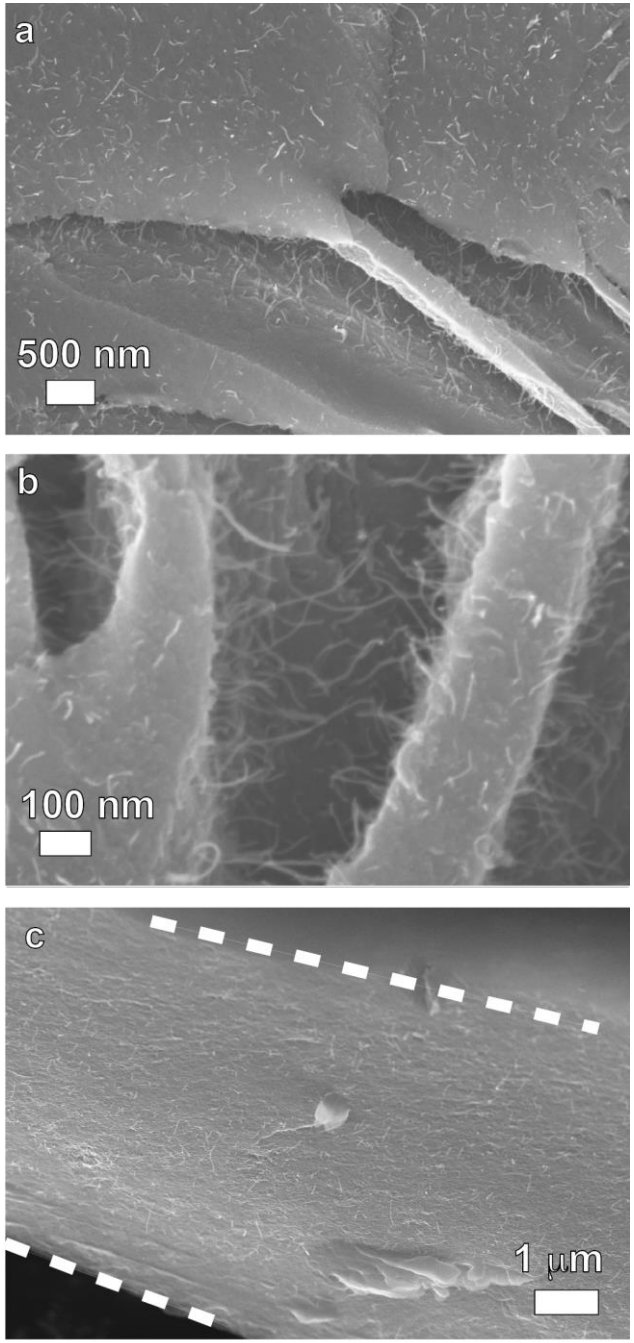
a
500 nm
b
100 nm
c
1 μm

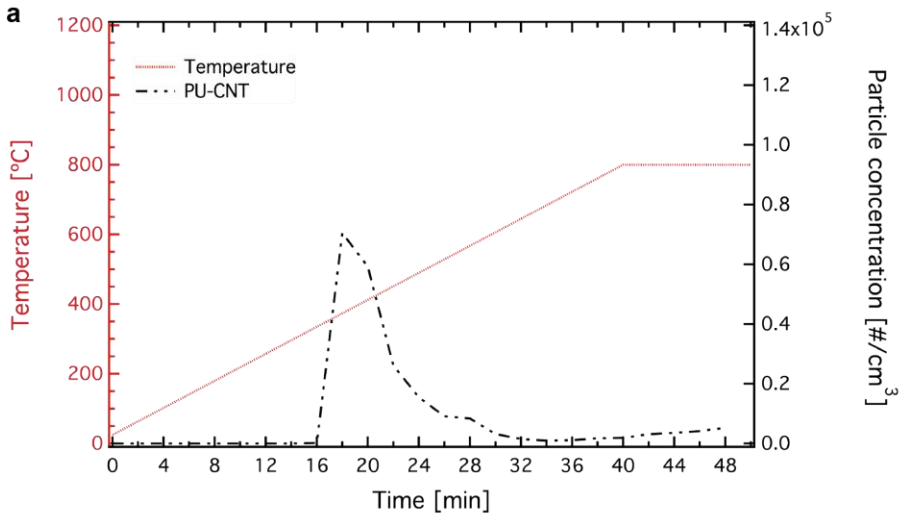
a
Temperature
PU-CNT
Temperature [°C]
Particle concentration [#/cm3]
Time [min]

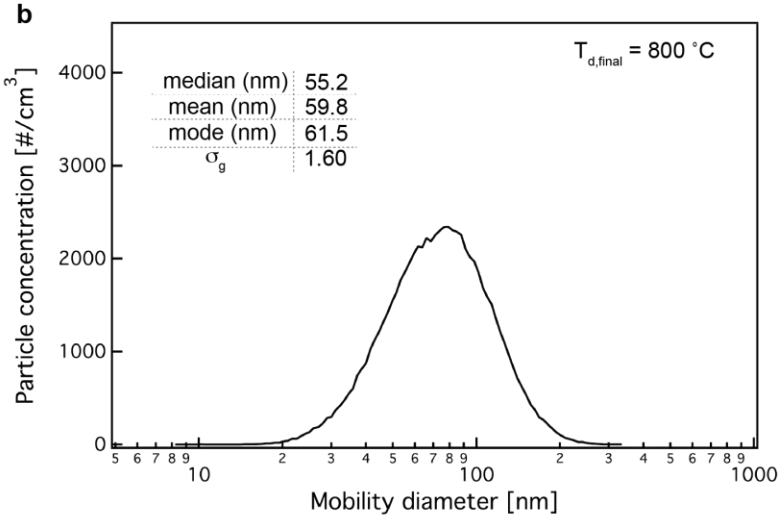
b
T d,final = 800 °C
median (nm) 55.2
mean (nm) 59.8
mode (nm) 61.5
σg 1.60
Particle concentration [#/cm3]
Mobility diameter [nm]

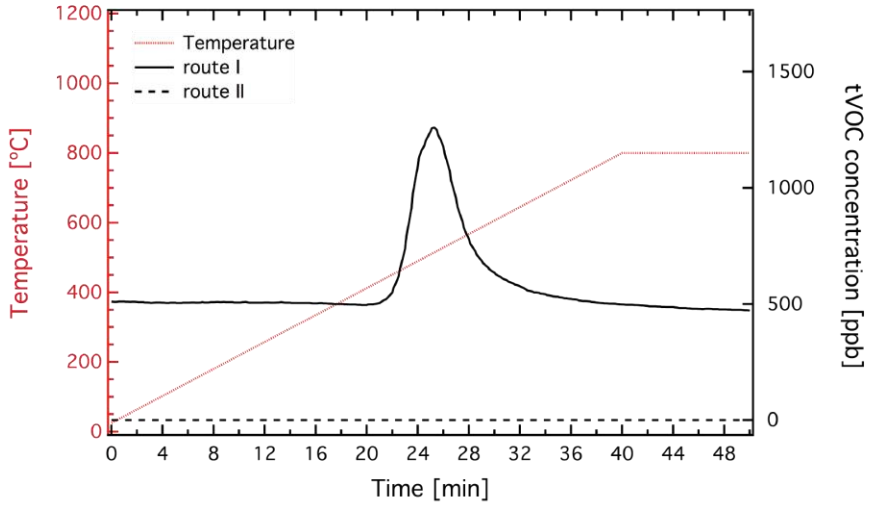
Temperature
route I
route II
Temperature [°C]
tVOC concentration [ppb]
Time [min]

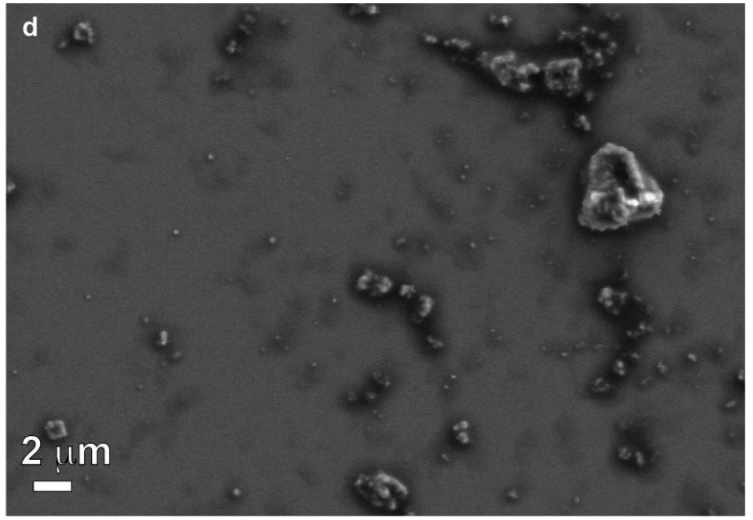
d
2 µm

NANOTOXICOLOGY 2015

S. Pirela, **G.A. Sotiriou**, D. Bello, M. Shafer, K. Lee Bunker, V. Castranova, T. Thomas & P. Demokritou. "Consumer exposures to laser printer-emitted nanoparticles: A case study of the life-cycle implications from nano-enabled products" *Nanotoxicology* **9**, 760-768 (2015).

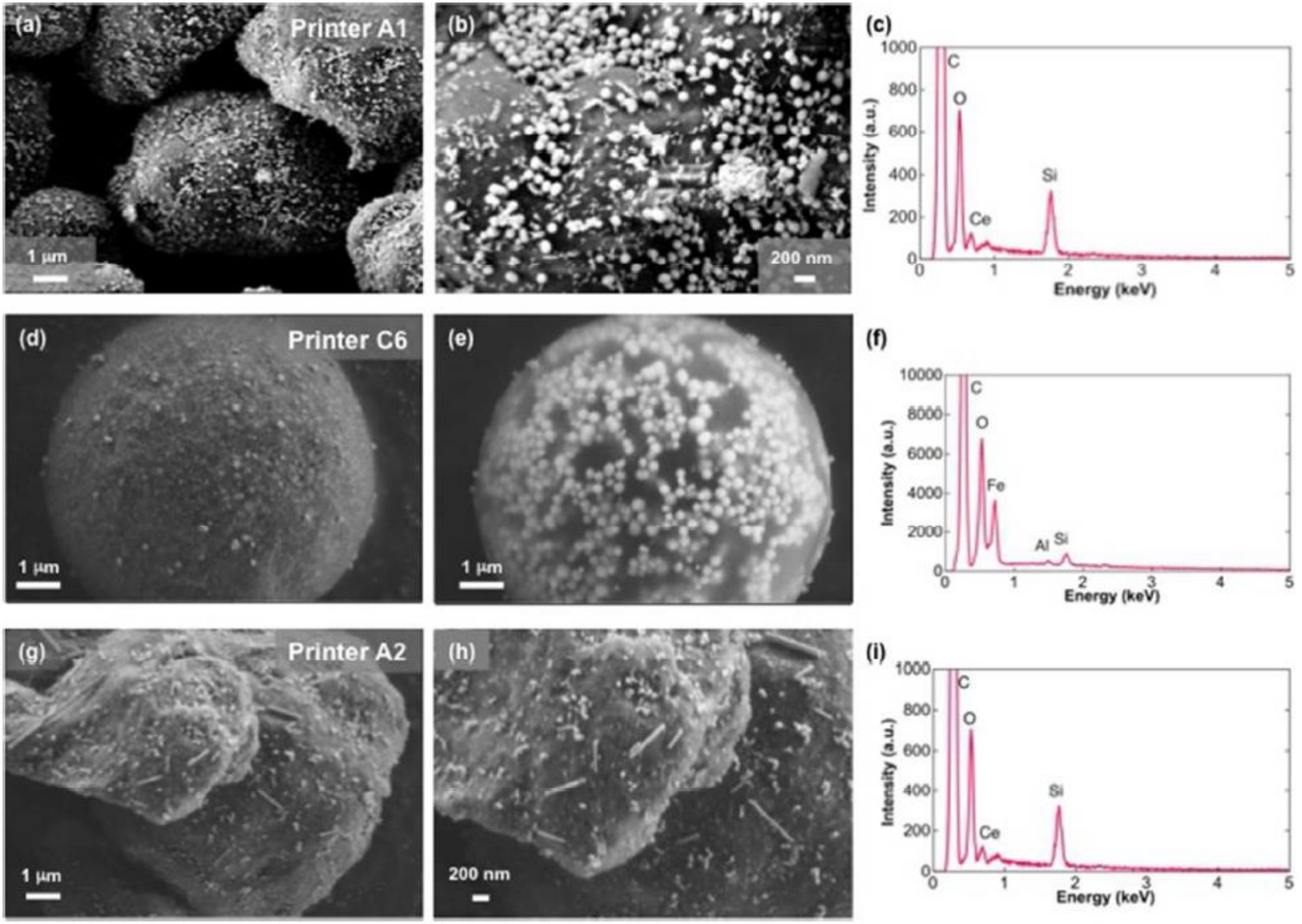
(a)
Printer A1
1 μm
(b)
200 nm
(c)
C
O
Ce
Si
Intensity (a.u.)
Energy (keV)
(d)
Printer C6
1 μm
(e)
1 μm
(f)
C
O
Fe
Al
Si
Intensity (a.u.)
Energy (keV)
(g)
Printer A2
1 μm
(h)
200 nm
(i)
C
O
Ce
Si
Intensity (a.u.)
Energy (keV)

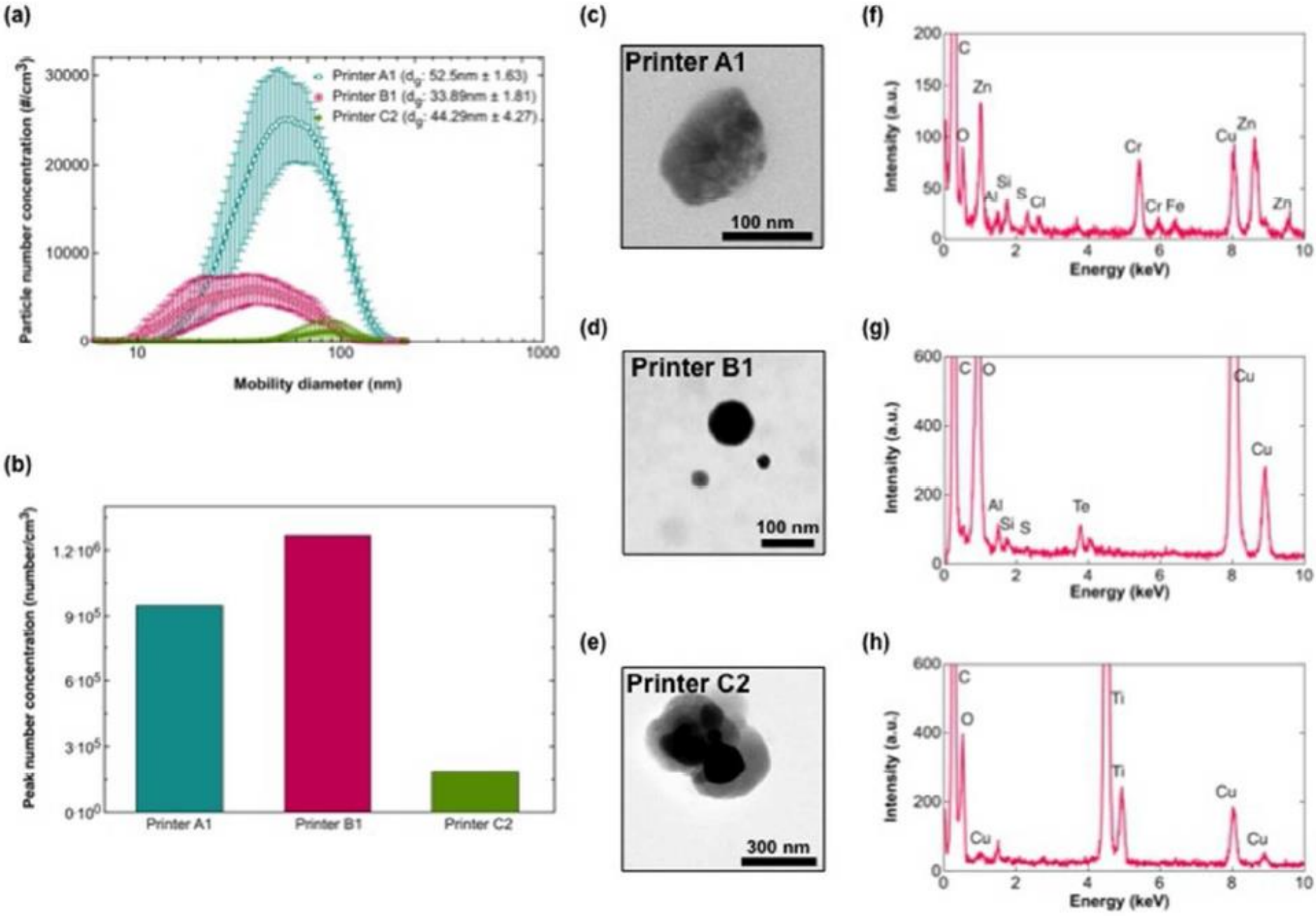
(a)
Printer A1 (dg: 52.5nm ± 1.63)
Printer B1 (dg: 33.89nm ± 1.81)
Printer C2 (dg: 44.29nm ± 4.27)
Particle number concentration (#/cm3)
Mobility diameter (nm)
(b)
Peak number concentration (number/cm3)
Printer A1
Printer B1
Printer C2
(c)
Printer A1
100 nm
(d)
Printer B1
100 nm
(e)
Printer C2
300 nm
(f)
Intensity (a.u.)
Energy (keV)
(g)
Intensity (a.u.)
Energy (keV)
(h)
Intensity (a.u.)
Energy (keV)

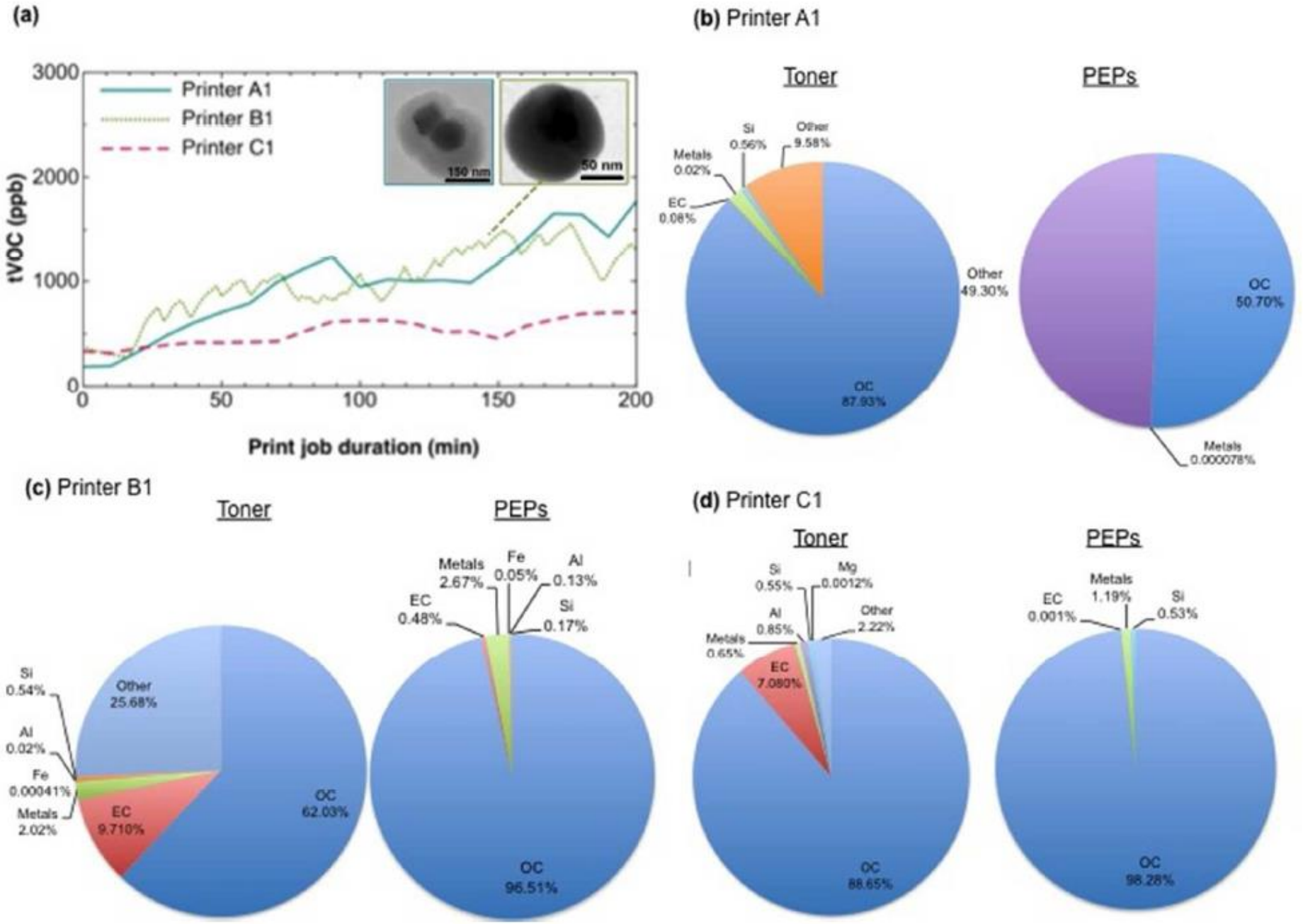
(a)
3000
2000
1000
0
tVOC (ppb)
0
50
100
150
200
Print job duration (min)
Printer A1
Printer B1
Printer C1
150 nm
50 nm
(b) Printer A1
Toner
PEPs
Metals 0.02%
Si 0.56%
Other 9.58%
EC 0.08%
Other 49.30%
OC 87.93%
OC 50.70%
Metals 0.000078%
(c) Printer B1
Toner
PEPs
Si 0.54%
Other 25.68%
Al 0.02%
Fe 0.00041%
Metals 2.02%
EC 9.710%
OC 62.03%
Metals 2.67%
Fe 0.05%
Al 0.13%
EC 0.48%
Si 0.17%
OC 96.51%
(d) Printer C1
Toner
PEPs
Si 0.55%
Mg 0.0012%
Al 0.85%
Other 2.22%
Metals 0.65%
EC 7.080%
OC 88.65%
EC 0.001%
Metals 1.19%
Si 0.53%
OC 98.28%

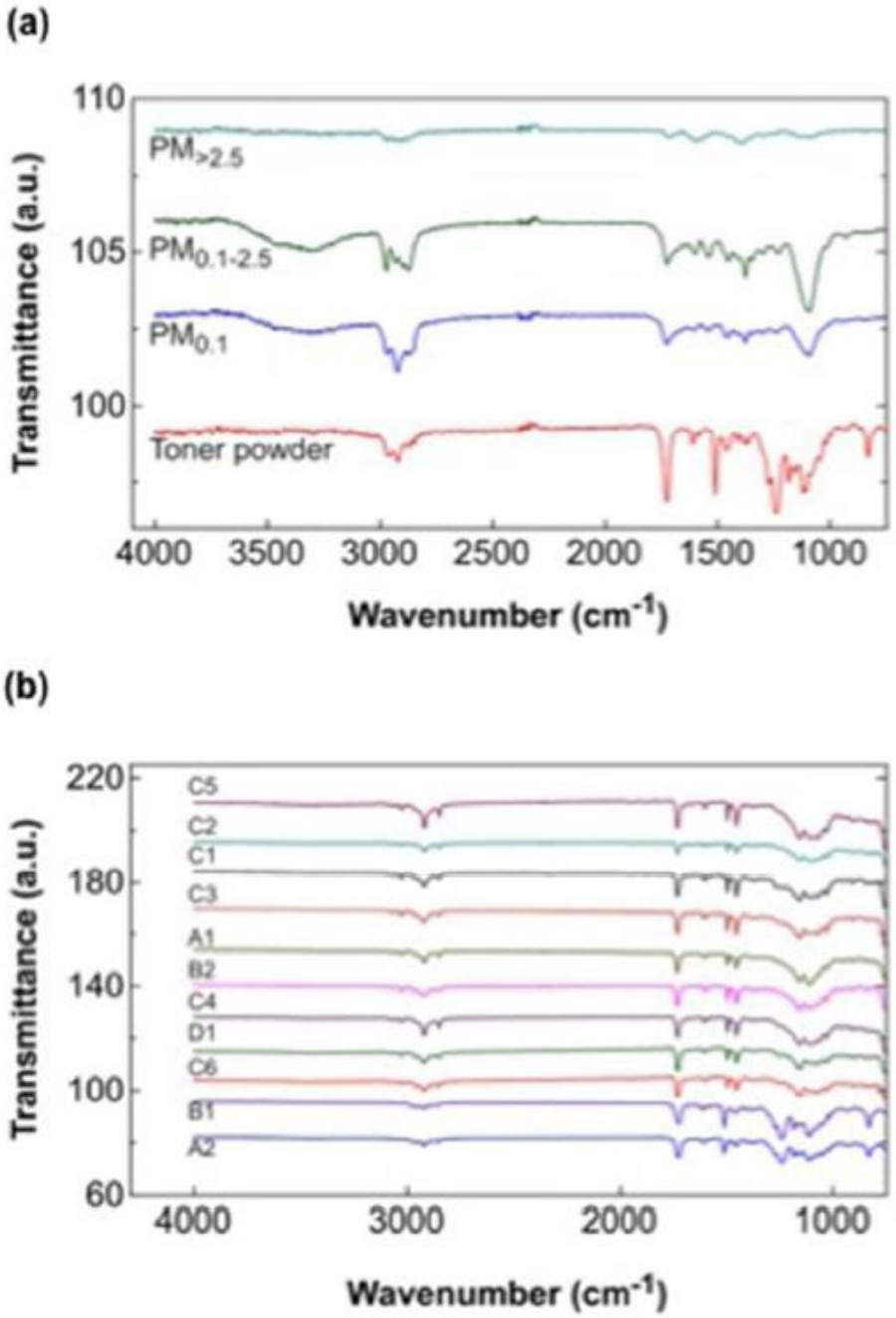
(a)
110
105
100
Transmittance (a.u.)
PM>2.5
PM0.1-2.5
PM0.1
Toner powder
4000
3500
3000
2500
2000
1500
1000
Wavenumber (cm-1)
(b)
220
180
140
100
60
Transmittance (a.u.)
C5
C2
C1
C3
A1
B2
C4
D1
C6
B1
A2
4000
3000
2000
1000
Wavenumber (cm-1)

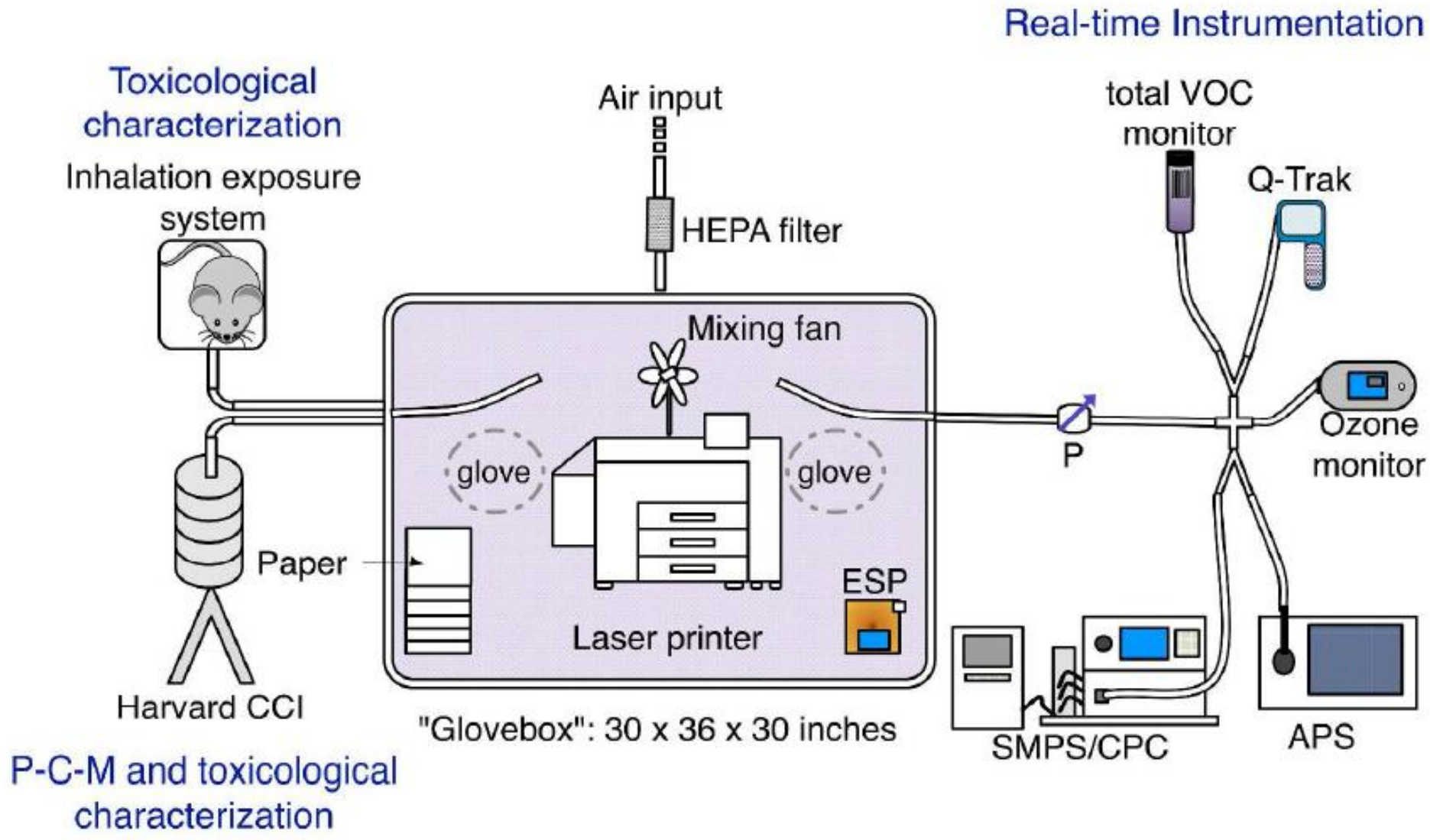
Real-time Instrumentation
Toxicological characterization
Inhalation exposure system
Air input
HEPA filter
total VOC monitor
Q-Trak
Mixing fan
glove
glove
P
Ozone monitor
Paper
ESP
Laser printer
Harvard CCI
"Glovebox": 30 x 36 x 30 inches
SMPS/CPC
APS
P-C-M and toxicological characterization

J HAZARD MATER 2016

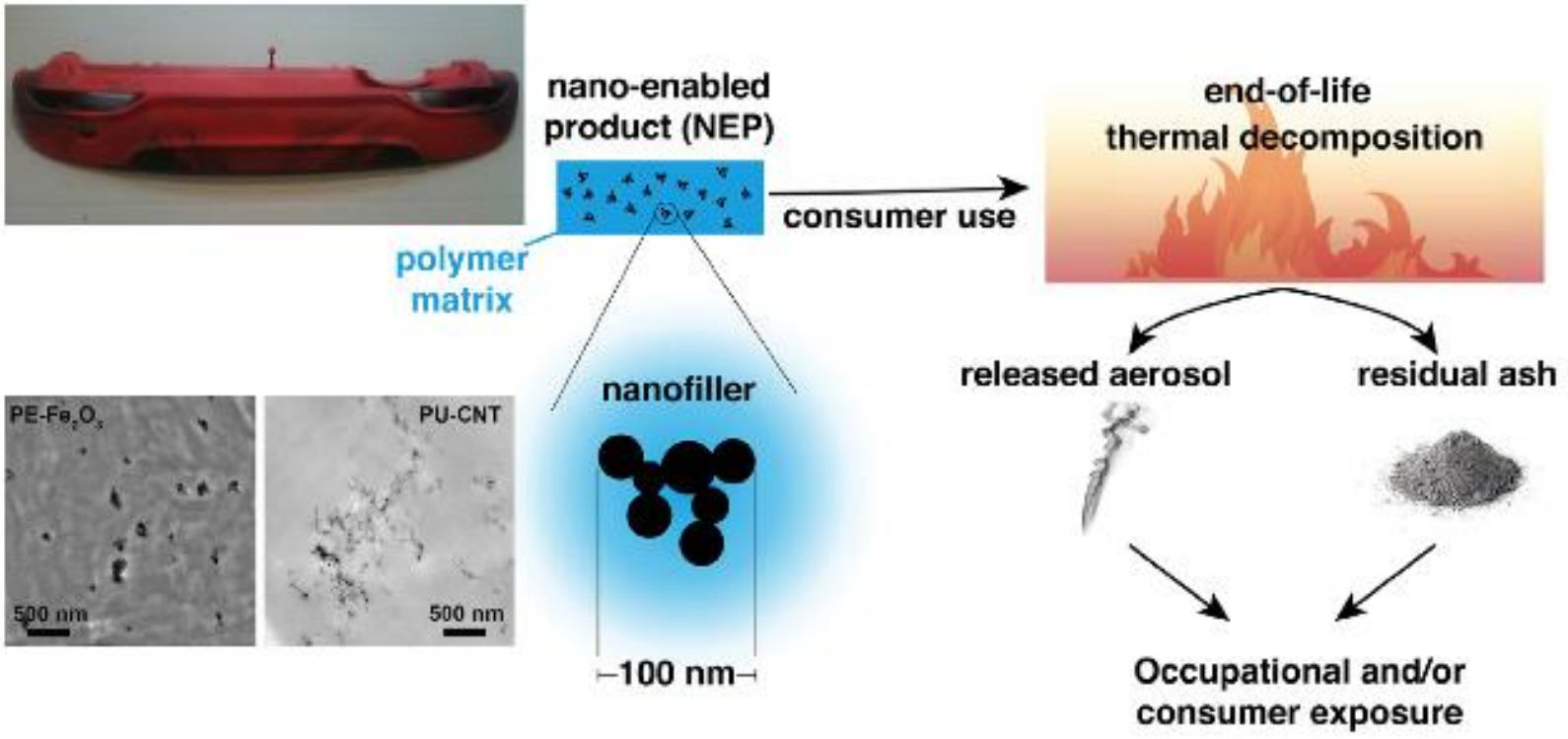

Table 1
Summary of all nano-enabled products (NEPs) analyzed in this study along with the main results regarding the yield, the EC/OC content as well as the Fe content for both the released aerosol and the residual ash.

NEPs				Released aerosol										Residual ash					
				500 °C					800 °C					500 °C				800 °C	
				Yield (%)		EC (%)	OC (%)	Fe (wt%)[b]	Yield (%)		EC(%)	OC (%)	Fe (wt%)[b]						
Sample ID	Filler	Size (nm)	Loading (wt%)	$PM_{0.1}$	$PM_{0.1-2.5}$				$PM_{0.1}$	$PM_{0.1-2.5}$				Yield (%)	EC (%)	OC (%)	Fe (wt%)[b]	Yield (%)	Fe (wt%)[b]
PU	–	–	–	1.65	0.44	0.9	99.1	–	3.41	1.07	0.8	99.2	–	5.0	84.9	15.1	–	–	–
PU-CB	CB	50–100	0.09	3.61	1.09	0.6	99.4	–	2.96	0.79	0.7	99.3	–	4.0	76.5	23.5	–	–	–
PU-CNT	CNT	10[a]	0.09	4.04	0.93	0.7	99.3	–	3.64[c]	1.84	0.9	99.1[d]	–	6.1	82.1	17.9	–	–	–
PE	–	–	–	4.08	3.66	0.4	99.6	–	3.46	3.25	0.3	99.7	–	0.9	78.2	21.8	–	–	–
PE-Fe_2O_3	Fe_2O_3	50–100	4	2.77	0.74	0.3	99.7	0.004	1.46	1.60	0.3	99.7	0.026	3.9	–	–	74.5	3.9	77.3
PE-org.	Org. pigm.	50–100	2	3.29	0.90	0.3	99.7	–	2.66	0.63	0.4	99.6	–	1.0	75.0	25.0	–	–	–

PU: polyurethane, CB: carbon black, CNT: carbon nanotube, PE: polyethylene, Org: organic pigment Red 254, EC: elemental carbon, OC: organic carbon.

[a] Size corresponds to diameter.

[b] Measured by ICP-MS.

[c] Standard deviation of 3 independent measurements: 1.4%.

[d] Standard deviation of 3 independent measurements: 0.2%.

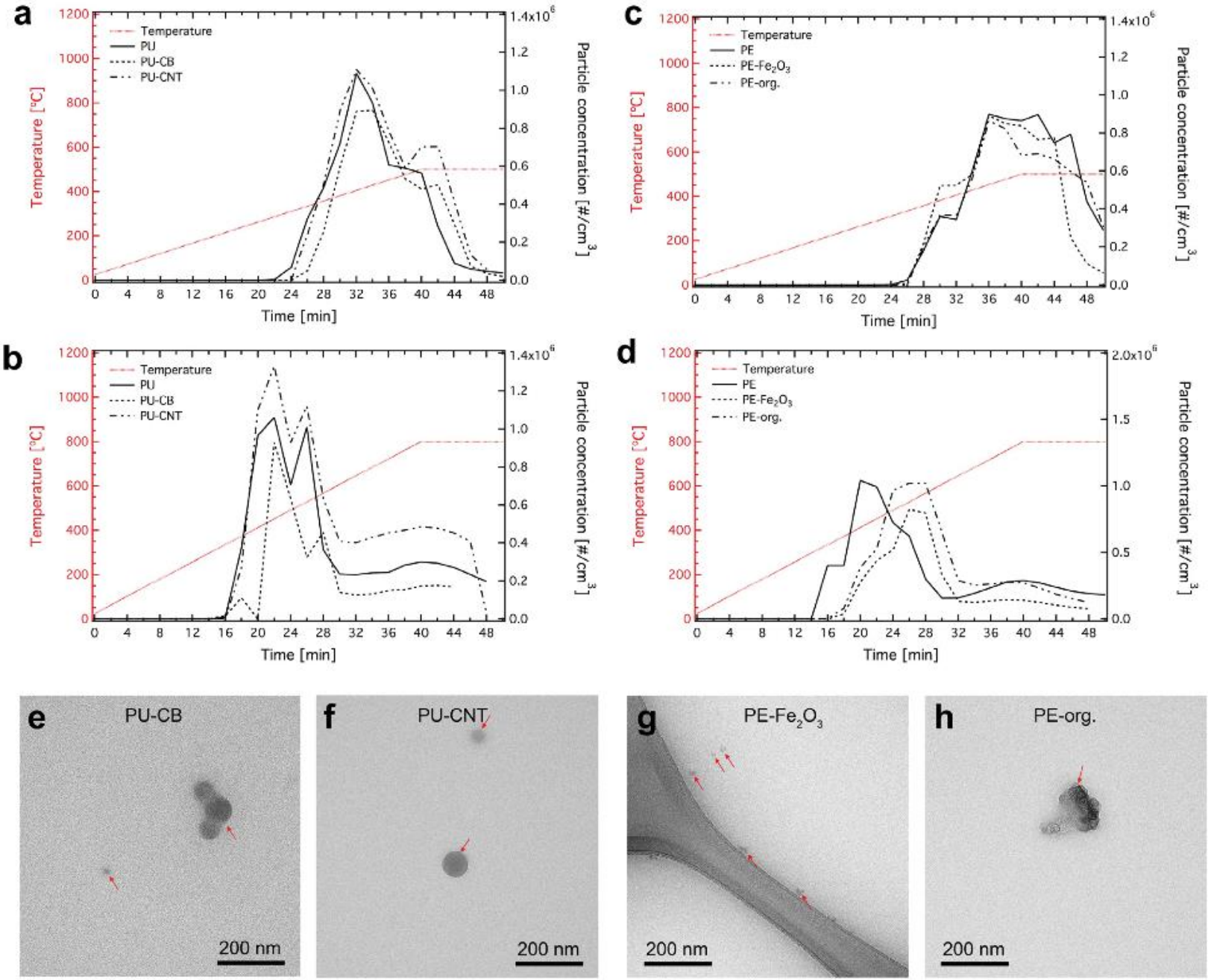
a
Temperature
PU
PU-CB
PU-CNT
Temperature [°C]
Particle concentration [#/cm³]
Time [min]
b
Temperature
PU
PU-CB
PU-CNT
Temperature [°C]
Particle concentration [#/cm³]
Time [min]
c
Temperature
PE
PE-Fe2O3
PE-org.
Temperature [°C]
Particle concentration [#/cm³]
Time [min]
d
Temperature
PE
PE-Fe2O3
PE-org.
Temperature [°C]
Particle concentration [#/cm³]
Time [min]
e
PU-CB
200 nm
f
PU-CNT
200 nm
g
PE-Fe2O3
200 nm
h
PE-org.
200 nm

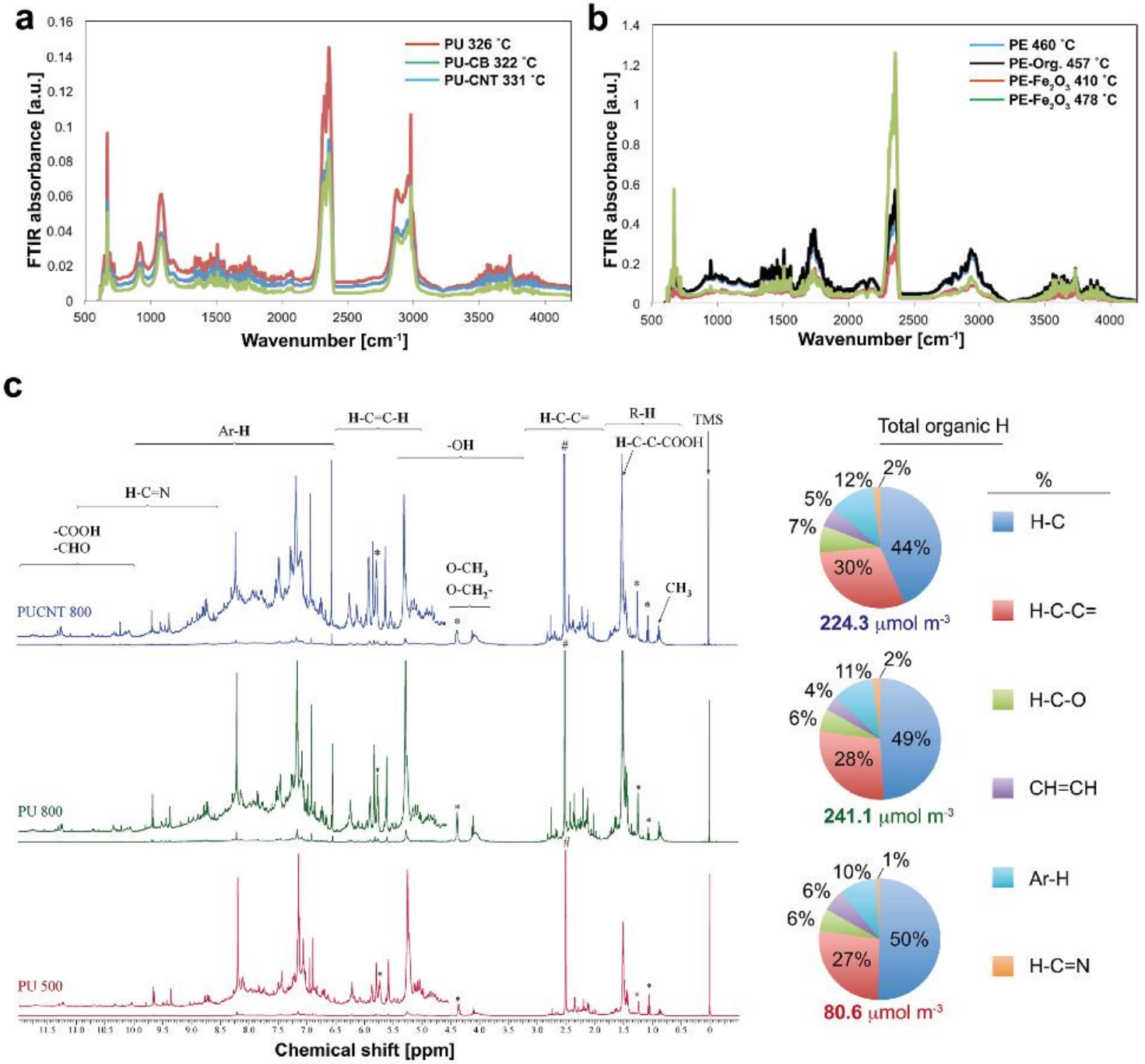
a
FTIR absorbance [a.u.]
Wavenumber [cm-1]
PU 326 °C
PU-CB 322 °C
PU-CNT 331 °C
b
FTIR absorbance [a.u.]
Wavenumber [cm-1]
PE 460 °C
PE-Org. 457 °C
PE-Fe2O3 410 °C
PE-Fe2O3 478 °C
c
Ar-H
H-C=C-H
-OH
H-C-C=
R-H
TMS
H-C-C-COOH
H-C=N
-COOH
-CHO
O-CH3
O-CH2-
CH3
PUCNT 800
PU 800
PU 500
Chemical shift [ppm]
Total organic H
%
H-C
H-C-C=
H-C-O
CH=CH
Ar-H
H-C=N
44%
30%
7%
5%
12%
2%
224.3 μmol m-3
49%
28%
6%
4%
11%
2%
241.1 μmol m-3
50%
27%
6%
6%
10%
1%
80.6 μmol m-3

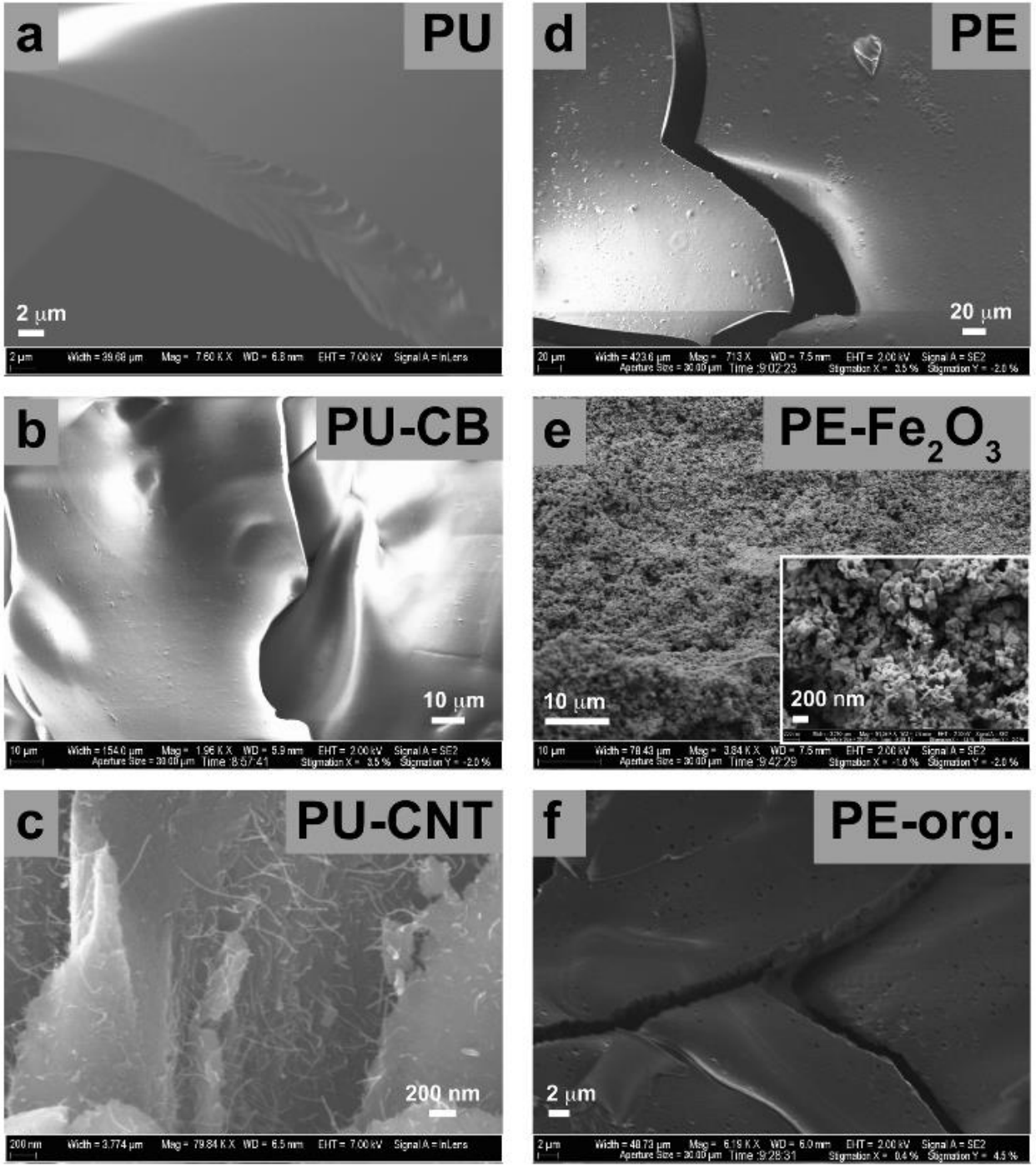
a
PU
2 μm
d
PE
20 μm
b
PU-CB
10 μm
e
PE-Fe2O3
10 μm
200 nm
c
PU-CNT
200 nm
f
PE-org.
2 μm

NANOMEDICINE 2016

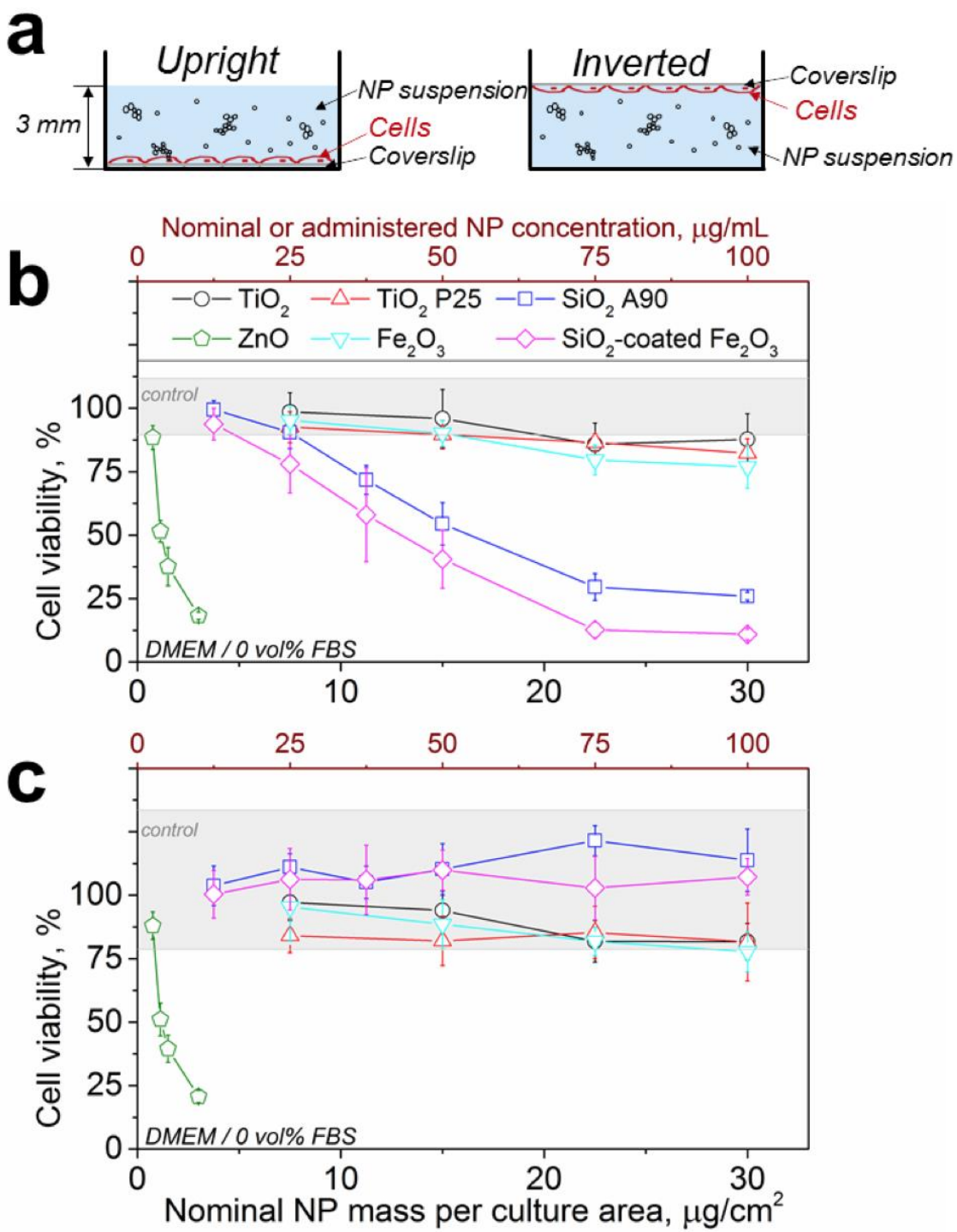
a
Upright
Inverted
3 mm
NP suspension
Cells
Coverslip
Coverslip
Cells
NP suspension
b
Nominal or administered NP concentration, µg/mL
0
25
50
75
100
TiO2
TiO2 P25
SiO2 A90
ZnO
Fe2O3
SiO2-coated Fe2O3
control
Cell viability, %
100
75
50
25
0
DMEM / 0 vol% FBS
0
10
20
30
c
0
25
50
75
100
control
Cell viability, %
100
75
50
25
0
DMEM / 0 vol% FBS
0
10
20
30
Nominal NP mass per culture area, µg/cm2

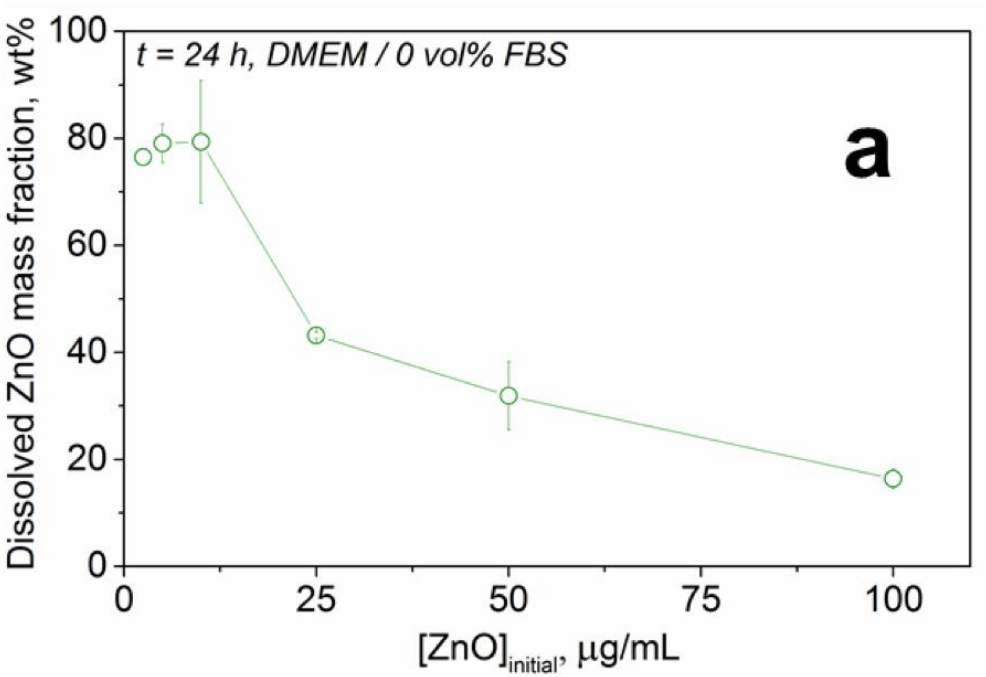
t = 24 h, DMEM / 0 vol% FBS
a
Dissolved ZnO mass fraction, wt%
0
20
40
60
80
100
0
25
50
75
100
[ZnO]initial, µg/mL

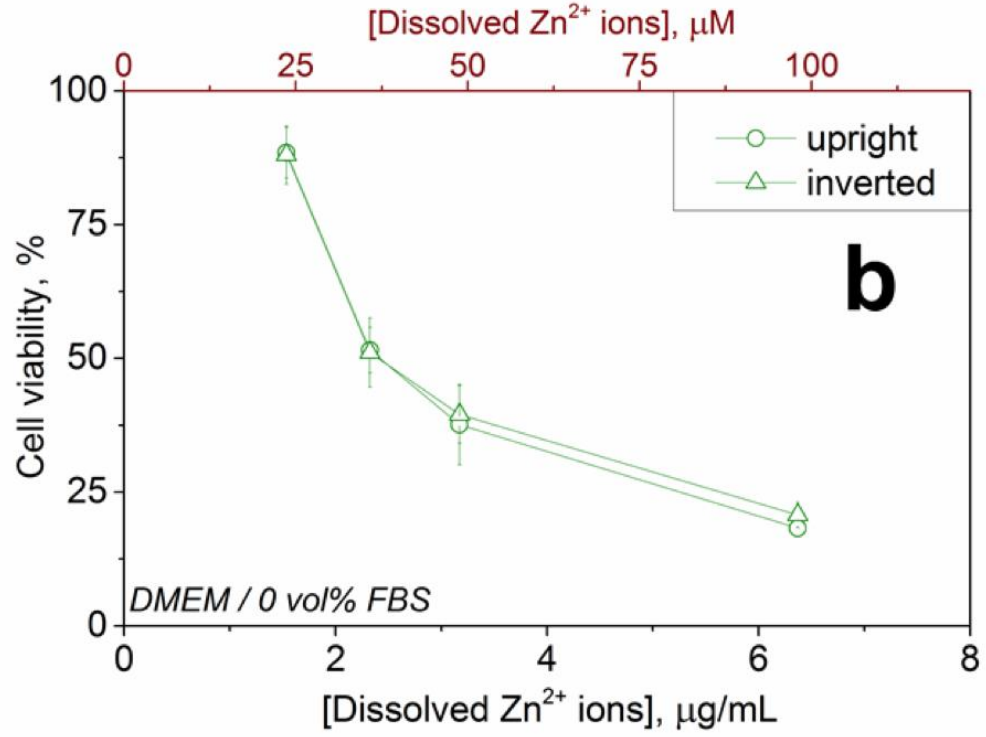
[Dissolved Zn2+ ions], µM
0
25
50
75
100
upright
inverted
b
Cell viability, %
0
25
50
75
100
DMEM / 0 vol% FBS
0
2
4
6
8
[Dissolved Zn2+ ions], µg/mL

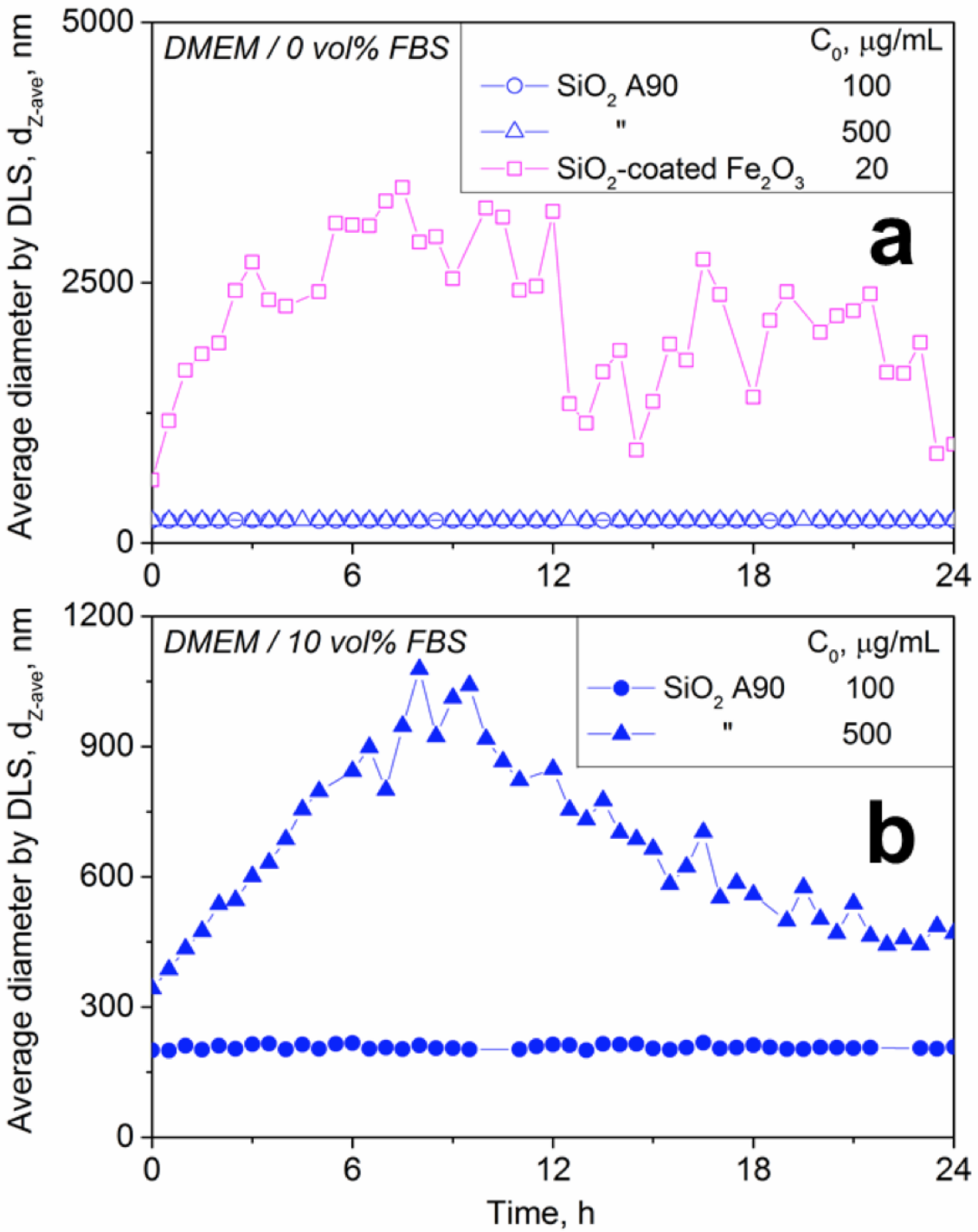
DMEM / 0 vol% FBS
C0, μg/mL
SiO2 A90 100
" 500
SiO2-coated Fe2O3 20
a
Average diameter by DLS, dZ-ave, nm
5000
2500
0
0
6
12
18
24
DMEM / 10 vol% FBS
C0, μg/mL
SiO2 A90 100
" 500
b
Average diameter by DLS, dZ-ave, nm
1200
900
600
300
0
0
6
12
18
24
Time, h

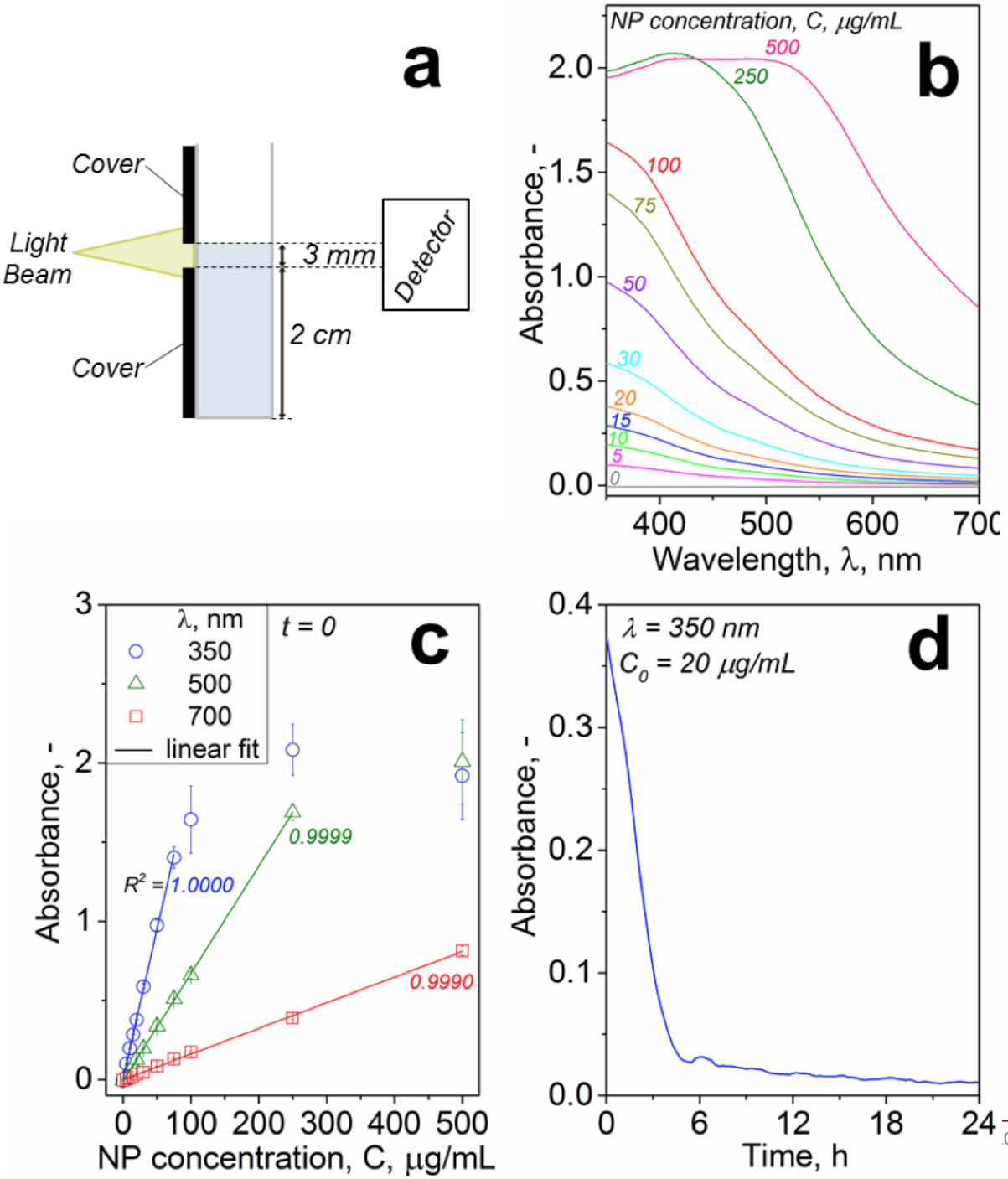
a
Cover
Light Beam
3 mm
Detector
2 cm
Cover
b
NP concentration, C, μg/mL
500
250
100
75
50
30
20
15
10
5
0
Absorbance, -
Wavelength, λ, nm
c
λ, nm
350
500
700
linear fit
t = 0
R² = 1.0000
0.9999
0.9990
Absorbance, -
NP concentration, C, μg/mL
d
λ = 350 nm
C0 = 20 μg/mL
Absorbance, -
Time, h

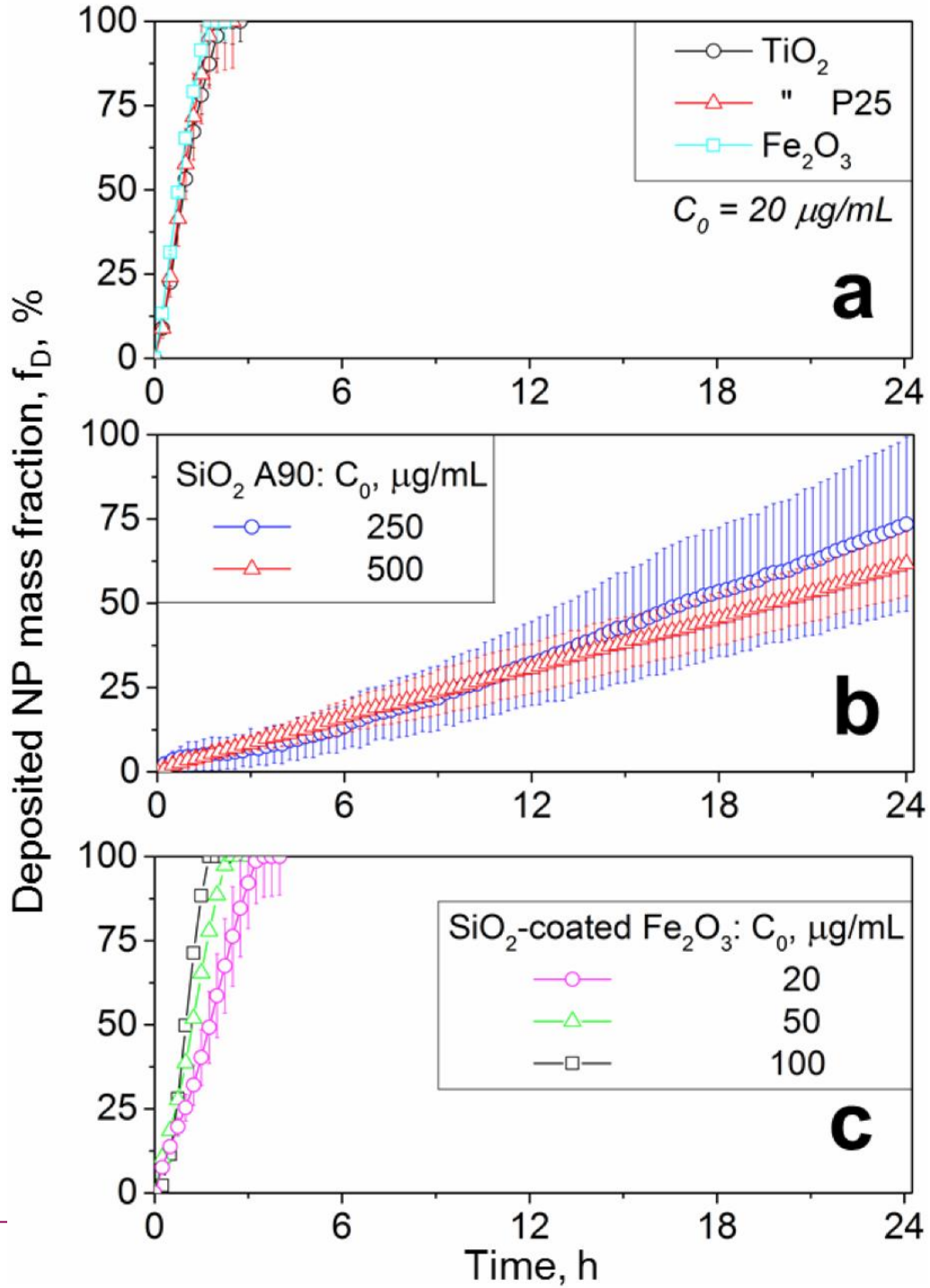
Deposited NP mass fraction, f_D, %
100
75
50
25
0
0
6
12
18
24
TiO_2
" P25
Fe_2O_3
C_0 = 20 µg/mL
a
SiO_2 A90: C_0, µg/mL
250
500
b
SiO_2-coated Fe_2O_3: C_0, µg/mL
20
50
100
c
Time, h

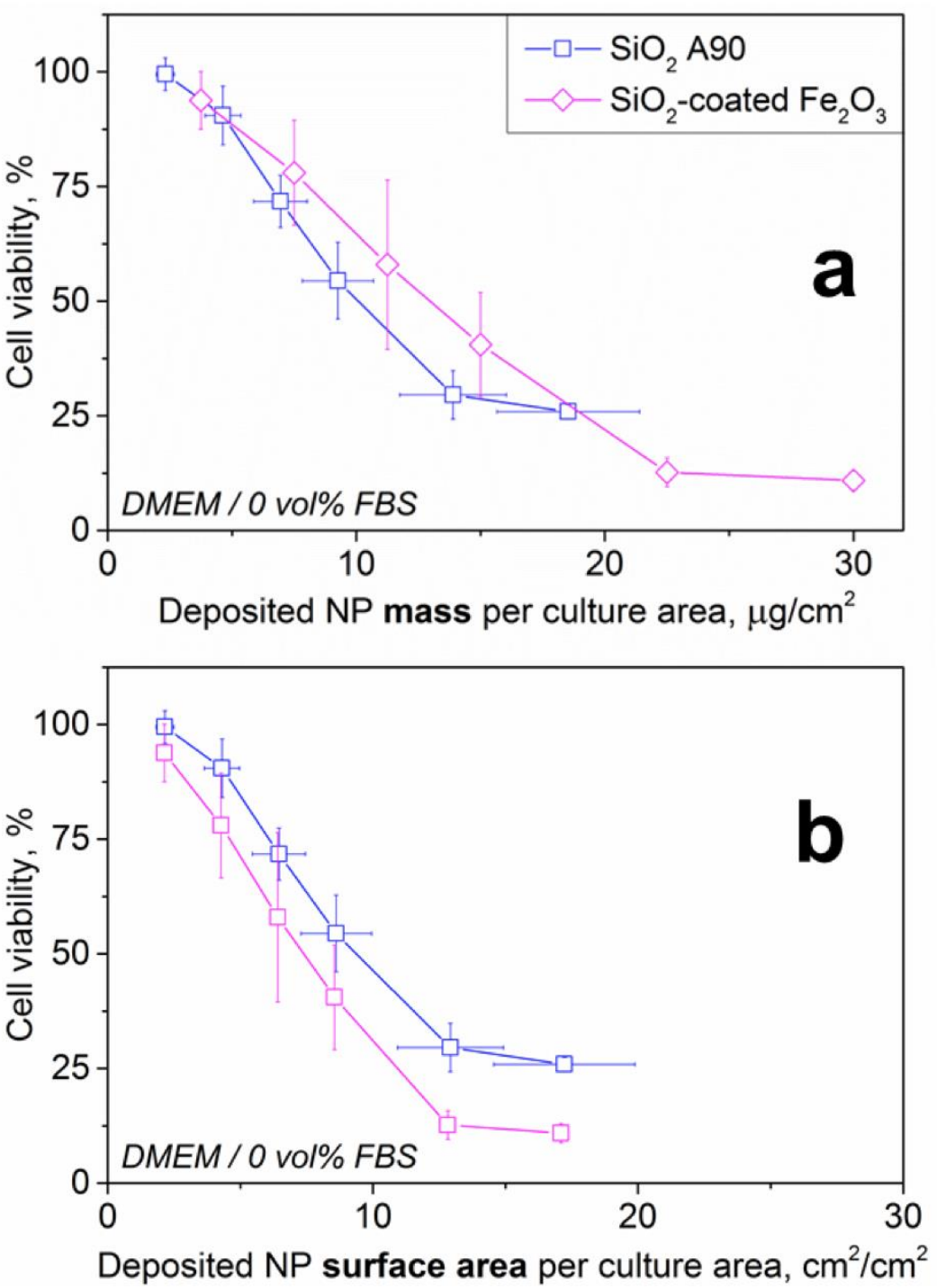
SiO2 A90
SiO2-coated Fe2O3
a
DMEM / 0 vol% FBS
Cell viability, %
Deposited NP mass per culture area, μg/cm2
b
DMEM / 0 vol% FBS
Cell viability, %
Deposited NP surface area per culture area, cm2/cm2

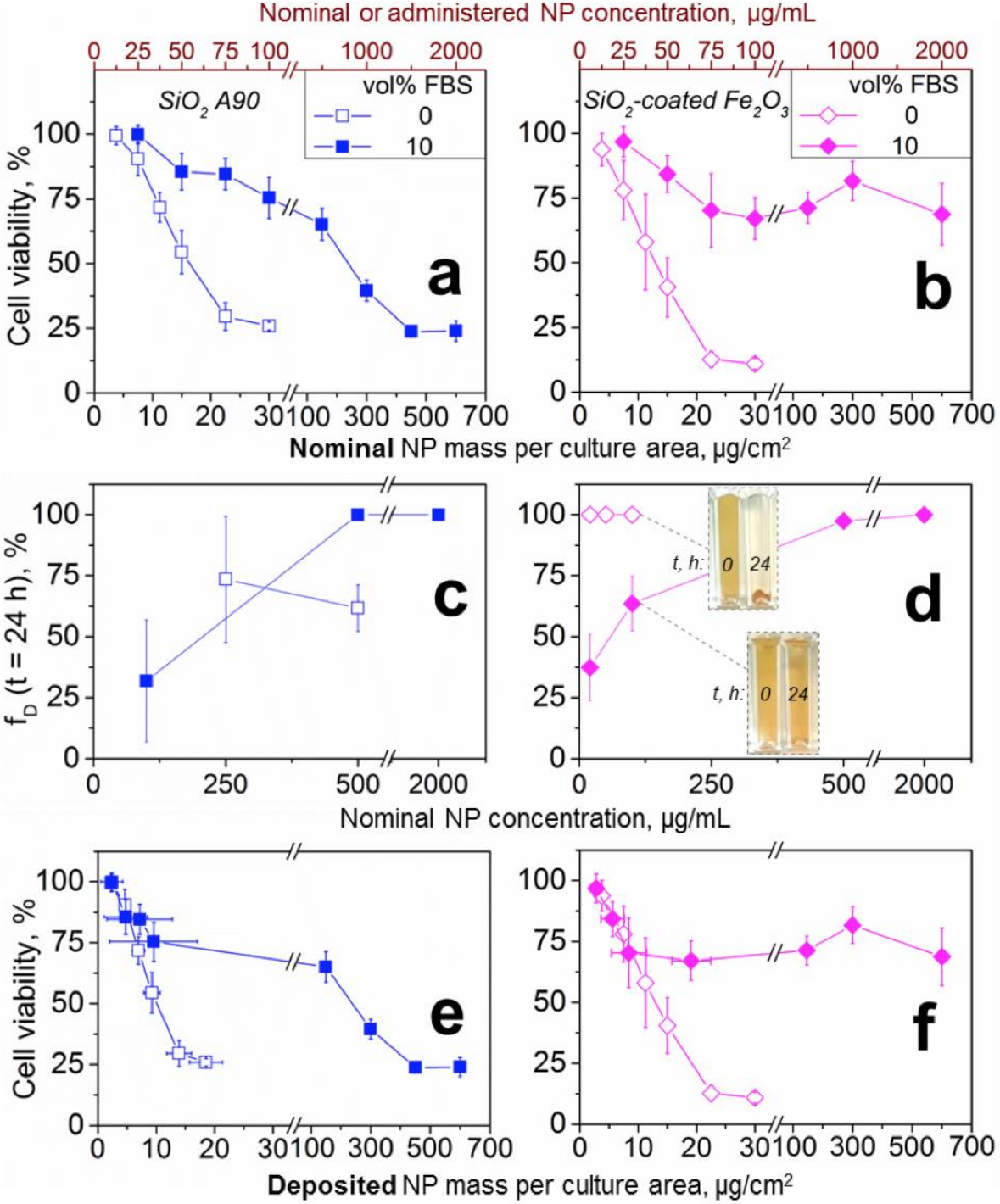
Nominal or administered NP concentration, μg/mL
0 25 50 75 100 1000 2000
SiO2 A90
vol% FBS
0
10
Cell viability, %
a
SiO2-coated Fe2O3
b
Nominal NP mass per culture area, μg/cm2
fD (t = 24 h), %
c
t, h: 0 24
d
Nominal NP concentration, μg/mL
e
f
Deposited NP mass per culture area, μg/cm2